FUNCTIONAL ROLE OF NEUROTRANSMITTERS IN THE VISUAL THALAMUS

by

YOUNG HA KWON

B.S. Biology, Massachusetts Institute of Technology
(1984)

M.D. Yale University
(1991)

Submitted to the Department of Brain and Cognitive Sciences
in partial fulfillment of the requirements for the degree of

DOCTOR OF PHILOSOPHY

at the

Massachusetts Institute of Technology
September, 1991

Signature of Author _____
Department of Brain and Cognitive Sciences
May 30, 1991

Certified by _____
Mriganka Sur
Associate Professor, Department of Brain and Cognitive Sciences
Thesis Supervisor

Accepted by _____
Emilio Bizzi, Chairman
Department of Brain and Cognitive Sciences

FUNCTIONAL ROLE OF NEUROTRANSMITTERS IN THE VISUAL THALAMUS

by

YOUNG HA KWON

Submitted to the Department of Brain and Cognitive Sciences on May 30, 1991
in partial fulfillment of the requirements for the degree of
Doctor of Philosophy in Neuroscience

ABSTRACT

Thalamic modulation of visual signals was investigated by examining the action of two known neurotransmitter systems in the dorsal lateral geniculate nucleus (dLGN) of the cat: the excitatory amino acid (EAA) system and acetylcholine (ACh) system. The former mediates direct retinogeniculate transmission, while the latter mediates the innervation from the brain stem to the dLGN.

Excitatory amino acid receptor antagonists were iontophoretically applied to neurons of the dLGN. The neurons were classified physiologically as on- or off-center, X or Y, and lagged or nonlagged types. Visual responses of *all* dLGN cell types were shown to be mediated by EAA receptors, thus confirming the notion that an EAA is the neurotransmitter at the retinogeniculate synapse. Two EAA receptor types, N-Methyl-D-Aspartate (NMDA) and non-NMDA receptors, were *both* responsible for thalamic transmission of retinal inputs to cortex. However, when quantitatively analyzed, NMDA receptors contributed proportionately more to the visual responses of lagged cells than those of nonlagged cells; no such preferential contribution was found for non-NMDA receptors.

The contribution of NMDA receptors to the visual response of dLGN cells was studied, by systematically varying stimulus contrast and size. When the contrast of an

optimal sized spot was varied, thereby changing the amount of retinal excitatory drive, NMDA receptor contributions to the visual response remained proportionately the same despite variations in the response amplitude. However, as the stimulus size (at a constant contrast) was increased, thereby recruiting more surround (intrageniculate) inhibition, the relative contribution of NMDA receptors decreased. Therefore, modulation of NMDA receptor contribution to visual response in the dLGN does not seem possible (at least when monitored extracellularly) by retinal excitatory drive alone. Altering the balance of excitation and inhibition by recruiting spatial inhibition may be necessary for modulation. This is consistent with the voltage-dependence of NMDA receptors; hyperpolarization causes the receptor channel to be blocked by Mg^{++} ions, even when appropriate ligand is bound, while depolarization removes this block. Once the block is removed, the proportional contribution of NMDA receptors is independent of the absolute level of depolarization.

Finally, ACh was iontophoretically applied to dLGN cells to study effect on temporal properties of the visual response. The visual responses of nonlagged cells became more *sustained* during Ach application; that of lagged cells became *less lagged.* Since retinal afferents to both lagged and nonlagged cells are of nonlagged type, these results are consistent with a hypothesis that (brain stem) cholinergic innervation of the dLGN facilitates faithful transmission of retinal signals to cortex in the temporal domain.

The studies described here suggest that the visual thalamus contains specific sets of neurotransmitter receptors that mediate transmission and modulation of visual signals. In general, these results underscore the role of the thalamus in "gating" peripheral sensory information *en route* to cortex.

Thesis Supervisor: Dr. Mriganka Sur
Title: Associate Professor of Brain and Cognitive Sciences

In memory

of

Jenny (Yong-Jin) Shin

ACKNOWLEDGEMENTS

Mriganka Sur, my thesis advisor, has been my mentor, teacher and friend for the past five years. He has been friendly and receptive to my ideas from the very beginning and has remained so throughout these years. He has also been the inspiration and force behind my thesis work. I am always indebted to him for helping me become more mature as a scientist, for his sense of humor which, sometimes, only the few "privileged" can understand, and for his patience with my grammar.

I am indebted to Richard Andersen, Peter Schiller, Ellen Hildreth and Nigel Daw for their supervision, helpful comments and encouragement. They have been influential in my thinking about the functional aspects of this thesis work and have provided different perspectives that helped shape and broaden my thinking about the brain.

I feel priviledged to have had a chance to work closely with Manuel Esguerra, Anna W. Roe, Louis Toth, Sacha Nelson and Lukas Ruecker. The work presented here would not have been possible without their collaborative efforts. Special thanks to Manuel Esguerra and Anna W. Roe for early collaborations and teaching me much of the electrophysiological techniques that I know today. I also would like to thank Manuel Esguerra, Anna W. Roe and Sarah Pallas for letting me actively participate in their own work and broaden the scope my graduate education.

Some of the most valuable experiences during the years at Mriganka Sur's laboratory come from the friendships that I have developed with many of my colleagues. Anna W. Roe, Manny Esguerra, Jong-On Hahm, Preston Garraghty, Louis Toth, Sacha Nelson, Laurie Carmen, Cheryl White, Sarah Pallas, Ary Ramoa, Terry Sullivan and other members of the lab. including Mriganka Sur have become my close friends. I thank them for being wonderful friends, for making everything seem all right during the worst of circumstances, and for making everything fun and memorable during more festive occasions.

Howard Rasmussen, director of the Medical Scientist Training Program at Yale University, and Robert Gifford, dean of student affairs at Yale University School of Medicine, as well as administrative officers, Ann DeCosta at Yale and Jan Ellertsen at M.I.T., receive deepest gratitude for making my graduate education possible in the first place. I admire their patience and understanding.

I thank my parents, Tae Sung Kwon and Hae Hong Kwon, for their unending support and encouragement. It is hard to imagine parents who are more dedicated to their children than they.

Finally, I am most deeply indebted to Laurie Collier whose encouragement and support have sustained me through my graduate years, and whose love, friendship and music have made my life a much more enriching experience.

Table of Contents

Abstract	2
Dedication and Acknowledgements	4
Chapter 1	
Literature Review: Neurotransmitter systems in the lateral geniculate nucleus	8
Chapter 2	
NMDA and non-NMDA receptors mediate visual responses of neurons in the cat's lateral geniculate nucleus	41
Chapter 3	
Effect of stimulus contrast and size on NMDA receptor activity in the cat lateral geniculate nucleus	96
Chapter 4	
Action of acetylcholine on temporal features of visual responses in the cat's lateral geniculate nucleus	158

CHAPTER 1

NEUROTRANSMITTER SYSTEMS IN THE LATERAL GENICULATE NUCLEUS

This chapter has four sections that provide the background for the research in this thesis. In the first section, I review the distribution of excitatory amino acid (EAA) receptors in the brain as determined from receptor-binding and uptake studies. In the second section, I review the physiological evidence for EAA receptors in transmission between retinal ganglion cell axons and postsynaptic cells in the dLGN. In the third section, I review the involvement of two other receptor systems (besides EAA receptors) on dLGN neurons in the modulation of dLGN activity: GABA receptors that mediate inhibitory input from intrinsic interneurons and neurons from the perigeniculate nucleus (PGN), and acetylcholine/norepinephrine receptors that mediate inputs from the brain stem. In the fourth section, I describe general aspects of the microiontophoresis method, which is the major experimental approach used to examine the role of EAA and acetylcholine receptors in the transmission and modulation of retinal activity by dLGN neurons.

Anatomical distribution of excitatory amino acids and their receptors in the central nervous system.

An excitatory amino acid (EAA) is now firmly established as a neurotransmitter in the mammalian central nervous system based on a number of criteria (for review, see Fonnum, 1984). These criteria include Ca^{++}-dependent release upon stimulation, high affinity uptake into nerve terminals, presence of EAAs and appropriate synthetic enzymes in nerve terminals, blockade of synaptic transmission by EAA receptor antagonists, and physiological identification of its action. The anatomical distribution of EAAs in the mammalian central nervous system has been extensively studied (for review, see Cotman et al., 1987). EAA-containing terminals can be identified by high affinity uptake of [^{3}H]D-aspartate (a false transmitter, that is, a transmitter analogue that cannot be metabolized by tissue) into tissue slices, by immunocytochemistry, by electrical stimulation- or K^+-evoked release, by the presence of enzymes that synthesize glutamate, or by anterograde/retrograde axonal transport. Radioligand binding can also reveal receptor distributions.

Early studies of the anatomical distribution of EAA receptors used [^{3}H]L-glutamate, a marker which labels all EAA receptors (Monaghan et al., 1983a; Greenamyre et al., 1984; Ottersen & Storm-Mathisen, 1984a; for review see Fonnum & Malthe-Sorenssen, 1981). Subsequently, subpopulations of EAA receptors have been defined, in part on the basis of their different affinities for a variety of synthetic agonists and antagonists. The EAA receptor subtypes include N-Methyl-D-Aspartate (NMDA), amino-3-hydroxy-5-methyl-4-isoxazolepropionic acid (AMPA), and kainate (KA) receptors. Neuroanatomical distributions of each of these EAA receptor subtypes have also been studied (Monaghan et al., 1983b; Greenamyre et al., 1985; for review see Monaghan & Cotman, 1986) and is briefly described below.

NMDA-sensitive [^{3}H]L-glutamate binding sites are numerous in the rat brain. The highest levels of binding are found in CA1 fields, frontal, anterior cingulate and pyriform cortices, basal ganglia, dorsal lateral septum, amygdala, as well as some sensory areas such as the *dorsal lateral geniculate nucleus (dLGN)*, superficial superior colliculus, dorsal medial geniculate nucleus, medial vestibular nucleus, olfactory bulb, olfactory nuclei, nucleus of the solitary tract and the spinal cord (Monaghan & Cotman, 1985). Complementary sets of studies using the competitive NMDA receptor antagonists [^{3}H]D-APV and [^{3}H]CPP have generally confirmed the distribution (Monaghan et al., 1984b; Olverman et al., 1986). The distribution of [^{3}H]CPP shows relatively lower binding levels within the striatum, septum and cerebellum, and relatively higher levels in thalamus. Noncompetitive antagonists such as [^{3}H]-1-(1-(2-thienyl)-cyclohexyl)piperidine ([^{3}H]TCP) or [^{3}H]MK-801, show distributions that correspons well with those found for NMDA-sensitive glutamate binding sites (Contreras et al., 1986; Maragos et al., 1986; Sircar & Zukin, 1985).

[^{3}H]-AMPA receptor sites are similar to those of NMDA; high levels are found in CA1, outer cortex, anterior olfactory nuclei, olfactory tubercles, nucleus accumbens, caudate/putamen, lateral septum, lateral and basolateral amygdala and cerebellar molecular layer (Monaghan et al., 1984a; Rainbow et al., 1984). Kainate ([^{3}H]KA) binding distributions are different and in general, complementary to those of the NMDA sites (Foster et al., 1981; Monaghan & Cotman, 1982; Unnerstall & Wamsley, 1983). Thus, specific KA sites tend to be in the regions of sparse NMDA sites, such as striatum lucidum, infragranular layers of cortex, hypothalamus and reticular nucleus of thalamus. Interestingly, some ventrally located structures, such as hypothalamus, mammillary bodies and pons, show a preferential binding of KA. This leads to an interesting speculation that NMDA receptors do not seem to be as important for ventrally-located, motor-associated nuclei as for more dorsally-located, sensory-associated systems such as

dLGN, medial vestibular nucleus, nucleus of the solitary tract, and dorsal cochlear nucleus (Cotman et al., 1987).

Uptake autoradiography in rodent brain tissue using [^{3}H]D-aspartate and [^{3}H]L-glutamate yields anatomical distributions that are very similar to those of receptor autoradiography (Fonnum et al.,1981; Ottersen & Storm-Mathisen, 1984b; Taxt & Storm-Mathisen, 1984). The regions of high uptake were the outer cortex, basal forebrain, and the *dLGN*. Using this approach, sensory and motor pathways have been proposed to utilize EAA an as the transmitter (for review, see Fagg & Foster, 1983; Fonnum, 1984; Ottersen & Storm-Mathisen, 1986). All sensory modalities are included, that is, visual, auditory, olfactory and somatosensory systems (Cotman et al., 1987).

It is interesting to note that a substantial portion of glutamate in the dLGN is derived from corticofugal input (for review, see Fonnum,1984). Following unilateral ablation of visual cortex there is a selective reduction in the high affinity uptake of both D-aspartate and L-glutamate in the ipsilateral dLGN (Fonnum, 1984; Fosse et al., 1989). Injection of the false transmitter, [^{3}H]D-aspartate, into the dLGN leads to retrograde labelling of cells in layer VI of the visual cortex (Baughman & Gilbert, 1980). Depolarization of LGN slices with K^+ leads to a Ca^{++}-dependent release of both endogenous glutamate and exogenously added [^{3}H]D-asparate. Furthermore, the release of both of these compounds was reduced after lesioning the corticofugal input (Fonnum, 1984; see also Karlsen & Fonnum, 1978; Fonnum et al., 1981; Young et al., 1981; Bromberg et al., 1981; Fosse et al., 1984; Fosse et al., 1986.)

Interestingly, *in vivo* dialysis sampling in the cat dLGN during local electrical stimulation shows selective increase in the level of glutamate, aspartate, GABA and taurine (Sandberg & Lindström, 1983). However, these authors did not study the effect of stimulation of the optic tract or visual cortex on the level of released glutamate.

In summary, there is much evidence that an EAA is a neurotransmitter localized in

specific parts of the brain, including the dLGN. Because of its ubiquitous presence as a metabolic precursor however, it has been difficult to determine whether glutamate or aspartate (or both) is the endogenous neurotransmitter at any particular synapse. Nevertheless, the selective anatomical distributions of EAAs and thier receptors seem to underscore specific functional roles mediated by the three receptor subtypes.

Physiological evidence for excitatory amino acid receptors in retinogeniculate transmission

N-Methyl-D-Aspartate receptors, one of the EAA receptor subtypes, has been shown to be important in the induction of a long-term potentiation in hippocampus (for review, see Brown et al. 1988) as well as for plasticity and development in the visual pathway (Artola and Singer 1987; Cline et al. 1987; Kleinschmidt et al. 1987; Hahm et al. 1991). However, there is also growing evidence that NMDA receptors as well as non-NMDA receptors (the AMPA or quisqualate type and the kainate type) are also involved in ongoing visual transmission. Excitatory amino acids have been suggested to be the neurotransmitter mediating retinal excitatory input to the dLGN in cats. Microiontophoresis of "first-generation" antagonists such as D-a-aminoadipate (D-a-AA, a weak NMDA receptor antagonist) and 1-hydroxy-3-amino-2-pyrrolidone (HA-966, a non-competitive NMDA receptor antagonist) *in vivo* resulted in a reduction of visual responses of dLGN neurons (Kemp & Sillito, 1982). No differences were observed in the antagonists' effects between on- and off-center or X and Y types of cells. More specific, "second-generation," NMDA receptor antagonists, d-2-amino-5-phosphonovaleric acid (d-APV) and 3-((+/-)-2-carboxypiperazin-4-yl)-propyl-1-phosphonic acid (CPP), also decreased the visual responses of on- and off-center cells as well as X and Y cells in the dLGN (Moody & Sillito, 1988; Sillito et al., 1988; Sillito et al. 1990b). Similarly, 6-cyano-7-nitroquinoxaline-2,3-dione (CNQX), a specific non-NMDA receptor antogonist, reduced the visual responses of dLGN neurons (Sillito et al. 1990a). These results suggest that both NMDA and non-NMDA receptors mediate retinal excitatory input to dLGN neurons. Monosynaptic retinogeniculate excitation has also been studied *in vitro* by intracellular recordings (Crunelli et al., 1985; Crunelli et al., 1987). In the ferret LGN, it has been shown that optic tract-evoked excitatory post-

synaptic potentials (EPSP) are sensitive to both d-APV and CNQX, confirming the results obtained in cats *in vivo* (Esguerra et al., 1989; 1991).

Recently, a novel physiological class of neurons termed "lagged" cells has been described in the dLGN (Mastronarde, 1987a;1987b; 1988; Humphrey & Weller, 1988a; 1988b). Lagged cells differ from "nonlagged" cells in their temporal properties of thier response to a flashing visual stimulus. Their responses show a long visual latency ($\geq$ 55 ms) to stimulus onset, lack of a transient onset discharge, and an "anomalous" offset discharge. Importantly, lagged properties are absent in the retinal ganglion cells that provide input to lagged cells in the dLGN; simultaneous recordings of a retinal ganglion and a dLGN lagged cell postsynaptic to the retinal afferent reveal that the retinal input is nonlagged (Mastronarde, 1987a). Thus the lagged response is an emergent property of the thalamus. Lagged visual responses were originally described in X cells; however, lagged Y cells have since been described as well (Saul & Humphrey, 1990; see also Kwon et al., 1991 and Chapter 2). Iontophoretic application of EAA receptor antagonists on lagged and nonlagged cells show that the two types of neuron are also different pharmacologically. Visual responses of lagged cells are more sensitive to NMDA receptor blockade while those of nonlagged cells are more sensitive to non-NMDA receptor blockade (Heggelund & Hartveit, 1990; Hartveit & Heggelund, 1990; however, see Kwon et al., 1991 and Chapter 2).

Modulation of retinogeniculate transmission in the visual thalamus

The idea that the transmission of retinal signals to cortex can be modulated in the thalamus is not new (Singer 1977; Burke & Cole, 1978; Crick, 1984; Ahlsén et al., 1985). This section discusses three broad neurotransmitter systems that modulate thalamic processing of sensory information (see Fig. 1).

Functional role of NMDA receptors in the dLGN

The evidence for EAA receptors mediating retinogeniculate transmission has been discussed above. This section focuses on the role of NMDA receptors in retinogeniculate transfer. Studies of NMDA receptors in the verterbrate central nervous system have recently been reviewed (Mayer & Westbrook, 1987). The NMDA receptor is not only ligand-gated but also voltage-dependent ; that is, the receptor channel opens when NMDA (or appropriate ligand) binds the receptor, but in the region between -70 to -30mV membrane potential the conductance through the channel is subject to voltage-dependent Mg^{++} block of the channel pore (see Fig. 2). Hence the receptor channel is in the greatest conductance state when the membrane potential is sufficiently depolarized (to about -30mV), while at more hyperpolarized potentials, there is decreasing amount of current flow (due to Mg^{++} block). In other words, the receptor is fully activated only when both a ligand is bound and the postsynaptic membrane is simultaneously depolarized. This requirement of simultaneous, dual conditions for activation has led to specific predictions about the synaptic physiology of NMDA receptors at the retinogeniculate synapse and several are listed below. First, the nonlinear nature of NMDA receptor activation (Fig. 2) suggests that low levels of retinal excitatory drive to LGN cells may engage proportionately a smaller amount of NMDA receptors contributing

to the visual response compared to high levels of retinal excitatory drive. Furthermore, simultaneous inhibitory input to the LGN cell may block full activation of NMDA receptors through the Mg^{++} block and thus decrease the NMDA receptor contribution to LGN cell responses (see Chapter 3). Finally, it has been proposed that simultaneous corticofugal excitatory input to LGN may be able to facilitate NMDA receptor activation at retinogeniculate synapses (Koch, 1987). That is, the activation of corticofugal input (to the distal dendrites, Guillery, 1967; Friedlander et al., 1981; Hamos et al., 1985; Hamos et al., 1987) depolarize more proximal dendrites of a LGN neuron, the sites of retinal inputs (Guillery, 1971; Hamos et al., 1987; Wilson et al., 1984). During activation of corticofugal input, NMDA receptors present at retinogeniculate synapses would be relieved of Mg^{++} block and consequently, there would be a corresponding increase in the retinogeniculate transfer ratio. Indeed this has been recently demonstrated *in vitro* (Esguerra & Sur, 1990; Esguerra, 1991).

Influences of corticofugal input on dLGN cells are both excitatory and inhibitory (Fig. 1). Corticogeniculate axons monosynaptically excite LGN relay cells as well as interneurons (Ahlsén et al., 1982). Anatomically corticogeniculate axon terminals make synaptic contacts with both GABA-containing interneurons as well as non-GABAergic neurons (presumably relay cells since only the interneurons in the LGN are GABAergic) with a ratio of 3:1 (Weber et al., 1989). Cross-correlation analysis between neurons in layer VI of visual cortex and LGN neurons show excitatory corticogeniculate connections when the receptive field centers of the two cells are separated by less than 1.7°, while larger separations produce inhibitory connections (Tsumoto et al., 1978). Functionally, Murphy and Sillito (1987) were able to abolish length-tuning of dLGN neurons when the corticofugal feedback was removed, suggesting the property was conferred by end-inhibited layer VI cells of the visual cortex. Varela and Singer (1987) showed an inhibitory effect on the responses of LGN neurons to a grating stimulus of

one orientation by presenting a grating stimulus of another orientation to the non-dominant eye. This inhibition was abolished upon removal of the visual cortex. While the exact nature of corticofugal influences on the dLGN remains elusive, these data are consistent with the idea that "matching" of cortical and retinal activity can increase the gain of thalamic transmission of retinal signals to cortex.

GABA receptors

One of the most important spatial operations carried out by dLGN is enhancement of the surround inhibition found in retinal receptive fields. This enhanced inhibition is GABAergic (for review see Sherman & Koch,1986). LGN relay cells receive inhibitory inputs from the axons of perigeniculate (PGN) neurons as well as from the axons and dendrites of local interneuron (Fig. 1). Each of these inhibitory processes is organized retinotopically, and is thus spatially localized in its operation (cf. Hamos et al., 1985; Cucchiaro et al. 1985). Dendritic appendages of interneurons provide local feed-forward inhibition, while perigeniculate cells provide both direct (via geniculate axon collaterals) and indirect (through cortex) feed-back inhibition (Dubin & Cleland, 1977; Ide, 1982). GABAergic inhibition in the LGN is mediated by two types of receptors: the $GABA_A$ receptor which produces "shunting" inhibition due to increased Cl^- conductance, and the $GABA_B$ receptor which actively hyperpolarizes through a K^+ channel (Curtis & Johnston, 1974; Dingledine & Langmoen, 1980; Segal & Barker, 1984; Crunelli & Leresche, 1991). Evidence for $GABA_A$ inhibition includes: 1) IPSPs recorded from relay cells are reversed by direct injection of Cl^- ions into the cell (Lindström 1982; cf. McIlwain & Creutzfeldt, 1967). 2) local application of bicuculline, a $GABA_A$ antagonist, leads to a loss of inhibitory mechanisms in dLGN neurons (Sillito & Kemp, 1983; Berardi & Morrone, 1984; Norton et al., 1989). There is also growing evidence

that $GABA_B$ receptors may be involved in conferring LGN inhibition. *In vivo* intracellular recording of relay cells reveal 3 types of IPSPs: short-, medium-, and long-duration. Based on reversal potentials, the short-duration IPSP is thought to be mediated by $GABA_A$ receptors while the medium- and long-duration IPSPs are thought to be mediated by $GABA_B$ receptors (Bloomfield & Sherman, 1988). *In vitro* studies have confirmed the presence of two pharmacologically distinct IPSPs in LGN neurons, a short-lasting IPSP mediated by $GABA_A$ receptors and a delayed, long-lasting IPSP mediated by $GABA_B$ receptors (for review, see Crunelli & Leresche, 1991). Both types of IPSPs are seen in LGN slice preparations that do not contain the PGN, thus suggesting that feedforward inhibition mediated by the intrinsic interneurons can be mediated by both types of GABA receptors.

Acetylcholine and Norepinephrine receptors

Ascending brain stem inputs capable of modulating neuronal responses in the LGN have been extensively studied (for review, see Singer, 1977; Burke & Cole, 1978). The ascensing brain stem input (Fig. 1) involves cholinergic and noradrenergic neurotransmitter systems (for review, see Sherman & Koch, 1986; McCormick 1989). In the cat, the dLGN is densely innervated by cholinergic fibers arising from the pedunculopontine tegmental nucleus and the parabigeminal nucleus (De Lima et al., 1985; De Lima & Singer, 1987) while the nucleus reticulares (nRt) receives cholinergic input from both brainstem and basal forebrain nuclei (Steriade & Llinás, 1988). Noradrenergic fibers from the locus coeruleus innervate both the dLGN and nucleus reticulares (De Lima & Singer, 1987). Acetylcholine (ACh) has both excitatory and inhibitory effects in the dLGN (cf. McCormick, 1989). It excites the relay neurons (both X and Y) by a nicotinic receptor-mediated increase in cation conductance followed by a muscarinic receptor-mediated decrease in potassium conductance; however, it inhibits the local circuit

neurons by a muscarinic M_2 receptor-mediated increase in K^+ conductance. Norepinephrine (NE) excites the relay neurons as well as neurons in the reticular thalamic nucleus by an α_2 adrenoceptor-coupled decrease in K^+ conductance.

Thalamic neurons show two states of intrinsic firing patterns depending upon their membrane potential: a "burst" mode at hyperpolarized potentials (less than -65 mV) and a "relay" mode at more depolarized potentials (McCormick, 1989). The burst and relay modes are well correlated with synchronized electroencephalogram (EEG) activity (i.e., slow wave sleep, drowsiness and inattentiveness) and desynchronized EEG activity (i.e., arousal, alertness and rapid eye movement (REM) sleep) respectively (Steriade & Deschênes, 1984; Steriade & Llinás, 1988; Hobson & Steriade, 1986). The ascending modulatory neurotransmitter systems may play a role in the shift from a period of drowsiness to a state of waking attentiveness by switching thalamic cells from burst to relay mode, thereby allowing thalamic cells to respond linearly to afferent inputs (McCormick & Prince, 1987; McCormick & Prince, 1988; McCormick, 1989).

It has recently been reported that stimulation of the parabrachial region of the brain stem can switch lagged visual reponses in the LGN to nonlagged-type responses (Uhlrich et al., 1990). The result suggests that the two physiological types of visual response are two cell types defined physiologically correspond to different response modes of the same LGN neuron. More generally, it implies that the parabrachial innervation can alter temporal patterns of LGN response in a specific manner. The most likely neurotransmitter mediating the parabrachial effects is ACh, which suggests that cholinergic input may have a powerful influence on temporal properties of LGN neurons (see Chapter 4).

Methods for microiontophoresis and general considerations

Multibarrel electrodes for *in vivo* microiontophoresis are made using conventional glass micropipettes (1mm, outside dimeter). An appropriate number of micropipette blanks (typically 6 in our experiments) are held together in a staggered fashion and fastened at their ends using heat-shrink tubing and fast-setting adhesive (e.g. Krazy Glue). The bottom of this assembly is then tightly clamped in the lower chuck of a vertical electrode puller (David Kopf Instruments). A 5-turn heating coil is used to gently melt the glass in the central portion of the assembly and the top portion is slowly rotated 360 ° by hand and pulled gently (0.5cm). The multibarrel assembly is then reclampted and allowed to cool and then pulled in a conventional way. Multibarrel electrodes pulled this way generally have a shank length of 1 - 1.3 cm with a fine tip diameter ($\leq 1\mu m$).

"Bumping" the tip of the electrode assembly is performed under a microscope against a rough surface (e.g. glass slide lined with very fine sand paper) using a micromanipulator. This usually produces an evenly broken tip, although several repetitions may be necessary to achieve the final tip size. We try to obtain final tip sizes (for the whole assembly) of 15 - 25 μm (outside diameter).

Each of the barrels is filled with a freshly mixed drug solution using a hypodermic syringe and needle; capillary pressure fills the solution to the tip. Recording through the central barrel is satisfactory for larger cells (that display extracellular spike amplitude of $\geq 100\ \mu V$) but may be difficult for smaller cells (with extracellular spike amplitude in the range of tens of microvolts, Stone, 1985). We circumvent this problem by combining a thick-wall micropipette with several thin-walled ones for the assembly. The thick-wall pipette when filled with 3M KCl is used for extracellular recording (with typical impedence of 5 - 10 MΩ) while the thin-wall micropipettes are used as ejection

barrels. Using this method (and depending on final tip size), we routinely obtain recording electrodes that are capable of recording most of the cell types in the cat dLGN regardless of size, i.e. X and Y as well as lagged and nonlagged types.

Some of the problems associated with recording with a multibarrel micropipette assembly as described above include risk of cell damage, effect of drug leakage and ejection current artifacts. The effects of drug leakage as well as ejection current artifacts can be minimized. Spontaneous efflux (leakage) of drug solutions lie in the range 1 fmol/sec to 1 pmol/sec for solutions in the 0.1 to 1 M concentration range, due to diffusion and hydrostatic pressure (Stone, 1985). The spontaneous efflux is prevented by applying a small retaining current (5 - 20 nA). In addition, we routinely plug the top end of ejection barrels so as to decrease the hydrostatic pressure that contributes to the leakage. Lowering the drug concentration and reducing the tip diameter can further reduce the leakage. Occasionally, if a microintophoretic electrode is located very close to a neuronal membrane, the passage of current from a barrel to ground may be enough to change the excitability of the recorded cell. We minimize such ejection current artifacts by employing a balance barrel containing NaCl (150 mM) and actively applying an opposite polarity current equal in magnitude to the algebraic sum of all currents being passed through the drug-containing barrels.

Tissue concentrations of ejected compounds can be estimated assuming a diffusional model (Carslaw and Jaeger, 1959; Stone, 1985). Using such model, Krnjevic and Phillis (1963) estimated that when neurones lay several tens of microns from the pipette tip, the concentration of glutamate effective in causing an excitatory effect was about 0.1mM. For APV (an NMDA receptor antagonist), it has been estimated that 10nA ejection current results in tip concentration of about 0.05 mM (Armstrong-James et al., 1981); effective concentration at a distance of 100 - 200 μm from the ejection barrel has been estimated to be about 6 μM (Fox et al., 1989).

The most effective way to establish specificity of an applied "dose" of antagonist is to adjust agonist "doses" to achieve a clear excitatory response, and titrate antagonist "doses" to ablolish (only) the appropriate agonist response (see Chapter 2 for documentation and details).

REFERENCES

Ahlsén, G., Lindström, S.and Lo, F-S. (1982). Functional distinction of perigeniculate and thalamic reticular neurons in the cat. Exp Brain Res. 46: 118-126.

Ahlsen, G., Lindström, S., and Lo, F-S. (1985). Interaction between inhibitory pathways to principal cells in the lateral geniculate nucleus of the cat. Exp. Brain Res. 58: 134-143.

Armstrong-James, M., Fox, K., Kruk, Z.L., and Millar, J. (1981). Quantitative iontophoresis of catecholamines using multibarrel carbon fibre microelectrodes. J. Neurosci. Methods, 4, 385-406.

Artola, A. and Singer, W. (1987). Long-term potentiation and NMDA receptors in rat visual cortex. *Nature* 330: 649-652.

Baughman, R.W. and Gilbert, C.D. (1980). Aspartate and glutamate as possible neurotransmitters of cells in layer 6 of the visual cortex. Nature, Lond. 287: 848-850.

Berardi, N. and Morrone, M.C. (1984). The role of g-aminobutyric acid mediated inhibition in the response properties of cat lateral geniculate nucleus neurones. J. Physiol (Lond) 357: 505-524.

Bloomfield, S.A. and Sherman, S.M. (1988). Postsynaptic potentials recorded in neurons of the cat's lateral geniculate nucleus following electrical stimulation of the optic chiasm. J. Neurophysiol. 60: 1924-1945.

Bromberg, M.B., Penney, J.B., Stephenson, B.S. and Young A.B. (1981). Evidence for glutamate as the neurotransmitter of corticothalamic and corticorubral pathways. Brain Res. 215: 369-374.

Brown, T.H., Chapman, P.F., Kairiss, E.W. and Keenam, C.L. (1988). Long-term synaptic potentiation. Science. 242:724-728.

Burke, W. and Cole, A.M. (1978). Extraretinal influences on the lateral geniculate nucleus. Rev. Physiol. Biochem. Pharmacol. 80: 105-166.

Carlslaw, H.S., and Jaeger, J.C. (1959). Conduction of Heat in Solids. Oxford University Press, London.

Cline, H. T., Debski, E. A., and Constantine-Paton, M. N-methyl-D-aspartate receptor antagonist desegregates eye-specific stripes. (1987). *Proc. Natl. Acad. Sci.USA* 84: 4342-4345.

Contreras, P.C., Quirion, R., and O'Donohue, T.L. (1986). Neurosci. Lett. 67:101-106.

Cotman, C.W., Monaghan, D.T., Ottersen O.P. and Storm-Mathisen, J. (1987). Anatomical organization of excitatory amino acid receptors and their pathways. Trends Neurosci. 10: No.7, 273-280.

Crick, F. (1984). The function of the thalamic reticular complex: the searchlight

hypothesis. Proc. Natl. Acad. Sci. USA 81: 4586-4590.

Crunelli, V., Kelly, J.S., Leresche, N. and Peirchio, M. (1987). On the excitatory postsynaptic potential evoked by stimulation of the optic tract in the rat lateral geniculate nucleus. J. Physiol. 384: 603-618.

Crunelli, V. and Leresche, N. (1991). A role for $GABA_B$ receptors in excitation and inhibition of thalamocortical cells. TINS 14: 16-21.

Crunelli, V., Leresche, N. and Pirchio, M. (1985). Non-NMDA receptors mediate the optic nerve input to the rat LGN in vitro. J. Physiol. 365: 40P.

Cucchiaro, J., Uhlrich, D.J., Hamos, J.E. and Sherman, S.M. (1985). Perigeniculate input to the cat's lateral geniculate nucleus: a light- and electron microscopic study of single, HRP-filled cells. Society for Neurosci. Abstr. 11:231.

Curtis, D.R. and Johnston, G.A.R. (1974). Amino acid transmitters in the mammalian central nervous system. Ergebn. Physiol. Biol. Chem. Exp. Pharmakol. 69: 97-188.

De Lima, A.D., Montero, V.M. and Singer, W. (1985). The cholinergic innervation of the visual thalamus: an EM immunocytochemical study. Exp. Brain Res. 59: 206-212.

De Lima, A.D. and Singer, W. (1987). J. Comp. Neurol. 259: 92-121.

Dingledine, R. and Langmoen, I.A. (1980). Conductance changes and inhibitory actions of hippocampal recurrent IPSPs. Brain Res. 185: 277-287.

Dubin, M.W. and Cleland, B.G. (1977). Organization of visual inputs to interneurons of lateral geniculate nucleus of the cat. J. Neurophysiol. 40: 410-427.

Esguerra, M. (1991). Synaptic transmission in the ferret lateral geniculate nucleus *in vitro*: modulation by membrane voltage and neurotransmitters. Doctoral Dissertation, Dept. of Brain and Cognitive Sciences, M.I.T.

Esguerra, M., Kwon, Y.H. and Sur, M. (1989). NMDA and non-NMDA receptors mediate retinogeniculate transmission in cat and ferret LGN *in vitro*. Society for Neurosci. Abstr. 75.7.

Esguerra, M., Kwon, Y.H. and Sur, M. (1991). Retinogeniculate EPSPs recorded intracellularly in the ferret lateral geniculate nucleus in vitro: role of NMDA receptors. submitted.

Esguerra, M. and Sur, M. Corticogeniculate feedback gates retinogeniculate transmission by activating NMDA receptors. (1990). *Soc. Neurosci. Abstr.* 16: 159.

Fagg, G.E. and Foster, A.C. (1983). Amino acid neurotransmitters and their pathways in the mammalian central nervous system. Neuroscience 9:701-719.

Fonnum, F. (1984). Glutamate: a neurotransmitter in mammalian brain. J. Neurochem. 42:1-11.

Fonnum, F., Fosse, V.M. and Allen, C.N. (1984). Identification of excitatory amino acid pathways in the mammalian nervous system. In *Excitotoxins*, K. Fuxe, P.J.

Roberts, and R. Schwarcz, eds., pp. 3-18, Plenum, New York.

Fonnum, F. and Malthe-Sorenssen, D. (1981). Identification of glutamatergic neurons. In *Glutamate. Transmitter in the Central Nervous System*, P.J. Roberts, J. Storm-Mathisen, and G.A.R. Johnston, eds., pp. 205-221, Wiley, New York.

Fonnum, F., Søreide, A., Kvale, I., Walker, J. and Walaas, I. (1981) in *Glutamate as a Neurotransmitter* (DiChiara, G. and Gessa, G.L., eds.), pp.29-41, Raven Press.

Fosse, V.M., Heggelund, P. and Fonnum, F. (1989). Postnatal development of glutamatergic, GABAergic, and cholinergic neurotransmitter phenotypes in the visual cortex, lateral geniculate nucleus, pulvinar, and superior colliculus in cats. J. of Neurosci. 9(2): 426-435.

Fosse, V.M., Heggelund, P., Iversen, E. and Fonnum, F (1984). Effects of Area 17 ablation on neurotransmitter parameters in efferents to Area 18, the lateral geniculate body, pulvinar and superior colliculus in the cat. Neurosci. Lett. 52: 323-328.

Fosse, V.M., Kolstad, J. and Fonnum, F. (1986). A bioluminescence method for the measurement of L-glutamate: Applications to the study of changes in the release of L-glutamate from lateral geniculate nucleus and superior colliculus after visual cortex ablation in rats. J. Neurochem. 47: 340-349.

Foster, A.C., Mena, E.E., Monaghan, D.T. and Cotman, C.W. (1981). Synaptic localisation of kainic acid binding sites. Nature 289, 73-75.

Fox, K., Sato, H., and Daw, N. (1989). The location and function of NMDA receptors in cat and kitten visual cortex, J. of Neurosci., 9(7), 2443-2454.

Friedlander, M.J., Lin, C.S., Stanford, L.R. and Sherman, S.M. (1981). Morphology of functionally identified neurons in the lateral geniculate nucleus of the cat. *J. Neurophysiol.* 46: 80-129.

Greenamyre, J.T., Olson, J.M.M., Penney, J.B. and Young, A.B. (1985). Autoradiographic characterization of N-methyl-D-aspartate-, quisqualate- and kainate-sensitive glutamate binding sites. J. Pharmacol. exp. Ther. 233: 254-263.

Greenamayre, J.T., Young, A.B. and Penney, J.B. (1984) Quantitative autoradiographic distribution of L-[^{3}H]glutamate-binding sites in rat central nervous system. J. Neurosci. 4:2133-2144.

Guillery, R.W. (1967).Patterns of fiber degeneration in the dorsal lateral geniculate nucleus of the cat following lesions in the visual cortex. J. Comp. Neuro. 130: 197:222.

Guillery, R.W. (1971). Patterns of synaptic interconnections in the dorsal lateral geniculate nucleus of the cat and monkey: a brief review. Vision Res. Suppl. 3: 211-227.

Hahm, J., Langdon, R.B. and Sur, M. (1991). Disruption of retinogeniculate afferent segregation by antagonists to NMDA receptors. Naure (Lond.) in press.

Hamos, J.E., Van Horn, S.C., Raczkowski, D. and Sherman, S.M. (1987). Synaptic circuits involving an individual retinogeniculate axon in the cat. J. Comp. Neurol. 259:

165-192.

Hamos, J.E., Van Horn, S.C., Raczkowski, D., Uhlrich, D.J., Sherman, S.M. (1985). Synaptic connectivity of a local circuit neuron in the cat's lateral geniculate nucleus. Nature 317, 618-621.

Hartveit, E. and Heggelund, P. (1990). Neurotransmitter receptors mediating excitatory input to cells in the cat lateral geniculate nucleus. II. Nonlagged cells. *J. Neurophys.* 63: 1361-1372.

Heggelund, P. and Hartveit, E. Neurotransmitter receptors mediating excitatory input to cells in the cat lateral geniculate nucleus. I. Lagged cells. *J. Neurophys.* 63: 1347-1360, 1990.

Hobson, J.A. and Steriade, M. (1986). Neuronal basis of behavioral state control. In: Handbook of Physiology. The Nervous System. Intrinsic Regulatory Systems of the Brain. pp. 401-823, Williams & Wilkins and the American Physiological Society.

Humphrey, A.L. and Weller, R.E. (1988a). Functionally distinct groups of X-cells in the lateral geniculate nucleus of the cat. J. Comp. Neurol. 268, 429-447.

Humphrey, A.L. and Weller, R.E. (1988b). Structural correlates of functionally distinct X-cells in the lateral geniculate nucleus of the cat. J. Comp. Neurol. 268, 448-468.

Ide, L.S. (1982). The fine structure of the perigeniculate nucleus in the cat. J. Comp. Neurol. 210: 317-334.

Karlsen, R.Lœ. and Fonnum, F. (1978). Evidence for glutamate as a neurotransmitter in the corticofugal fibers to the dorsal lateral geniculate body and the superior colliculus in rats. Brain Res. 151:457-467.

Kemp, J.A. and Sillito, A.M. (1982). The nature of the excitatory transmitter mediating X and Y cell inputs to the cat dorsal lateral geniculate nucleus. J. Physiol. 323, 377-391.

Kleinschmidt, A., Bear, M. F., and Singer, W. (1987). Blockade of "NMDA" receptors disrupts experience-dependent plasticity of kitten striate cortex. *Science* 238: 355-358.

Koch, C. (1987). The action of the corticofugal pathway on sensory thalamic nuclei: a hypothesis. Neurosci. 23, 399-406.

Krnjevic,K., and Phillis, J.W. (1963). Iontophoretic studies of neurones in the mammalian cerebral cortex, J. Physiol., 165, 274-304.

Kwon, Y.H., Esguerra, M. and Sur, M. (1991). NMDA and non-NMDA receptors mediate visual responses of neurons in the cat's lateral geniculate nucleus. J. Neurophysiol. in press.

Lindström, S. (1982). Synaptic organization of inhibitory pathways to principal cells in the lateral geniculate nucleus of the cat. Brain Res. 234: 447-453.

Maragos, W.F., Chu, D.C.M., Greenamyre, J.T., Penney, J.B. and Young, A.B. (1986) Eur. J. Pharmacol. 123:173-177.

Mastronarde, D.N. (1987a). Two classes of single-input X-cells in cat lateral geniculate nucleus. I. Receptive-field properties and classification of cells. J. Neurophysiol. 57, 357-380.

Mastronarde, D.N. (1987b). Two classes of single-input X-cells in cat lateral geniculate nucleus. II. Retinal inputs and the generation of receptive-field properties. J. Neurophysiol. 57, 381-413.

Mastronarde, D.N. (1988). Branching of X and Y functional pathways in cat lateral geniculate nucleus. *Soc. Neurosci. Abstr.* 14: 309.

Mayer, M.L. and Westbrook, G.L. (1987). The physiology of excitatory amino acids in the vertebrate central nervous system. Progress in Neurobiol. 28, 197-276.

McCormick, D.A. (1989). Cholinergic and noradrenergic modulation of thalamocortical processing. TINS 12: 215-221.

McCormick, D.A. and Prince, D.A. (1987). Actions of acetylcholine in the guinea-pig and cat medial and lateral geniculate nuclei. J. Physiol. (London) 392: 147-165.

McCormick, D.A. and Prince, D.A. (1988). Noradrenergic modulation of firing pattern in guinea pig and cat thalamic neurons, In Vitro. J. Neurophysiol. 59: 978-996.

McIlwain, J.T. and Creutzfeldt, O.D. (1967). Microelectrode study of synaptic excitation and inhibition in the lateral geniculate nucleus of the cat. J. Neurophysiol. 30: 1-21.

Monaghan, D.T. and Cotman, C.W. (1982). The distribution of [^{3}H] kainic acid binding sites in rat CNS as determined by autoradiography. Brain Res. 252: 91-100.

Monaghan, D.T. and Cotman, C.W. (1985). Distribution of N-methyl-D-aspartate-sensitive L-[^{3}H]Glutamate-binding sites in rat brain. J. Neurosci. 5:2909-2919.

Monaghan, D.T., and Cotman, C.W. (1986). Anatomical organization of NMDA, kainate and quisqualate receptors. In: *Excitatory Amino Acids*, Ed. P.J. Roberts. MacMillan Press.

Monaghan, D.T., Holets, V.R., Toy, D.W. and Cotman, C.W. (1983a). Anatomical distributions of four pharmacologically distinct [^{3}H]-L-glutamate binding sites. Nature 306: 176-179.

Monaghan, D.T., Yao, D. and Cotman, C.W. (1983b). L-[^{3}H]glutamate binds to kainate, NMDA-, and AMPA-sensitive binding sites: an autoradiographic analysis. Brain Res. 340: 378-383.

Monaghan, D.T., Yao, D. and Cotman, C.W. (1984a) Brain Res. 324:160-164.

Monaghan, D.T., Yao, D.T., Olverman, H.J., Watkins, J.C. and Cotman, C.W. (1984b). Autoradiography of D-2-[^{3}H]-amino-5-phosphonopentanoate binding sites in rat brain. Neurosci. Lett. 52: 253-258.

Moody, C.I. and Sillito, A.M. (1988). The role of the N-methyl-D-aspartate (NMDA)

receptor in the transmission of visual information in the feline dorsal lateral geniculate nucleus (dLGN). J. Physiol. 396: 62P.

Norton, T.T., Hodefer, R.N. and Godwin, D.W. (1989). Effects of bicuculline on receptive field center sensitivity of relay cells in the lateral geniculate nucleus. Brain Research. 488: 348-352.

Murphy, P.C. and Sillito, A.M. (1987). Corticofugal feedback influences the generation of length tuning in the visual pathway. Nature 329: 727-729.

Olverman, H.J., Monaghan, D.T., Cotman, C.W. and Watkins, J.C. (1986) Eur. J. Pharmacol. 131: 161-162.

Ottersen, O.P. and Storm-Mathisen, J. (1984a) Glutamate- and GABA-containing neurons in the mouse and rat brain, as demonstrated with a new immunocytochemical technique. J. Comp. Neurol. 229: 374-392.

Ottersen, O.P. and Storm-Mathisen, J. (1984b) in *Handbook of Chemical Neuroanatomy* (Vol. 3) (Björklund, A., Hökfelt, T. and Kuhar, M.J., eds.), pp. 141-246, Elsevier.

Ottersen, O.P. and Storm-Mathisen, J. (1986) in *Excitatory Amino Acids and Epilepsy* (Ben-Ari, Y. and Schwarcz, R., eds), pp. 263-284, Plenum press.

Rainbow, T.C., Wieczorek, C.M. and Halpain, S. (1984) Brain Res. 309:173-177.

Sangerg, M. and Lindström, S. (1983). Amino acids in the dorsal lateral geniculate nucleus of the cat: collection in vivo. J. Neurosci. Meth. 9: 65-74.

Saul, A and Humphrey, A.L. (1990). Spatial and temporal response properties of lagged and non-lagged cells in the cat lateral geniculate nucleus. *J. Neurophys.* 64: 206-224.

Segal, M. and Barker, J.L. (1984). Rat hippocampal neurons in culture: properties of GABA-activated Cl^- ion conductance. J. Neurophysiol. 51: 500-515.

Sherman, S.M. and Koch, C. (1986). The control of retinogeniculate transmission in the mammalian lateral geniculate nucleus. Exp. Brain Res. 63, 1-20.

Sillito, A.M. and Kemp, J.A. (1983). The influence of GABAergic inhibitory processes on the receptive field structure of X and Y cells in the cat dorsal lateral geniculate nucleus (dLGN). Brain Res. 277: 63-77.

Sillito, A.M., Murphy, P.C. and Moody, I. (1988). The role of N-methyl-D-aspartate and quisqualate receptors in mediating the retinal input to the lateral geniculate nucleus. in *Frontiers in Excitatory Amino Acid Research*, 429-434, Alan R. Liss, Inc.

Sillito, A.M., Murphy, P.C. and Salt, T.E. (1990a). The contribution of the non-N-Methyl-D-Aspartate group of excitatory amino acid receptors to retinogeniculate transmission in the cat. *Neuroscience* 34: 273-280.

Sillito, A.M., Murphy, P.C., Salt, T.E. and Moody, C.I. (1990b). Dependence of retinogeniculate transmission in cat on NMDA receptors. *J. Neurophys.* 63: 347-355.

Singer, W. (1977). Control of thalamic transmission by corticofugal and ascending reticular pathways in the visual system. Physiol. Rev. 57: 386-420.

Sircar, R. and Zukin, S. (1985) Brain Res. 344:142-145.

Steriade, M. and Deschênes, M. (1984). The thalamus as a neuronal oscillator. Brain Res. Rev. 8: 1-63.

Steriade, M. and Llinás, R.R. (1988). The functional states of the thalamus and the associated neuronal interplay. Physiol. Rev. 68: 649-742.

Stone, T.W. (1985). *Microiontophoresis and Pressure Ejection*, John Wiley and Sons.

Taxt, T. and Storm-Mathisen, J. (1984) Neuroscience 11: 79-100.

Tsumoto, T., Creutzfeldt, O.D. and Legéndy, C.R. (1978). Functional organization of the corticofugal system from visual cortex to lateral geniculate nucleus in the cat. Exp. Brain Res. 32: 345-364.

Uhlrich, D.J., Tamamaki, N. and Sherman, S.M. (1990). Brainstem control of response modes in neurons of the cat's lateral geniculate nucleus. *Proc. Natl. Acad. Sci. USA* 87: 2560-2563.

Unnerstall, J.R. and Wamsley, J.K. (1983) Eur. J. Pharmacol. 86:361-371.

Varela, F.J. and Singer, W. (1987). Neuronal dynamics in the visual corticothalamic pathway revealed through binocular rivalry. Exp. Brain Res. 66: 10-20.

Weber, A.J., Kalil, R.E. and Behan, M. (1989). Synaptic connections between corticogeniculate axons and interneurons in the dorsal lateral geniculate nucleus of the cat. J. Comp. Neurol. 289, 156-164.

Wilson, J.R., Friedlander, M.J. and Sherman, S.M. (1984). Ultrastructural morphology of identified X- and Y-cells in the cat's lateral geniculate nucleus. Proc. R. Soc. B. 221:411-436.

Young, A.B., Bromberg, M. B. and Penney, J. B. (1981). Decreased glutamate uptake in subcortical areas deafferented by sensorimotor cortex ablation in the cat. J. Neurosci. 1: 241-249.

FIGURE LEGEND

Fig.1. Schematic diagram illustrating the functional relationship between the various inputs to geniculate relay cells. Excitatory and inhibitory terminals are shown by open and closed triangles respectively. Brain stem includes midbrain and pontine components of reticular formation; PGN, perigeniculate nucleus (a part of the nucleus reticularis); EAA, excitatory amino acid; Ach, acetylcholine. Both retinogeniculate and corticogeniculate feedback projections to LGN relay cells are excitatory and mediated by EAAs. GABAergic inhibition is provided by local intrinsic LGN interneurons as well as by neurons originating in the PGN. Finally, one of the most prominent brain stem inputs, the cholinergic innervation, is excitatory to LGN relay neurons while inhibitory to LGN intrinsic interneurons and PGN neurons (modified from Sherman & Koch, 1986).

Fig. 2. The set of current-voltage plots show results obtained for quisqualic acid and NMDA recorded over a wide range of membrane voltage potentials from spinal cord neurons under two electrode voltage clamp. Note the similar reversal potential for both quisqualic acid and NMDA, close to 0 mV, and the negative slope conductance for NMDA, but not quisqualic acid, over the membrane potential range -30 to -70 mV (from Mayer & Westbrook, 1987).

Fig. 1

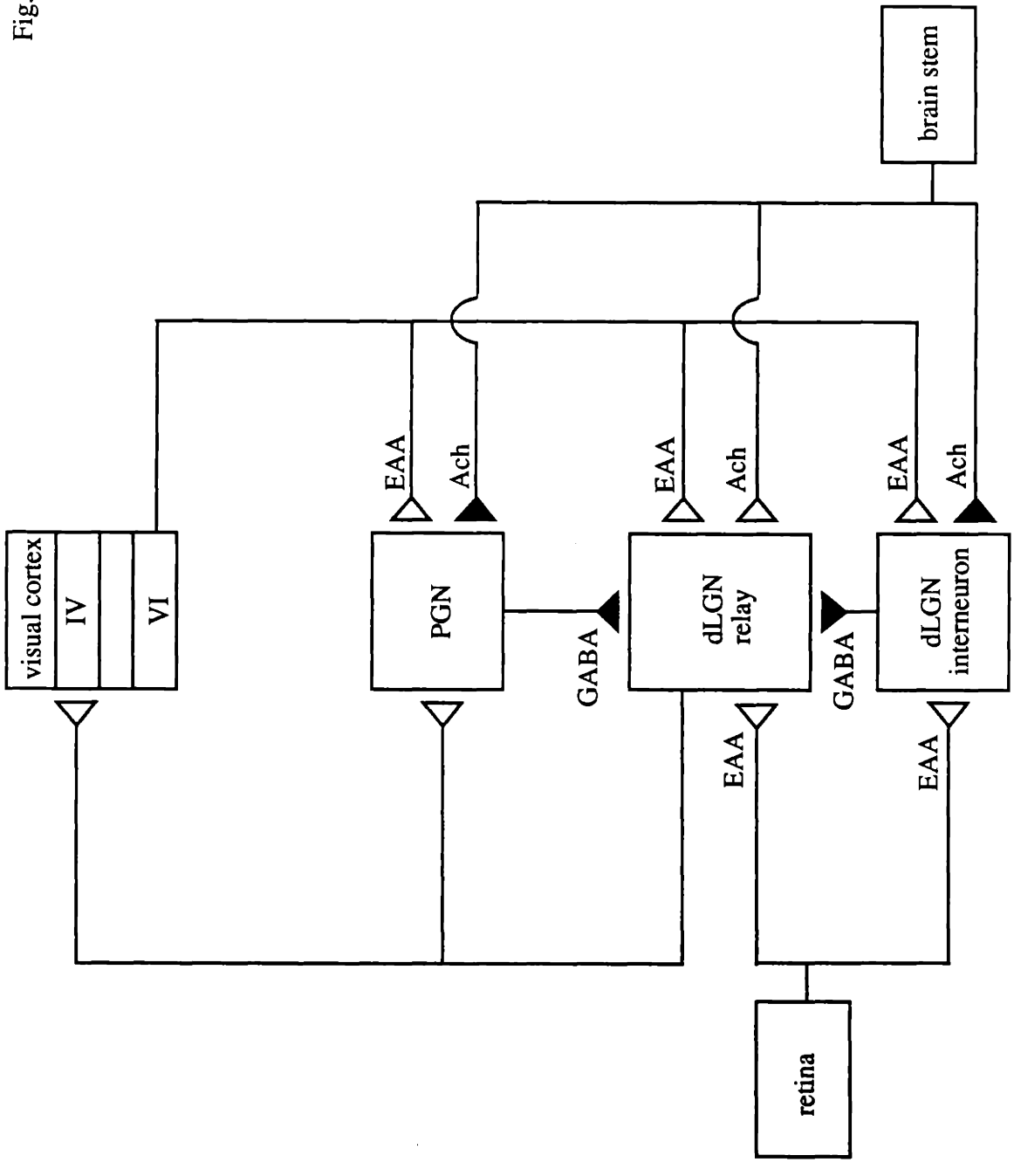
brain stem
visual cortex
IV
VI
EAA
Ach
PGN
GABA
dLGN relay
EAA
Ach
GABA
dLGN interneuron
EAA
Ach
EAA
EAA
retina

Fig. 2

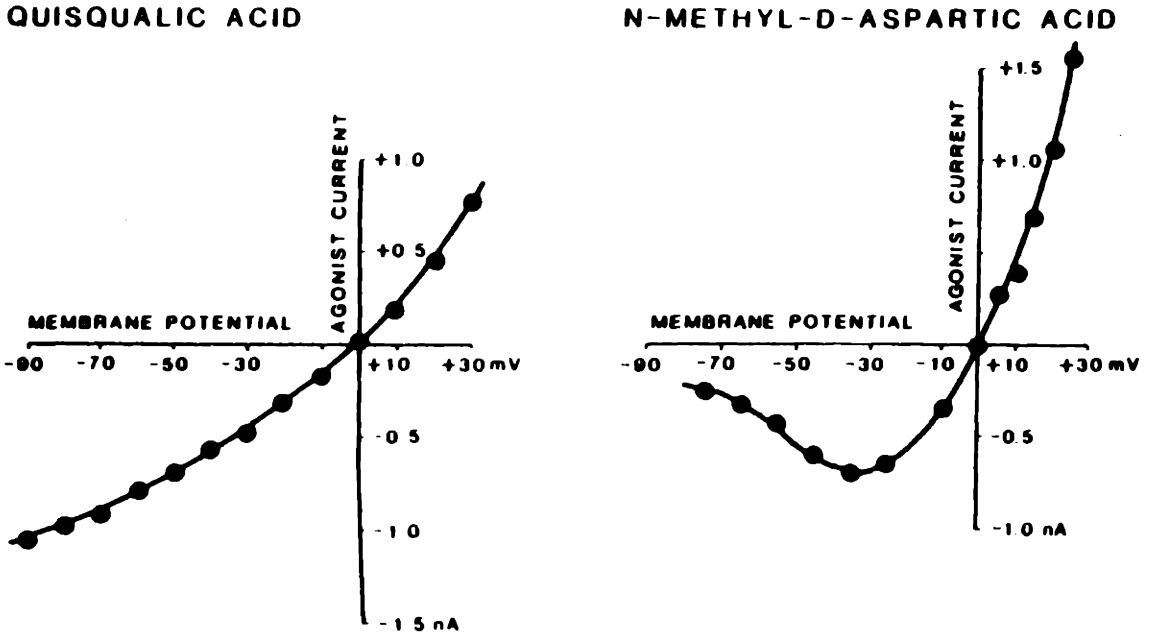
QUISQUALIC ACID
AGONIST CURRENT
+1.0
+0.5
MEMBRANE POTENTIAL
-90
-70
-50
-30
+10
+30 mV
-0.5
-1.0
-1.5 nA
N-METHYL-D-ASPARTIC ACID
AGONIST CURRENT
+1.5
+1.0
MEMBRANE POTENTIAL
-90
-70
-50
-30
-10
+10
+30 mV
-0.5
-1.0 nA

CHAPTER 2

NMDA AND NON-NMDA RECEPTORS MEDIATE VISUAL RESPONSES OF NEURONS IN THE CAT'S LATERAL GENICULATE NUCLEUS

SUMMARY AND CONCLUSIONS

1. We have examined the effects of iontophoresing specific antagonists to excitatory amino acid receptors on the visual responses of cells in lamina A or A1 of the cat's lateral geniculate nucleus (LGN).

2. Cells were classified as On- or Off-center, X or Y, and lagged or nonlagged. The effects of antagonists were studied while cells were stimulated with spots of the appropriate contrast covering the receptive field center.

3. The NMDA receptor antagonists d-2-amino-5-phosphonovaleric acid (d-APV) and 3-((+/-)-2-carboxypiperazin-4-yl)-propyl-1-phosphonic acid (CPP), when iontophoresed at doses that specifically antagonized NMDA-induced responses but not Kainate-induced responses, reduced the responses of all cell types in the LGN, including X and Y cells, lagged and nonlagged cells, and On- and Off-center cells.

4. The non-NMDA receptor antagonist 6-cyano-7-nitroquinoxaline-2,3-dione (CNQX), when applied at doses that specifically antagonized Kainate-induced responses but not NMDA-induced responses, also reduced the visual responses of each of the cell types in the LGN.

5. We analyzed quantitatively the effects of d-APV and CNQX on LGN cells. D-APV reduced the responses of lagged cells to a greater extent than the responses of nonlagged cells. CNQX reduced the responses of lagged and nonlagged cells to a similar extent. There was no difference in the effect of d-APV or of CNQX on X and Y cells, or On- and Off-center cells.

6. We analyzed the effects of the antagonists on separate components of responses, including an early component comprising the first 100 ms of response and a late

component comprising the next 300 ms of response. D-APV reduced the late component of lagged cell responses to a greater extent than either the early component of the same cells, or the early or late component of nonlagged cells. CNQX had nearly equivalent effects on both response components of all cell types. 7. These data indicate that NMDA and non-NMDA receptors make similar contributions to the responses of On- and Off-center and X and Y cells in the LGN. Lagged and nonlagged cells are not differentiated with respect to the contribution of non-NMDA receptors to their visual responses. The greater contribution of NMDA receptors to the responses of lagged cells is consistent with the large contribution made by these receptors to the late response components of lagged cells. It is possible, then, that the degree of participation of NMDA receptors in the visual responses of LGN cells is a function of the response characteristics of cells rather than a fundamental distinguishing feature of LGN cell types.

INTRODUCTION

Excitatory amino acid (EAA) receptors are involved in synaptic transmission in many areas of the vertebrate central nervous system (Cotman et al. 1987; Mayer and Westbrook 1987). EAA receptors can be broadly categorized into two groups, the N-Methyl-D-Aspartate (NMDA) and non-NMDA receptor types (which include the kainate [KA] and quisqualate subtypes), based on their specific agonists and antagonists as well as the ionic composition of their receptor-associated conductances. To date, the most potent and specific NMDA receptor antagonists include d-2-amino-5-phosphonovaleric acid (d-APV) and 3-((+/-)-2-carboxypiperazin -4-yl)-propyl-1-phosphonic acid (CPP) while those for non-NMDA receptors include 6-cyano-7-nitroquinoxaline-2,3-dione (CNQX) and 6,7-dinitro-quinoxaline-2,3-dione (DNQX) (Watkins and Olverman 1987; Honore et al. 1988).

In the cat's lateral geniculate nucleus (LGN), visual responses have been shown to be sensitive to the blockade of excitatory amino acid receptors (Kemp and Sillito 1982). More recent studies have shown that iontophoretic applications of the NMDA receptor antagonists d-APV and CPP, as well as the non-NMDA receptor antagonist CNQX, attenuate the visual responses of both X and Y cells in the LGN (Sillito et al. 1990a,b). Optic tract evoked postsynaptic responses in slices of the LGN maintained in vitro are attenuated by NMDA (Esguerra et al. 1989; Scharfman et al. 1990) and non-NMDA (Crunelli et al. 1987) receptor antagonists. These results together support the notion that an EAA is the optic nerve transmitter in the LGN, and that both NMDA and non-NMDA receptor types are

involved in retinogeniculate transmission.

It is now thought that the two main parallel pathways, comprised of X and Y cells, that arise in the cat's retina are further divided in the LGN into two physiologically distinct groups. These cell types have been termed lagged and non-lagged cells based on temporal properties of their visual responses (Mastronarde 1987a,b; Mastronarde 1988; Humphrey and Weller 1988a; Saul and Humphrey 1990). Lagged and nonlagged cells may correspond to different response modes of the same neuron (Uhlrich et al. 1990), though one study indicates that lagged and non-lagged X cells have different dendritic morphology (Humphrey and Weller 1988b). A recent iontophoresis study suggests that the visual responses of lagged cells are very sensitive to NMDA receptor blockade but insensitive to non-NMDA receptor blockade, while the visual responses of non-lagged cells are more sensitive to non-NMDA receptor blockade and less sensitive to NMDA receptor blockade (Heggelund and Hartveit 1990; Hartveit and Heggelund 1990). These experiments raise the possibility that lagged and nonlagged cells in the cat LGN are distinguished pharmacologically as well as physiologically.

We have examined the physiological division of LGN cells into lagged and nonlagged types, and asked whether the visual responses of these cell types are indeed affected differently by NMDA and non-NMDA receptor antagonists. We find that X and Y cells in the cat LGN can be divided reliably into lagged and nonlagged types. However, the visual responses of all cell types are reduced by NMDA and non-NMDA receptor antagonists. When examined quantitatively, we find that the responses of lagged cells are affected significantly more by d-APV than the responses of nonlagged cells. CNQX, on the other hand, affects the

responses of both lagged and nonlagged cells to a similar extent. These results indicate that lagged and nonlagged cell types in the cat LGN are less distinct than suggested previously (Heggelund and Hartveit 1990; Hartveit and Heggelund 1990), at least with respect to the contribution of non-NMDA receptors to their visual responses.

METHODS

Experiments were performed on adult cats that were prepared for electrophysiological recording from the LGN using procedures that have been described previously (Sur et al. 1987). Animals were anesthetized (70% N_2O/30% O_2, 0.6-1% Halothane), paralyzed (3.6 mg/hr gallamine triethiodide and 0.7 mg/hr d-tubocurarine) and artificially ventilated. End-tidal CO_2 was monitored and maintained at 4%. Body temperature was maintained at 38 deg. C. Vital signs were monitored continuously throughout the experiment and an adequate level of anesthesia maintained at all times by increasing the dose of Halothane if necessary. Pupils were dilated and nictitating membranes retracted with topical application of atropine sulfate and phenylephrine hydrochloride. Appropriate contact lenses were used to focus the eyes on an oscilloscope screen 57 cm in front of the animal. The sharpness of focus was assessed using an ophthalmic retinoscope, and by reflecting the image of retinal landmarks onto a tangent screen. A pair of bipolar stimulating electrodes was placed across the optic chiasm.

A six-barreled glass micropipette assembly was used for extracellular single-unit recording as well as iontophoresis of drugs. The iontophoresis pipettes were made from thin-walled capillary glass while the recording pipette was made from thick-walled capillary glass; the recording pipette thus had a finer tip and significantly higher impedance than the iontophoresis pipettes. The tip of the whole assembly was shaped to an outside diameter of 20-25 um. The recording barrel was filled with 1-3M KCl. One of the iontophoresis barrels was filled with 150 mM NaCl and was used as a balance barrel. The rest were filled with one of the

following solutions (in H_2O): NMDA (50 mM, pH 8.0), KA (20 mM, pH 8.0), d-APV (50 mM, pH 8.0), CNQX (12.5 mM, pH 9.8) and CPP (25 mM, pH 8.0).

Each cell's receptive field was plotted on a tangent screen and the cell classified as On- or Off-center and X or Y. The latter classification was based on a battery of tests, including receptive field center size, response latency to optic chiasm stimulation, and linearity of summation in response to a counterphasing grating stimulus (Sherman and Spear 1982; Shapley and Lennie 1985; Sur et al. 1987). X and Y cells were further divided into lagged and nonlagged types based on the temporal characteristics of their responses to a spot of the appropriate contrast (bright spot for On-center cells, dark spot for Off-center cells). A spot flashing at 1 Hz was placed at the center of the receptive field, and peristimulus time histograms (5 ms bin width) were collected and averaged over 15 trials. Two onset latencies, from start of stimulus to start of response (start-rise) and from start of stimulus to half the peak response (half-rise), and two offset latencies (start-fall and half-fall) were obtained. We then applied criteria that have been reported previously to distinguish lagged from nonlagged cells (Mastronarde 1987a, 1988; Humphrey and Weller 1988a; Saul and Humphrey 1990).

Once a cell was classified as On- or Off-center, X or Y, and lagged or nonlagged, a visual stimulus consisting of a spot alternating between brighter and darker than background at 1 Hz and covering only the receptive field center was continuously presented throughout the duration of recording. The stimulus was produced with a "Picasso" stimulus generator (Innisfree Inc., Cambridge, MA) and presented on a Tektronix 620 monitor at a mean luminance of 36 cd/m^2 and a contrast of up to 0.84. In order to establish effective antagonist doses, we applied

the agonist NMDA or KA at an ejection current level that produced a clear excitatory response equivalent to the visual response of the cell (the agonist current levels were typically 30-90nA). Then an antagonist was applied simultaneously in increasing "doses" of current until it completely blocked the agonist response (antagonist current levels were typically 80-90nA for d-APV and CNQX and 30-40 nA for CPP). This dose of antagonist was then applied to test whether it blocked the response to the other agonist. The antagonist dose was finally applied alone to determine its effect on the visual response of the cell. At all times, retaining currents of 5-10 nA were applied to prevent spontaneous leakage from the drug barrels.

We collected two types of data. First, free-running histograms of visual responses over a long time scale (1 s bin width, each bin equal to one stimulus cycle) were continuously collected from each cell before, during and after drug ejection. Second, peristimulus time (PST) histograms corresponding to one stimulus cycle, with bin widths of 5 or 10 ms and averaged over 10 or 15 stimulus cycles, were collected intermittently during each phase of drug application. In later experiments, we continuously recorded cell responses, stimulus luminance signals, and drug ejection times onto videotape using a data encoder (Neurocorder DR-886, Neuro Data Instruments, New York, NY), so that PST histograms could be constructed off-line.

Antagonist effects were measured from the data collected before, during and after iontophoresis. For each cell, we calculated the mean pre-drug visual response in successive 15 sec. segments over 3 min. preceding drug iontophoresis, and determined the maximum fluctuation between segments. These values for the cells

in a class were pooled to provide baseline measures of (maximum) fluctuation for a population against which antagonist effects were evaluated. To determine the effect of an antagonist, we compared the control response during 15 sec. preceding iontophoresis with the mean response in successive 15 sec. segments from the start of iontophoresis and up to 2 min. after the end of iontophoresis, and determined the maximum change from the control response. Apart from antagonist effects on overall visual responses, we calculated the effects on different response components by comparing the PSTH obtained immediately before iontophoresis with the PST histogram obtained during the segment showing maximum effect of antagonist. We divided each histogram into an early component comprising the first 100 ms of response and a late component comprising the next 300 ms of response, and determined the reduction in each component. All statistical comparisons were done using the Mann-Whitney U-test.

After each experiment, the cat was overdosed with sodium pentobarbital and perfused with saline followed by 10% formalin. The fixed brain was sectioned on a freezing microtome in the coronal plane, and sections stained with cresyl violet. Electrode tracks through the LGN were identified to confirm recording locations.

RESULTS

We recorded a total of 119 cells from laminae A and A1 of the LGN in 18 adult cats. Our sample of cells included 67 X, 46 Y and 6 unclassified cells. Receptive fields of these cells lay within 20 degs. of the area centralis. We obtained enough data from 63 X cells and 39 Y cells to classify them as lagged or nonlagged; the X cells included 39 nonlagged, 1 partially lagged and 23 lagged cells, while the Y cells included 34 nonlagged and 5 lagged cells. We obtained a full complement of data for at least one antagonist (i.e. data before, during and after drug iontophoresis) from 77 cells (51 X and 26 Y cells). The X cells included 32 nonlagged and 19 lagged cells, while the Y cells included 23 nonlagged and 3 lagged cells.

Classification of lagged and nonlagged cells

We attempted to follow previous criteria (Mastronarde 1987a, 1988; cf. Humphrey and Weller 1988a; Saul and Humphrey 1990) as closely as possible in classifying X and Y cells as lagged or nonlagged. The principal criteria are based on the visual latencies of cells at spot onset and offset. We derived latencies at spot onset (using a bright spot for On-center cells and a dark spot for Off-center cells) for every cell, including the latency from start of stimulus to start of response (start-rise latency) and the latency to half the peak response (half-rise latency). However, we found it more difficult to reliably measure latencies at spot offset, for two reasons. First, consistent with previous reports (Saul and Humphrey 1990; Heggelund and Hartveit 1990), latencies at spot offset could only be

obtained for those cells that showed some tonic response component at the end of the excitatory stimulus. In 15 X cells and 12 Y cells, the response to a spot stimulus had decayed to background levels by the time the stimulus turned off. Second, 10 Y cells exhibited clear on/off (or "frequency doubled") responses to spot onset and offset. While the offset response was weak in most cases, consistent with the fact that the nonlinear mechanisms that lead to rectified on/off responses are only modestly engaged by large spots (Hochstein and Shapley 1976), it was clear that offset latencies represent a complicated response measure for Y cells.

We thus initially divided cells into lagged and nonlagged types based on onset latencies alone. These latencies for the cells in our sample are shown in Tables 1 and 2. The mean start-rise and half-rise latencies of lagged X cells were greater than those of nonlagged X cells ($p<.001$ for each comparison; Table 1). Similarly, the start-rise and half-rise latencies of lagged Y cells were greater than those of nonlagged Y cells ($p<.001$ for each comparison; Table 2). For X and Y cells pooled together as well, lagged cells had greater start-rise and half-rise latencies than nonlagged cells ($p=.0001$ for each comparison). Operationally, in our sample, start-rise and half-rise latencies of 45 ms and 55 ms respectively separated lagged X cells from nonlagged X cells, and lagged Y cells from nonlagged Y cells. These values are nearly identical to those obtained by Mastronarde (1987a) and Heggelund and Hartveit (1990) as dividing lagged from nonlagged cells. Humphrey and Weller (1988a) and Saul and Humphrey (1990) suggested somewhat higher values but employed barbiturate anesthesia and a slightly different stimulus paradigm, and Humphrey and Weller (1988a) report using a spot a little larger than the hand-plotted receptive field center, a stimulus that might increase onset

latencies.

Offset latencies, for those X cells for which they could be defined reliably (see above), correlated well with the onset latencies (Table 1). Lagged X cells had higher start-fall and half-fall latencies than nonlagged X cells ($p<.001$ for each comparison). Start-fall and half-fall latencies of 40 ms and 50 ms respectively separated lagged X from nonlagged X cells; of 48 X cells for which we obtained offset latencies, 47 could be classified as lagged or nonlagged based on the combined criteria for the two onset and two offset latencies. One X cell had a half-rise latency slightly lower than 55 ms but a half-fall latency slightly greater than 50 ms. Following Mastronarde (1987a), we classified this cell as "partially lagged", but excluded it from subsequent analyses (this cell is not included in Table 1). For reasons noted above, we did not define offset latencies for any of the Y cells in our sample.

We calculated peak firing rates for lagged and nonlagged cells from PST histograms. Consistent with previous reports (Humphrey and Weller 1988a; Saul and Humphrey 1990), peak firing rates of lagged X cells (mean=131 spikes/s, SE=6.9) were lower than those of nonlagged X cells (mean=201 spikes/s, SE=13.7; $p<.001$), and rates for lagged Y cells (mean=112 spikes/s, SE=18.5) were lower than those of nonlagged Y cells (mean=216 spikes/s, SE=21.2; $p<.01$). Peak firing rates for lagged cells pooled together (mean=128 spikes/s, SE=11.7) were lower than those of nonlagged cells pooled together (mean=207 spikes/s, SE=6.6; $p=.0001$).

Specificity of drug doses

Fig. 1 shows the effects of typical doses (iontophoresis current levels) of antagonists on the agonist-induced responses of an Off-center Y cell. Application of 89 nA of the agonist KA transiently increased the cell's firing rate (Fig. 1A). This excitation was blocked almost completely by concurrent ejection of 90 nA of CNQX; 89 nA of d-APV, however, had no effect on the KA-induced excitation. Fig. 1B shows that application of 90 nA of NMDA to this cell in the absence of visual stimulation had no effect. However, when NMDA ejection was superimposed on the response to a flashing visual stimulus, there was a clear excitatory response. This excitation was subsequently blocked by concurrent ejection of 89 nA of d-APV but not by 89 nA of CNQX.

We carried out control trials such as these on each cell in which we challenged visual responses with antagonists. Agonist current levels and durations, and spot contrasts, were titrated so that the mean levels of agonist and visual responses were equivalent. The antagonist doses that selectively blocked agonist responses were then applied to the visual responses. The mean current levels used for iontophoresing d-APV and CNQX were 89 nA and 86 nA respectively. These levels were independent of cell class.

Cells with very low levels of background activity (such as the cell in Fig. 1) characteristically showed little or no response to NMDA iontophoresed alone, without concurrent visual stimulation. Cells that had higher levels of background activity, however, responded robustly to NMDA alone (see, for example, Fig. 7).

Overall effects of d-APV and CNQX on LGN cell responses

Figs. 2 shows long time scale histograms indicating that both d-APV and CNQX reduced the visual responses of nonlagged and lagged X cells, and Fig. 3 shows similar data for nonlagged and lagged Y cells. Only small segments of free running histograms are shown; we tried different drugs in succession, and in early experiments, PST histograms interrupted the continuous collection of long time scale histograms. In Fig. 2, d-APV reduced the visual response of an On-center nonlagged X cell by 43% while CNQX reduced the visual response of the cell by 67%. D-APV reduced the visual response of an Off-center lagged X cell by 72%, and CNQX reduced its response by 78%. When d-APV and CNQX were applied simultaneously to the nonlagged X cell of Fig. 2, its visual response was reduced by 85% (data not shown). In Fig. 3, d-APV reduced the visual response of an On-center nonlagged Y cell by 69% while CNQX reduced its response by 70%. Similarly, d-APV reduced the response of an On-center lagged Y cell by 76%, and CNQX by 45%.

These cells, chosen as representative examples of the effects of d-APV and CNQX on the visual responses of nonlagged and lagged X and Y cells, show unequivocally that both NMDA and non-NMDA receptors participate in the visual responses of all cell types in the LGN. When results from all cells in our sample are pooled together, we find that blocking NMDA receptors has a greater effect on the visual responses of lagged cells than nonlagged cells, while blocking non-NMDA receptors has equivalent effects on all cell classes (see below).

Effects of NMDA receptor blockade

In addition to long time scale free-running histograms of the sort shown in Figs. 2 and 3, we examined the effects of blocking NMDA and non-NMDA receptors in short time scale PST histograms. Such histograms allowed us to examine antagonist effects not only on overall visual responses but also on separate components of responses. Fig. 4 shows the effect of d-APV on histograms obtained from a nonlagged X cell and a lagged X cell. The visual response of the On-center nonlagged X cell was reduced by 46%, and most of the effect appeared to be confined to the late, sustained, portion of the visual response. The On-center lagged X cell had 59% of its visual response reduced by d-APV, and again there was a tendency for the late response component to be more affected. In general, the late component of lagged X cell responses was consistently reduced by d-APV, while there was more variability in the effect on the early component or on nonlagged X cells (see below).

Fig. 5 shows an Off-center nonlagged Y cell and an On-center lagged Y cell that had 41% and 57% respectively of their visual responses reduced by d-APV. The visual responses of both cells were quite phasic, and in both, the very early transient response as well as somewhat later responses were reduced by d-APV. We were able to test the effect of d-APV on only one lagged Y cell; other lagged Y cells were tested with CPP (see below). Other nonlagged Y cells that we tested with d-APV were affected in generally similar fashion to that shown for the cell in Fig. 5.

Effects of d-APV on the population of cells that we examined with the antagonist are shown in Fig. 6. D-APV reduced the responses of X cells by 36.5% (SE=3.4, n=37) and those of Y cells by 32.0% (SE=5.4, n=20; Fig. 6A), effects

that were not significantly different from each other. Responses of lagged cells were reduced by 49.0% (SE=3.9, n=17) while those of nonlagged cells were reduced by 28.9% (SE=3.3, n=40; Fig. 6C); the effect of d-APV on lagged cells was significantly greater than on nonlagged cells ($p<.001$). Lagged X cell responses, reduced an average of 48.5% (SE=4.1, n=16), were affected more ($p=.001$) than nonlagged X cell responses, which were reduced by 27.3% (SE=4.1, n=21). The response of one lagged Y cell was reduced by 57.6%, and the responses of nonlagged Y cells were reduced an average of 30.6% (SE=5.5, n=19). Importantly, while the effect of d-APV on the visual responses of cells in our sample covered a substantial range (Fig. 6B,D), each category of cell contained neurons whose responses were nearly abolished by d-APV (eg. cells whose visual responses were reduced by close to 80%), suggesting that NMDA receptors contribute very substantially to the visual responses of at least some neurons in each class of LGN cell.

Since the visual responses of most lagged X cells are considerably more sustained than the visual responses of nonlagged X cells, we asked whether d-APV affected tonic (or late) components of visual responses to different extents in the different cell classes. We divided the visual responses of our cells arbitrarily into an early component containing the first 100 ms of response and a late component containing the next 300 ms (we used light on and off times of 500 ms, and for 4 lagged X cells with start-rise latencies greater than 100 ms, the late response component was curtailed to fit within 500 ms). Table 3 shows the effect of d-APV on the early and late response components of the cells in our sample. The late components of lagged (X and Y) cell responses were affected significantly more

than either the late components of nonlagged cells ($p<.001$) or the early components of lagged cells ($p<.05$). Similarly, d-APV reduced late components of lagged X cell responses more than either the early component of these same cells ($p<.05$) or the late components of nonlagged X cells ($p<.01$). [The number of cells in Table 3 is a subset of the cells in Fig. 6 because Table 3 was derived from short time scale PST histograms compiled from the same data as the long time scale histograms used for Fig. 6; in early experiments, we could not derive PST histograms from the long time scale records. The overall effects of d-APV are highly consistent between Table 3 and Fig. 6, however].

To further analyze why lagged cell responses were reduced more than nonlagged cell responses following blockade of NMDA receptors, we examined the effects of d-APV on our population of cells as a function of visual response level just prior to antagonist ejection. We reasoned that lagged cells might have higher overall levels of visual responses than nonlagged cells, which might relate in turn to a greater contribution by NMDA receptors to the visual responses of these cells. We found little correlation between the effect of d-APV and the mean pre-drug visual response level of our cells ($r=.17$). The mean response level of the cells that we challenged with d-APV was 29.5 spikes/s (SE=3.1, n=57). Lagged cells had a mean response level of 23.8 spikes/s (SE=4.6, n=17) while nonlagged cells had a response level of 31.9 spikes/s (SE=3.9, n=40). The distributions of these responses did not differ significantly from each other.

Finally, we tested 11 X cells (1 lagged, 10 nonlagged) and 5 Y cells (2 lagged, 3 nonlagged) with CPP. In particular, we wished to examine with another NMDA receptor antagonist whether or not the responses of nonlagged cells were

influenced by blockade of NMDA receptors (cf. Hartveit and Heggelund 1990). Fig. 7 shows representative data from an Off-center nonlagged X cell. Control trials show that the cell was excited by KA and NMDA, and CPP antagonized the NMDA-induced response but not the KA-induced one. The same dose of CPP was then applied when the cell was responding to a flashing spot at a mean rate (of about 8 spikes/s) similar to the firing rate induced by NMDA iontophoresis. CPP reduced both the onset transient and the sustained response of the cell, causing a mean reduction in response of 55%.

The effects of CPP on the cells that we tested were qualitatively similar to the effects of d-APV. Thus, the responses of X cells were reduced 29.3% by CPP (SE=3.0) and the responses of Y cells were reduced 31.5% (SE=9.9). The visual responses of lagged cells were reduced an average of 22.5% (SE=4.2) while the responses of nonlagged cells were reduced 31.7% (SE=4.2).

Effects of non-NMDA receptor blockade

The effect of CNQX on nonlagged and lagged X cells is shown in Fig. 8. CNQX reduced the visual response of the On-center nonlagged X cell by 54%. In this cell, as in other nonlagged X cells, both the early and late response components were reduced. The effect of CNQX on the lagged X cells in our sample was somewhat more variable than the effect on nonlagged X cells: some cells were affected relatively little, while other cells were affected substantially. An example of a lagged X cell that showed a fairly prominent reduction is shown in Fig. 8D. This was an On-center lagged X cell whose visual response was reduced 71% by CNQX.

At the doses that we used, all antagonists could affect severely a small proportion of the cells that we tested. One example of such an effect is shown in Fig. 9A-C, in which CNQX reduced by 97% the response of an On-center nonlagged Y cell. The On-center lagged Y cell in Fig. 9D had its response reduced by 76%. In general, both early and late response components of nonlagged and lagged cells were affected by CNQX.

Effects of CNQX for our entire population of cells is shown in Fig. 10. CNQX reduced the responses of X cells by 38.3% (SE=5.0, n=46), and the responses of Y cells by 30.8% (SE=6.0, n=21). These effects did not differ significantly from each other. The effects on both X and Y cells included a range of effects that varied from very little or no effect on some cells to nearly a complete block of the visual response for a few cells (Fig. 9, 10B). CNQX reduced the responses of lagged cells to a greater extent, on average, than the responses of nonlagged cells, though the difference was not significant (Fig. 10C). Again, a few nonlagged as well as lagged cells had their visual responses reduced severely (with an effect of 80-100%) by CNQX, indicating that non-NMDA receptors can contribute substantially to the visual responses of at least some cells of each type.

Effects of CNQX on nonlagged and lagged X and Y cells separately were as follows. CNQX reduced the responses of nonlagged X cells by 34.1% (SE=6.2, n=29) compared to 45.3% for lagged X cells (SE=8.7, n=17). These effects did not differ significantly from each other. Nonlagged Y cell responses were reduced by 27.3% (SE=5.6, n=18) while lagged Y cell responses were reduced by 51.7% (SE=25.7, n=3); these effects were also not significantly different.

We examined whether CNQX differentially affected early and late components of responses of nonlagged and lagged X and Y cells. Table 4 shows the effects of CNQX on the early (first 100 ms of response) and late (next 300 ms of response) components for the cells for which we obtained PST histograms before, during and after CNQX iontophoresis. In each category of cell, CNQX had similar effects on the two response components; the early and late response components for each cell class were not significantly different from each other or the corresponding components for any other cell class.

We examined whether the reduction of visual responses by CNQX correlated with the pre-drug visual response levels of our cells. We found no correlation between these variables (r=.077). The mean visual response of the cells that we tested with CNQX was 31.5 spikes/s (SE=3.1, n=67). The response level of lagged cells in this sample (mean=22.0, SE=3.0, n=20) differed only marginally from the response level of nonlagged cells (mean=35.5, SE=4.2, n=47; $p<.1$).

Effects of NMDA and non-NMDA receptor blockade on the same cells

We examined the effects of NMDA and non-NMDA receptor blockade on 19 lagged cells (16 were studied with d-APV and CNQX, 3 with CPP and CNQX) and 45 nonlagged cells (34 were studied with d-APV and CNQX, 11 with CPP and CNQX). Heggelund and Hartveit (1990) suggested that the visual responses of lagged cells are mediated largely by NMDA receptors while the visual responses of nonlagged cells are mediated largely by non-NMDA receptors. If this were true, we would expect that individual lagged cells would have their response reduced significantly by d-APV or CPP and little by CNQX, while individual nonlagged

cells would show the converse. In fact, consistent with the description above, we found that individual lagged and nonlagged cells were affected by blockade of both NMDA and non-NMDA receptors (Fig. 11; note that Fig. 11 shows responses as a proportion of control rather than response reductions). Most cells, regardless of type, clustered around the 45 deg. line, indicating that the greater the sensitivity of a cell to NMDA receptor blockade, the greater its sensitivity to non-NMDA receptor blockade. Both lagged and nonlagged cells were distributed evenly around the 45 deg. line, confirming that the visual responses of individual cells of both types are mediated by NMDA and non-NMDA receptors.

Effects on On- and Off-center cells

We examined the effect of d-APV on 37 On-center and 20 Off-center cells and found that they were affected to nearly identical extents (Table 5A). On-center X cells were not affected differently by d-APV than Off-center X cells. Similarly, the effect of d-APV on On-center Y cells was no different than the effect on Off-center Y cells. We examined the effect of CNQX on 45 On-center cells and 22 Off-center cells; the effects were again very similar (Table 5B). While there was no difference in the effect of CNQX on On-center X cells and Off-center X cells, we found a slight tendency for On-center Y cells to be affected more than Off-center Y cells ($p=.1$). On-center nonlagged and lagged cells were affected to much the same extent by d-APV and CNQX, as were Off-center nonlagged and lagged cells (Figs. 4 and 5 show side-by-side comparisons of the effects of d-APV on representative lagged and nonlagged X and Y cells of the same center sign, and Figs. 8 and 9 show similar comparisons of the effects of CNQX).

DISCUSSION

There are four main results of our study. First, we have confirmed that X and Y cells in the cat LGN can be divided into lagged and nonlagged types based on their latencies at spot onset (start-rise and half-rise latencies). Latencies at spot offset (start-fall and half-fall latencies), obtained for those X cells that had some tonic response component at the end of the excitatory stimulus, are highly consistent with the onset latencies. Second, both NMDA and non-NMDA receptors participate in the visual responses of all cell types in the LGN. D-APV and CPP, antagonists of NMDA receptors, and CNQX, an antagonist of non-NMDA receptors, reduce the visual responses of X and Y, nonlagged and lagged, and On-center and Off-center cells in the LGN. Third, d-APV reduces the responses of lagged cells to a greater extent than the responses of nonlagged cells. CNQX affects the responses of nonlagged and lagged cells to a similar extent. Fourth, d-APV reduces the late component of lagged cell responses to a greater extent than the early response component of the same cells, or either component of nonlagged cells. CNQX has nearly equivalent effects on both response components of all cell types.

Comparison with previous studies of the cat LGN

Sillito et al. (1990a,b) have shown that iontophoresis of NMDA and non-NMDA receptor antagonists reduces the visual responses of X and Y cells in the cat LGN. While our results are qualitatively similar, in the present report lagged cells are distinguished from nonlagged cells, and the drug sensitivities of different

components of responses are analyzed quantitatively.

The mean overall reductions in the visual responses of X and Y cells that we observe with NMDA receptor antagonists are lower than reductions found previously (Sillito et al. 1990a). We took great care not to exceed antagonist doses determined to be specific against agonist-evoked responses (that were equivalent in level to visual responses). The effects of these antagonist doses on individual cells in our sample could be very high, leading to a reduction of 80-100% for some cells (Fig. 6B,D). Importantly, in comparing the relative effects of d-APV or CPP on X and Y cells, Sillito et al. (1990a) found the two cell classes to be affected to similar extents, and our results indicate the same. The effects of CNQX that we observe are very similar to those found by Sillito et al. (1990b), both in overall levels of reduction and in the relative effects on X and Y cells. Again, our doses of CNQX caused substantial reductions (of 80-100%) in the visual responses of some cells in our sample (Fig. 10B,D).

Heggelund and Hartveit (1990) and Hartveit and Heggelund (1990) studied the effects of CPP and DNQX (6,7-dinitroquinoxaline-2,3-dione) on lagged and nonlagged cells in the cat LGN. In their sample, CPP reduced the visual responses of 31 lagged cells by an average of 94% and the responses of 72 nonlagged cells by an average of 22%. D-APV also suppressed the responses of 5 lagged cells and 8 nonlagged cells, though reportedly to a lesser extent; the actual reductions are not stated. In our study, the effect of d-APV on lagged cells is lesser, and the effect on nonlagged cells somewhat greater, than the effect of CPP on these cell types found by Hartveit and Heggelund. Still, our results are at least qualitatively similar, for we find the effect of d-APV to be significantly greater on lagged cells

than on nonlagged cells.

The effect of CNQX in our study is quite different from the effect of DNQX found by Heggelund and Hartveit. In their study, DNQX reduced the responses of 24 nonlagged cells by an average of 74%, while the responses of 11 lagged cells were not reduced but even increased by an average of 27%. In contrast, we find that CNQX reduces the responses of 47 nonlagged cells by an average of 32% and the responses of 20 lagged cells by an average of 46%. When one considers the effects of NMDA and non-NMDA receptor antagonists on the same cells (Fig. 11), the difference becomes quite dramatic. In particular, we do not find a distinct cluster of lagged cells that show high NMDA sensitivity and low non-NMDA sensitivity, and nonlagged cells that show the reverse.

We have considered carefully the possible sources of this discrepancy. First, it is possible that the different effects of DNQX and CNQX on lagged and nonlagged cells are due to major differences in effectiveness of the two antagonists on the two LGN cell types. However, given the similarity of the two drugs in structure and in antagonizing kainate/quisqualate induced responses in other preparations (Honore et al. 1988), such a possibility seems unlikely. Second, it is possible that cells have been classified differently in the two studies. However, the criteria for classifying cells as nonlagged or lagged in both studies are based closely on previous criteria and seem quite similar. Heggelund and Hartveit (1990) found onset latencies to be more reliable than offset latencies in classifying cells, and their mean latencies are similar to those found by Mastronarde (1987a), as are ours (see Results). Importantly, we encountered similar proportions of lagged and nonlagged cells, and employed very similar anesthetic regimens. Third, it is

possible that the different effects of CNQX or DNQX relate to the way antagonists were applied to examine lagged and nonlagged cells in the two studies. The selectivity of CNQX (or DNQX) for non-NMDA receptors and its effect at higher concentrations at the strychnine-insensitive glycine site of NMDA receptors (Birch et al. 1988; Harris and Miller 1989) is an issue in iontophoresis studies. We employed CNQX doses that were titrated carefully against agonist responses (see above), and our overall mean reductions for X and Y cells after CNQX application are similar to those found by Sillito et al. (1990b). In any case, our observation that CNQX affects nonlagged cells less and lagged cells more than the effects found by Heggelund and Hartveit would require that, in our hands, CNQX nonselectively affects lagged cells but is somehow not effective enough for nonlagged cells. We consider this unlikely, for we studied the two cell types using current levels that used each cell as its own control. Lagged and nonlagged cells were routinely recorded in the same penetration, using the same electrode. Furthermore, we examined the effects of antagonists without classifying cells on-line as lagged or nonlagged, and hence without overt knowledge of cell identity.

It is difficult to interpret the claim of Heggelund and Hartveit (1990) that lagged cell responses are not reduced by DNQX. Of 11 lagged cells that were examined with DNQX, 1 cell had its response reduced 89% "when DNQX was applied concurrently with NMDA". PST histograms from one lagged X cell, examined with one current level, are shown to document the lack of effect of DNQX on lagged cells compared to control responses (Fig. 4 of Heggelund and Hartveit 1990). In contrast, the effect of CPP on lagged cells, and the effect of DNQX on nonlagged cells (Hartveit and Heggelund 1990), was examined with

increasing levels of current to show increasing magnitudes of effect. It is unclear how the current levels used for examining the effect of DNQX on lagged cells were chosen, and whether increasing the antagonist dose would affect lagged cells more than that reported.

NMDA receptors and retinogeniculate transmission

Our results, along with those of Sillito et al. (1990a) and Heggelund and Hartveit (1990), indicate clearly that both NMDA and non-NMDA receptors are involved fundamentally in retinogeniculate transmission. This stands in contrast to an in vitro study of retinogeniculate transmission in the rat LGN (Crunelli et al. 1987), that showed that epsp's recorded in LGN cells after stimulation of the optic tract could be reduced by non-NMDA receptor antagonists but not by d-APV. More recent reports of in vitro LGN experiments, however, support the view that both NMDA and non-NMDA receptors mediate optic tract evoked postsynaptic responses (Soltesz et al. 1989; Esguerra et al. 1989; Scharfman et al. 1990; Esguerra and Sur 1990). In particular, the early and late components of epsp's in most LGN cells following optic tract stimulation are sensitive to d-APV, although the magnitude of the effect varies among cells (Scharfman et al. 1990; Esguerra and Sur 1990).

Our results suggest that, on the whole, NMDA and non-NMDA receptors each mediate the entire response of LGN cells to visual stimuli, including early and late response components. Retinal axons have fairly high rates of background activity (Kaplan et al. 1987; cf. Sur et al. 1987). Thus, even in the absence of overt visual stimulation, the steady barrage of retinogeniculate epsp's would be

sufficient to lift, at least to some extent, the Mg++ block of NMDA receptors on LGN cells. It would follow, then, that NMDA (and non-NMDA) receptors would be involved in retinogeniculate transmission at all times, and thus contribute to all components of visual responses.

There is considerable variation, however, in the contribution of NMDA and non-NMDA receptors to the responses of LGN cells (Figs. 6, 10, 11; see also below). The contribution of the two receptor classes to an individual cell's visual response would depend both on the relative proportion of these receptors and the effectiveness of the NMDA receptors; the latter is a function, in turn, of the cell's level of depolarization. Our observation that there is no clear relationship between the pre-drug visual response level and the effect of d-APV on LGN cells is very likely a reflection of these sources of variability in the contribution of NMDA receptors to the responses of cells that make up our population. Cells on which NMDA receptors are fully unblocked would show no dependence of the NMDA contribution on visual response level, while other cells would. For an individual cell (where also the proportion of NMDA and non-NMDA receptors is not a variable), we would expect the level of visual response to correspond well with the proportional contribution of NMDA receptors, at least at low levels of cell activity.

Excitatory amino acid receptors at corticogeniculate synapses

It has been suggested that the feedback projection from visual cortex to the LGN is also glutamatergic (Baughman and Gilbert 1980), and intracellular recordings of optic radiation evoked epsp's from LGN cells in vitro indicate that corticogeniculate synaptic transmission involves both NMDA and non-NMDA

receptors (Esguerra and Sur 1990). Consequently, iontophoretic application of EAA receptor antagonists could affect visual responses by blocking transmission at corticogeniculate as well as at retinogeniculate synapses. We cannot exclude this possibility; however, the severity of antagonist effects on visual responses suggests that the drugs are acting primarily at retinogeniculate sites. Attenuation of corticofugal influence by other means, such as reversible cooling (Kalil and Chase 1970; Geisert et al. 1981) or ablation of cortex (Murphy and Sillito 1987), produces rather subtle and complex changes in the visual responses of LGN cells. Furthermore, this modulation may be better detected when moving bars or other less conventional stimuli are used to activate the corticofugal projection (Kalil and Chase 1979; Murphy and Sillito 1987; Marrocco et al. 1982); the flashing spots used in the present study probably evoke minimal corticofugal activity.

Excitatory amino acid receptors and lagged/nonlagged cells

D-APV reduces the responses of lagged cells to a greater extent than the responses of nonlagged cells, suggesting that NMDA receptors play a larger role in mediating the visual responses of lagged cells. Lagged cells respond more tonically, in general, to maintained visual stimuli, and the large role of NMDA receptors in lagged cell responses would be due at least in part to the large contribution of NMDA receptors to the late response component of these cells.

One issue raised by these results is the relationship between NMDA receptors and the peculiar physiological characteristics of lagged cells. It is tempting to suggest that NMDA receptors, which play a prominent role in the visual responses of lagged cells, are in some way responsible for their unique

features. However, visual responses of lagged cells do not become nonlagged with blockade of NMDA receptors; their visual latencies before and after application of NMDA antagonists do not change appreciably. Similarly, the visual latencies of nonlagged cells do not change with NMDA receptor blockade. Therefore it is unlikely that the NMDA receptor by itself is sufficient to generate the features characteristic of lagged cells. Rather, intrageniculate inhibition may be crucial for the response properties of these cells (Humphrey and Weller 1988b; Heggelund and Hartveit 1990).

Our results indicate that lagged and nonlagged cells in the LGN are not as distinct with respect to the role of EAA receptors in their visual responses as suggested previously (Heggelund and Hartveit 1990; Hartveit and Heggelund 1990). Not only do non-NMDA receptors participate to very similar extents in the visual responses of lagged and nonlagged cells, even the differential contribution of NMDA receptors to lagged cell responses is more a quantitative distinction than a qualitative one. Thus, we find a range of effects of NMDA antagonists on lagged and nonlagged cells (Fig. 6D, 11), including cells in both groups that are affected very little and cells that are affected substantially. While it remains possible that lagged and nonlagged cells indeed represent distinct cell classes that contain different complements of NMDA receptors, these findings are consistent with the view that the two types of cell represent different response modes of the same neuron (Uhlrich et al. 1990; McCormick 1990; cf. Humphrey and Weller 1988b).

Our results would suggest then that NMDA receptors participate more in the lagged than in the nonlagged mode, and we can speculate briefly on how this might happen. One possibility concerns the visual stimuli that are used to classify

cells as lagged or nonlagged, and that have been used by us and others to study the sensitivity of responses to NMDA and non-NMDA receptor antagonists; these stimuli, which are spots of moderate to high contrast that abruptly turn on or off, might bias the responses of nonlagged cells towards non-NMDA receptors. Lagged cells in effect filter the onset transients in such stimuli so that their responses contain only gradual onsets. Since the kinetics of the ionic conductances associated with NMDA receptors are slower than those of non-NMDA receptors (Cull-Candy and Usowicz 1987), gradual response onsets allow NMDA receptors to participate more fully in the responses of lagged cells. A specific prediction would be that slowly varying stimuli (with ramp or sinusoidal onsets, for example) would allow NMDA receptors on nonlagged cells to participate equally effectively. Another, related, possibility is that the contribution of NMDA receptors to (lagged or nonlagged) LGN cells is a function of the tonic response level. The greater effect of NMDA receptor blockade on lagged cells is consistent with this possibility, and more detailed analyses of NMDA-sensitive response components and the maintained activity of cells might reveal such a general relationship.

Concluding remarks

The present results support the notion that NMDA receptors play a role not only in development and plasticity in the visual pathway (Artola and Singer 1987; Cline et al. 1987; Kleinschmidt et al. 1987; Hahm et al. 1990), but also in ongoing visual function. A similar functional role has been proposed for NMDA receptors in area 17 of visual cortex, where APV blocks visual responses in adult cats when administered either by infusion (Miller et al. 1989) or by iontophoresis

(Fox et al. 1989). Significantly, d-APV sensitivity is found through all cortical layers in kittens, but persists in only the supragranular layers in adults, suggesting both developmental and functional roles for the same receptor (Fox et al. 1989). In the LGN, it has been proposed that the massive corticofugal input may modulate NMDA receptors at retinogeniculate synapses, thereby gating the efficacy of thalamic transmission (Koch 1987; Esguerra and Sur 1990). In this regard, it is of some interest that lagged cells, whose properties emerge in the LGN, are the very cells whose visual responses are most dependent on NMDA receptors.

Acknowledgements

We thank Louis Toth and Lukas Ruecker for helping with some of the experiments, Teresa Sullivan for excellent assistance with histology, and Allen Humphrey for his comments on the manusscript. Supported by National Institutes of Health grant EY 07023 (MS). YHK is supported by National Institute of General Medical Sciences training grant GM07484, and ME by the Whitaker Health Sciences Fund.

REFERENCES

Artola, A. and Singer, W. Long-term potentiation and NMDA receptors in rat visual cortex. Nature 330: 649-652, 1987.

Baughman, R. W. and Gilbert, C. D. Aspartate and glutamate as possible neurotransmitters of cells in layer 6 of the visual cortex. Nature Lond. 287: 848-850, 1980.

Birch, P.J., Grossman, C.J., and Hayes, A.G. 6,7-Dinitro-quinoxaline-2,3-dion and 6-nitro,7-cyano-quinoxaline-2,3-dion antagonize responses to NMDA in the rat spinal cord via an action at the strychnine-insensitive glycine receptor. Eur. J. Pharmacol. 156: 177-180, 1988.

Cline, H. T., Debski, E. A., and Constantine-Paton, M. N-methyl-D-aspartate receptor antagonist desegregates eye-specific stripes. Proc. Natl. Acad. Sci.USA 84: 4342-4345, 1987.

Cotman, C.W., Monaghan, D.T., Ottersen, O.P. and Storm-Mathisen, J. Anatomical organization of excitatory amino acid receptors and their pathways. Trends in Neurosci. 10: 273-280, 1987.

Crunelli, V., Kelly, J.S., Leresche, N., and Pirchio, M. On the excitatory post-synaptic potential evoked by stimulation of the ooptic tract in the rat lateral geniculate nucleus. J. Physiol. Lond. 384: 603-618, 1987.

Cull-Candy, S.G. and Usowicz, M.M. Multiple-conductance channels activated by excitatory amino acids in cerebellar neurons. Nature Lond. 325: 525-528, 1987.

Esguerra, M., Kwon, Y.H., and Sur, M. NMDA and non-NMDA receptors mediate retinogeniculate transmission in cat and ferret LGN in vitro. Soc. Neurosci. Abstr.

15: 175, 1989.

Esguerra, M. and Sur, M. Corticogeniculate feedback gates retinogeniculate transmission by activating NMDA receptors. Soc. Neurosci. Abstr. 16: 159, 1990.

Fox, K., Sato, H. and Daw, N. The location and function of NMDA receptors in cat and kitten visual cortex. J. Neurosci. 9: 2443-2454, 1989.

Geisert, E. E., Langsetmo, A., and Spear, P. D. Influence of the cortico-geniculate pathway on response of cat lateral geniculate neurons. Brain Res. 208: 409-415, 1981.

Hahm, J., Langdon, R.B. and Sur, M. NMDA antagonists disrupt normal on/off sublaminar segregation of ferret retinogeniculate axons. Soc. Neurosci. Abstr. 16: 1128, 1990.

Harris, K.M. and Miller, R.J. CNQX antagonizes NMDA-evoked [3H]GABA release from cultured cortical neurons via an inhibitory action at the strychnine-insensitive glycine site. Brain Res. 489: 185-189, 1989.

Hartveit, E. and Heggelund, P. Neurotransmitter receptors mediating excitatory input to cells in the cat lateral geniculate nucleus. II. Nonlagged cells. J. Neurophys. 63: 1361-1372, 1990.

Heggelund, P. and Hartveit, E. Neurotransmitter receptors mediating excitatory input to cells in the cat lateral geniculate nucleus. I. Lagged cells. J. Neurophys. 63: 1347-1360, 1990.

Hochstein, S. and Shapley, R.M. Quantitative analysis of retinal ganglion cell classifications. J. Physiol. London 262: 237-264, 1976.

Honore, T., Davies, S.N., Drejer, J., Fletcher, E.J., Jacobsen, P., Lodge, D. and Nielsen, F.E. Quinoxalinediones: potent competitive non-NMDA glutamate receptor

antagonists. Science 241: 701-703, 1988.

Humphrey, A.L. and Weller, R.E. Functionally distinct groups of X-cells in the lateral geniculate nucleus of the cat. J. Comp. Neurol. 268: 429-447, 1988a.

Humphrey, A.L. and Weller, R.E. Structural correlates of functionally distinct X-cells in the lateral geniculate nucleus of the cat. J. Comp. Neurol. 268: 448-468, 1988b.

Kalil, R. E., and Chase, R. Corticofugal influence on activity of lateral geniculate neurons in the cat. J. Neurophysiol. 33: 459-474, 1970.

Kaplan, E., Purpura, K., and Shapley, R.M. Contrast affects the transmission of visual information through the mammalian lateral geniculate nucleus. J. Physiol. London 391: 267-288, 1987.

Kemp, J.A. and Sillito, A.M. The nature of the excitatory transmitter mediating X and Y cell inputs to the cat dorsal lateral geniculate nucleus. J. Physiol. 323: 377-391, 1982.

Kleinschmidt, A., Bear, M. F., and Singer, W. Blockade of "NMDA" receptors disrupts experience-dependent plasticity of kitten striate cortex. Science 238: 355-358, 1987.

Koch, C. The action of the corticofugal pathway on sensory thalamic nuclei: a hypothesis. Neuroscience 23: 399-406, 1987.

McCormick, D.A. Possible ionic basis for lagged visual responses in cat LGNd relay neurons. Soc. Neurosci. Abstr. 16: 159, 1990.

Marrocco, R. T., McClurkin, J. W., and Young, R. A. Modulation of lateral geniculate nucleus cell responsiveness by visual activation of the corticogeniculate pathway. J. Neurosci. 2: 256-263, 1982.

Mastronarde, D.N. Two classes of single-input X-cells in cat lateral geniculate nucleus. I. Receptive-field properties and classification of cells. J. Neurophysiol. 57: 357-380, 1987a.

Mastronarde, D.N. Two classes of single-input X-cells in cat lateral geniculate nucleus. II. Retinal inputs and the generation of receptive-field properties. J. Neurophysiol. 57: 381-413,1987b.

Mastronarde, D.N. Branching of X and Y functional pathways in cat lateral geniculate nucleus. Soc. Neurosci. Abstr. 14: 309, 1988.

Mayer, M.L. and Westbrook, G.L. The physiology of excitatory amino acids in the vertebrate central nervous system. Progress in Neurobiology 28: 197-276, 1987.

Miller, K. D., Chapman, B., and Stryker, M. P. Visual responses in adult cat visual cortex depend on N-methyl-D-aspartate receptors. Proc. Natl. Acad. Sci. USA 86: 5183-5187, 1989.

Murphy, P. C. and Sillito, A. M. Corticofugal feedback influences the generation of lenth tuning in the visual pathway. Nature 329: 727-729, 1987.

Saul, A and Humphrey, A.L. Spatial and temporal response properties of lagged and non-lagged cells in the cat lateral geniculate nucleus. J. Neurophys. 64: 206-224, 1990.

Scharfman, H.E., Lu, S.-M., Guido, W., Adams, P.R., and Sherman, S.M. N-Methyl-D-aspartate receptors contribute to excitatory postsynaptic potentials of cat lateral geniculate neurons recorded in thalamic slices. Proc. Natl. Acad. Sci. USA 87: 4548-4552, 1990.

Shapley, R. and Lennie, P. Spatial frequency analysis in the visual system. Ann. Rev. Neurosci. 8: 547-583, 1985.

Sherman, S.M. and Spear, P.D. Organization of visual pathways in normal and visually deprived cats. Physiol. Rev. 62: 738-855, 1982.

Sillito, A.M., Murphy, P.C., Salt, T.E. and Moody, C.I. Dependence of retinogeniculate transmission in cat on NMDA receptors. J. Neurophys. 63: 347-355, 1990a.

Sillito, A.M., Murphy, P.C. and Salt, T.E. The contribution of the non-N-Methyl-D-Aspartate group of excitatory amino acid receptors to retinogeniculate transmission in the cat. Neuroscience 34: 273-280, 1990b.

Soltesz, I., Haby, M., Jassik-Gerschenfeld, D., Leresche, N., and Crunelli, V. NMDA and non-NMDA receptors mediate both high and low frequency synaptic potentials in the rat lateral geniculate nucleus. Soc. Neurosci. Abstr. 15: 1310, 1989.

Sur, M., Esguerra, M., Garraghty, P. E., Kritzer, M. F., and Sherman, S. M. Morphology of physiologically identified retinogeniculate X- and Y-axons in the cat. J. Neurophysiol. 52: 1-32, 1987.

Uhlrich, D.J., Tamamaki, N. and Sherman, S.M. Brainstem control of response modes in neurons of the cat's lateral geniculate nucleus. Proc. Natl. Acad. Sci. USA 87: 2560-2563, 1990.

Watkins, J.C. & Olverman, H.J. Agonists and antagonists for excitatory amino acid receptors. Trends in Neurosci. 10: 265-272, 1987.

FIGURE LEGENDS

FIG. 1. Responses to EAA agonists recorded from an Off-center Y cell and the effect of antagonists. A. Specificity of CNQX for the KA-induced response. Iontophoresis of KA increased the cell's activity (left); the increase was unaffected by d-APV (middle) but antagonized by CNQX (right). The bars above each free-running histogram (bin width, 1s) represent periods of application of the drugs indicated. B. Specificity of d-APV for the NMDA-induced response. Iontophoresis of NMDA without visual stimulation had no effect on the cell (far left). A spot flashing at 1 Hz in the cell's receptive field caused the cell to respond vigorously (arrow). NMDA application then increased the cell's response; the increase was unaffected by CNQX but antagonized by d-APV. The d-APV dose was just enough to abolish only the NMDA-induced response increase. The scale in A applies as well to B.

FIG. 2. Effects of d-APV and CNQX on nonlagged and lagged X cells. These are free-running histograms showing the response of each cell to a spot in its receptive field flashing at 1 Hz (0.5 s on, 0.5 s off), and the effect of antagonist application for the duration indicated by the bar above each histogram. A. An On-center nonlagged X cell. B. An Off-center lagged X cell.

FIG. 3. Effects of d-APV and CNQX on nonlagged and lagged Y cells. Conventions as in Fig. 2. A. An On-center nonlagged Y cell. B. An On-center lagged Y cell.

FIG. 4. Effect of d-APV on nonlagged and lagged X cells. These are PST histograms (bin width, 5 ms) showing responses to a spot in the receptive field flashing 'on' for 0.5 s and 'off' for 0.5 s. The line below each column of histograms shows the light 'on' period. All control histograms were made just prior to antagonist application. A-C. Responses from an On-center nonlagged X cell taken (A) before, (B) during, and (C) 2 min. post-iontophoresis. D-F. Responses from an On-center lagged X cell taken (D) before, (E) during, and (F) 3.5 min. post-iontophoresis.

FIG. 5. Effect of d-APV on nonlagged and lagged Y cells. Conventions as in Fig. 4. A-C. Responses from an Off-center nonlagged Y cell taken (A) before, (B) during, and (C) 4 min. post-iontophoresis. D-E. Responses from an Off-center lagged Y cell taken (D) before, (E) during, and (F) 40 s post-iontophoresis.

FIG. 6. Effect of d-APV on the population of cells examined. A. Percent reduction in the visual responses of X and Y cells, shown as mean effects with SE bars. B. Same data as in A, now showing the distribution of effects on X and Y cells. C. Percent reduction in the visual responses of lagged and nonlagged cells. D. Same data as in C, now showing the distribution of effects on lagged and nonlagged cells.

FIG. 7. Effect of CPP on KA- and NMDA-induced excitation, and on the visual response of an Off-center nonlagged X cell. A. Iontophoresis of KA increased the

cell's activity. B. Iontophoresis of NMDA also increased the cell's activity. C. Iontophoresis of CPP concurrent with KA had no effect on the KA-induced excitation. D. Iontophoresis of CPP concurrent with NMDA abolished the NMDA-induced excitation. E-G. PST histograms of visual responses taken (E) before, (F) 20 s after, and (G) 2 min. 20 s after the end of CPP iontophoresis. Conventions as in Fig. 4.

FIG. 8. Effect of CNQX on nonlagged and lagged X cells. A-C. Responses of an On-center nonlagged X cell taken (A) before, (B) 40 s after, and (C) 3 min. 20 s after the end of iontophoresis. D-F. Responses of an On-center lagged X cell taken (D) before, (E) 2 min. after, and (F) 14 min. after the end of iontophoresis. Conventions as in Fig. 4.

FIG. 9. Effect of CNQX on nonlagged and lagged Y cells. A-C. Responses of an On-center nonlagged Y cell taken (A) before, (B) just after, and (C) 4 min. after the end of iontophoresis. D-F. Responses of an On-center lagged Y cell taken (D) before, (E) 20 s after, and (F) 4 min. after the end of iontophoresis. Conventions as in Fig. 4.

FIG. 10. Effect of CNQX on the population of cells examined. A. Percent reduction in the visual responses of X and Y cells, shown as mean effects with SE bars. B. Same data as in A, now showing the distribution of effects on X and Y cells. C. Percent reduction in the visual responses of lagged and nonlagged cells. D. Same data as in C, now showing the distribution of effects on lagged and

nonlagged cells.

FIG. 11. Scatterplot of lagged and nonlagged cells showing the effect of blocking NMDA and non-NMDA receptors. The axes show the response remaining after blockade as percent of the control response. Cells were tested with either d-APV or CPP, and with CNQX. Antagonists were applied successively, after recovery from the previous antagonist. The dashed line at 45 degs. indicates the location of cells that would be affected equally by NMDA and non-NMDA receptor blockade.

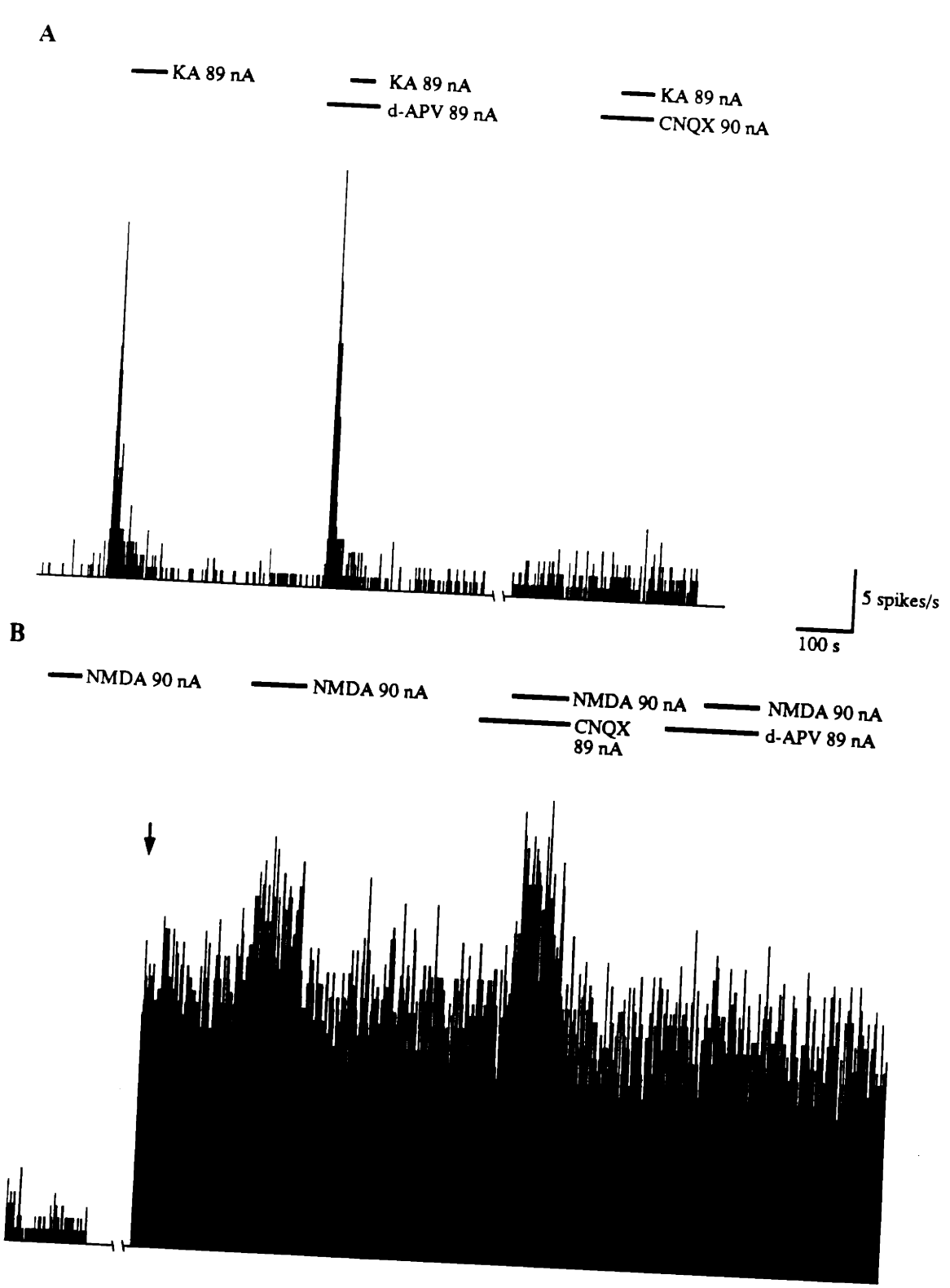
Off-center Y cell
A
KA 89 nA
KA 89 nA
d-APV 89 nA
KA 89 nA
CNQX 90 nA
5 spikes/s
100 s
B
NMDA 90 nA
NMDA 90 nA
NMDA 90 nA
CNQX
89 nA
NMDA 90 nA
d-APV 89 nA

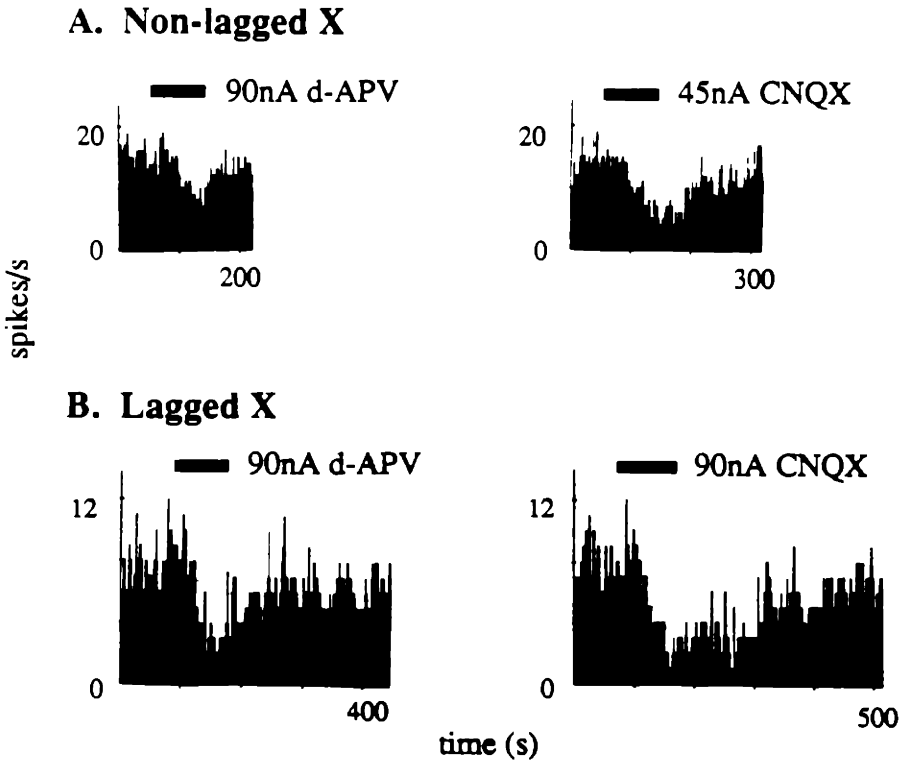
A. Non-lagged X
90nA d-APV
45nA CNQX
20
0
200
300
spikes/s
B. Lagged X
90nA d-APV
90nA CNQX
12
0
400
500
time (s)

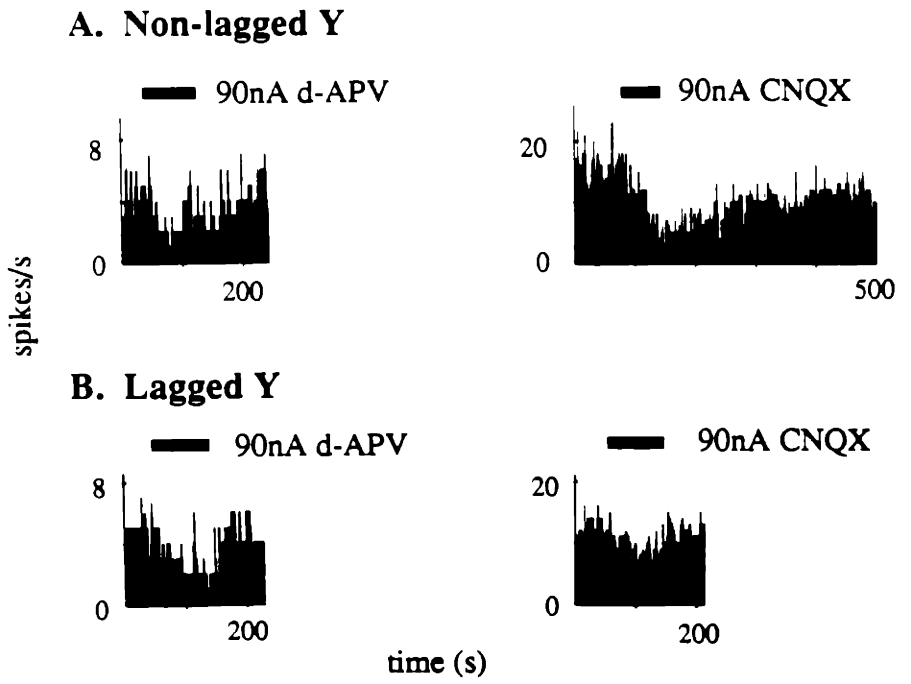
A. Non-lagged Y
90nA d-APV
90nA CNQX
8
0
200
20
0
500
spikes/s
B. Lagged Y
90nA d-APV
90nA CNQX
8
0
200
20
0
200
time (s)

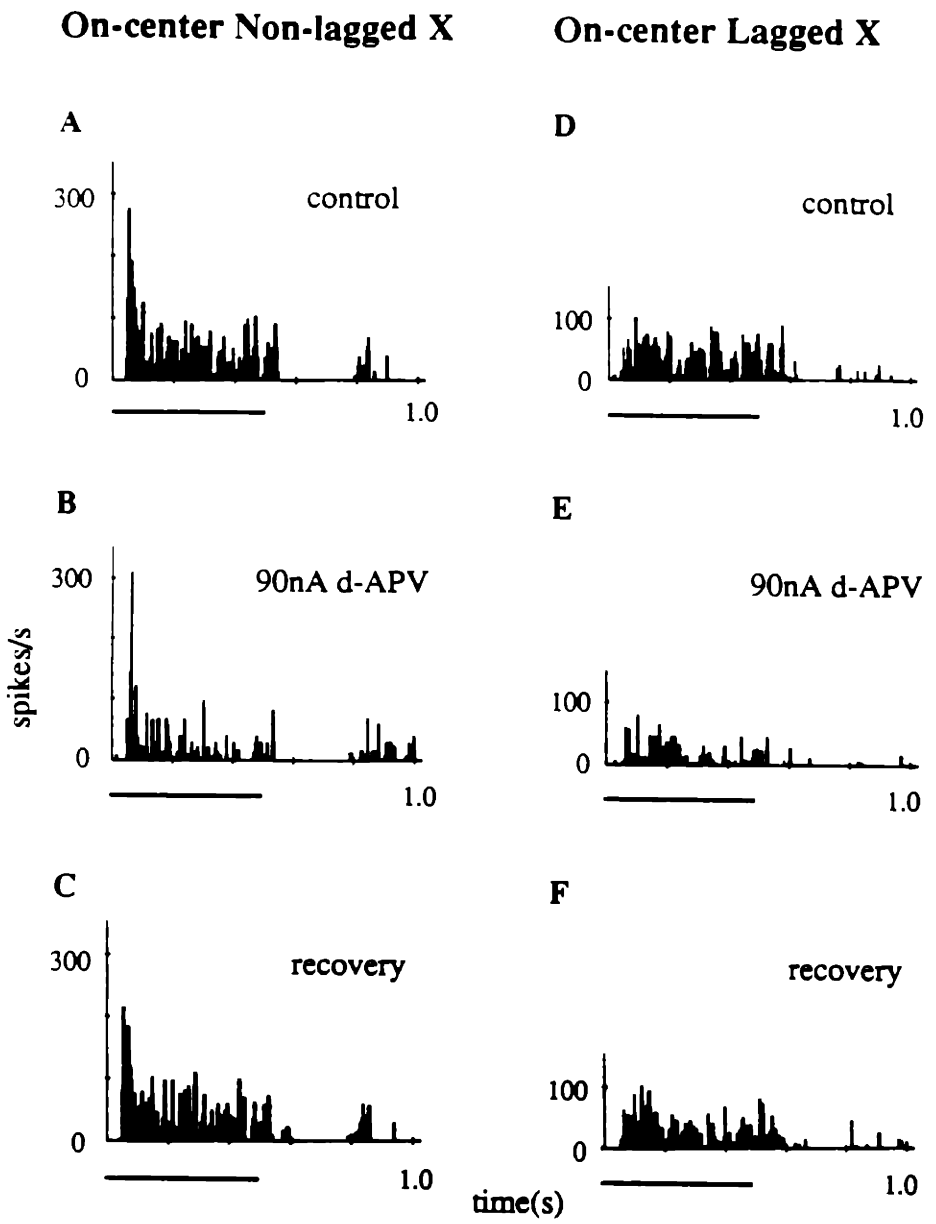
On-center Non-lagged X
On-center Lagged X
A
D
300
control
control
100
0
1.0
B
E
300
90nA d-APV
90nA d-APV
spikes/s
100
0
1.0
C
F
300
recovery
recovery
100
0
1.0
time(s)

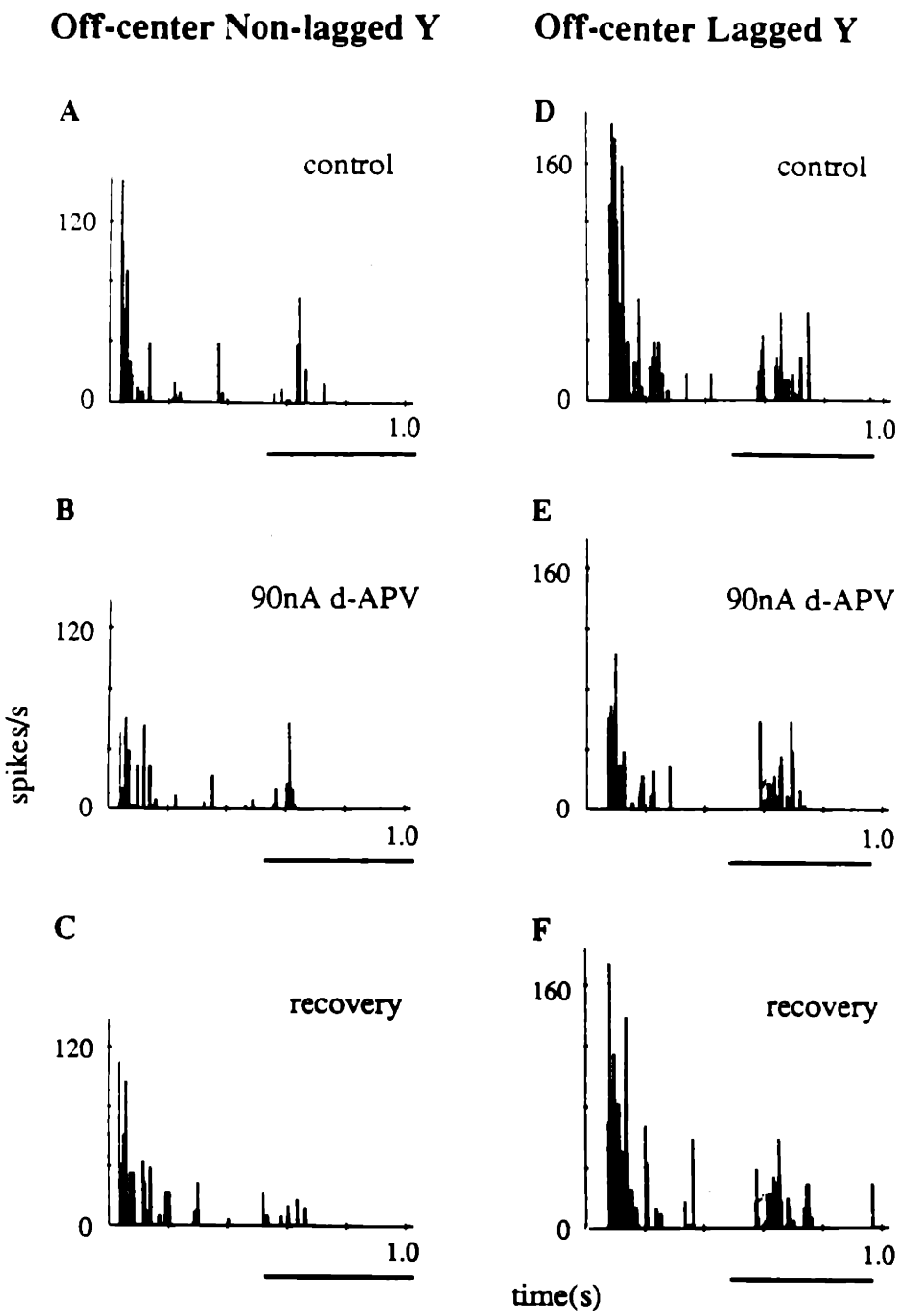
Off-center Non-lagged Y
Off-center Lagged Y
A
control
120
0
1.0
D
160
control
0
1.0
B
90nA d-APV
120
0
1.0
E
160
90nA d-APV
0
1.0
spikes/s
C
recovery
120
0
1.0
F
160
recovery
0
1.0
time(s)

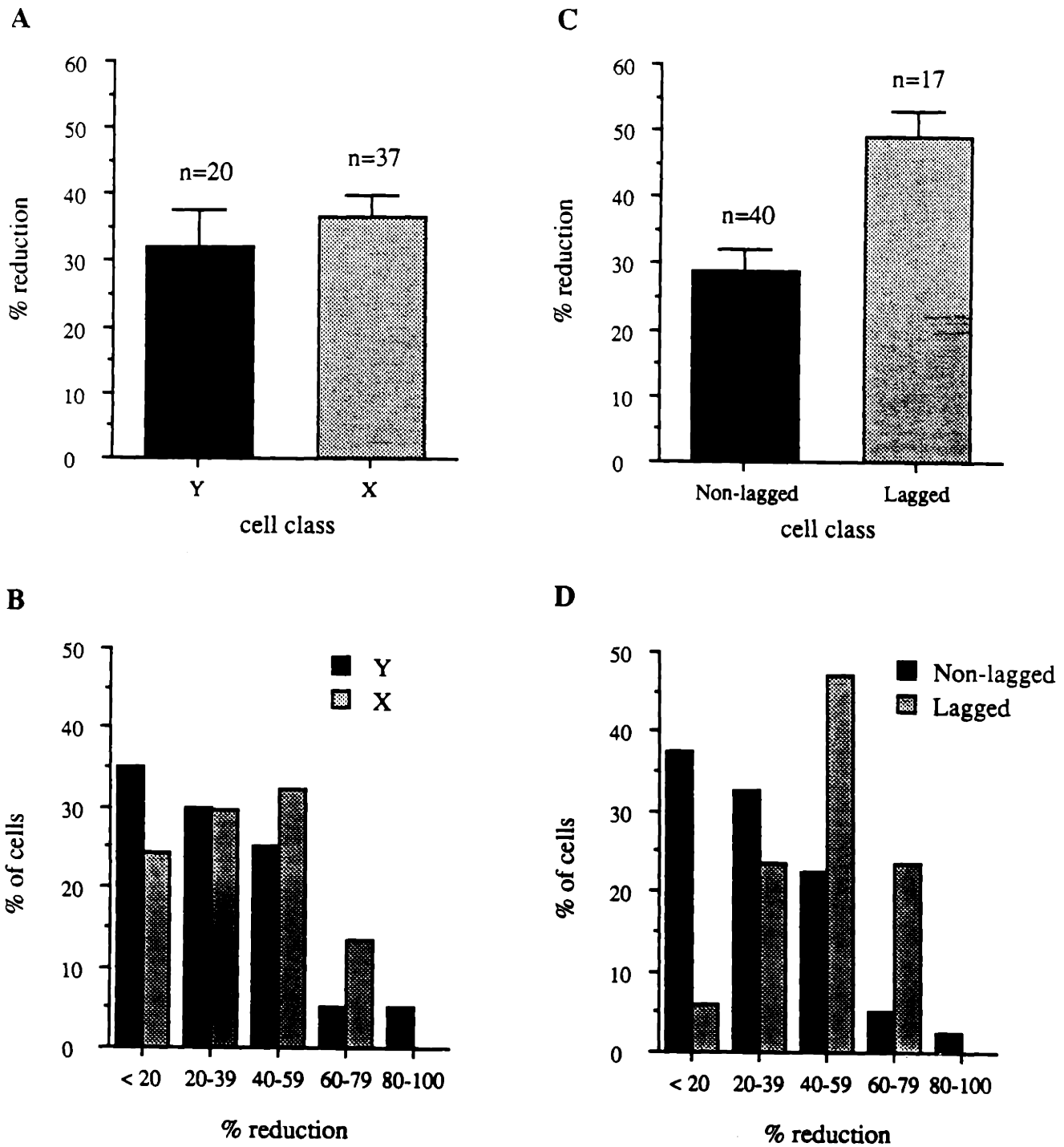
A
60
50
40
30
20
10
0
% reduction
n=20
n=37
Y
X
cell class
C
60
50
40
30
20
10
0
% reduction
n=40
n=17
Non-lagged
Lagged
cell class
B
50
40
30
20
10
0
% of cells
Y
X
< 20
20-39
40-59
60-79
80-100
% reduction
D
50
40
30
20
10
0
% of cells
Non-lagged
Lagged
< 20
20-39
40-59
60-79
80-100
% reduction

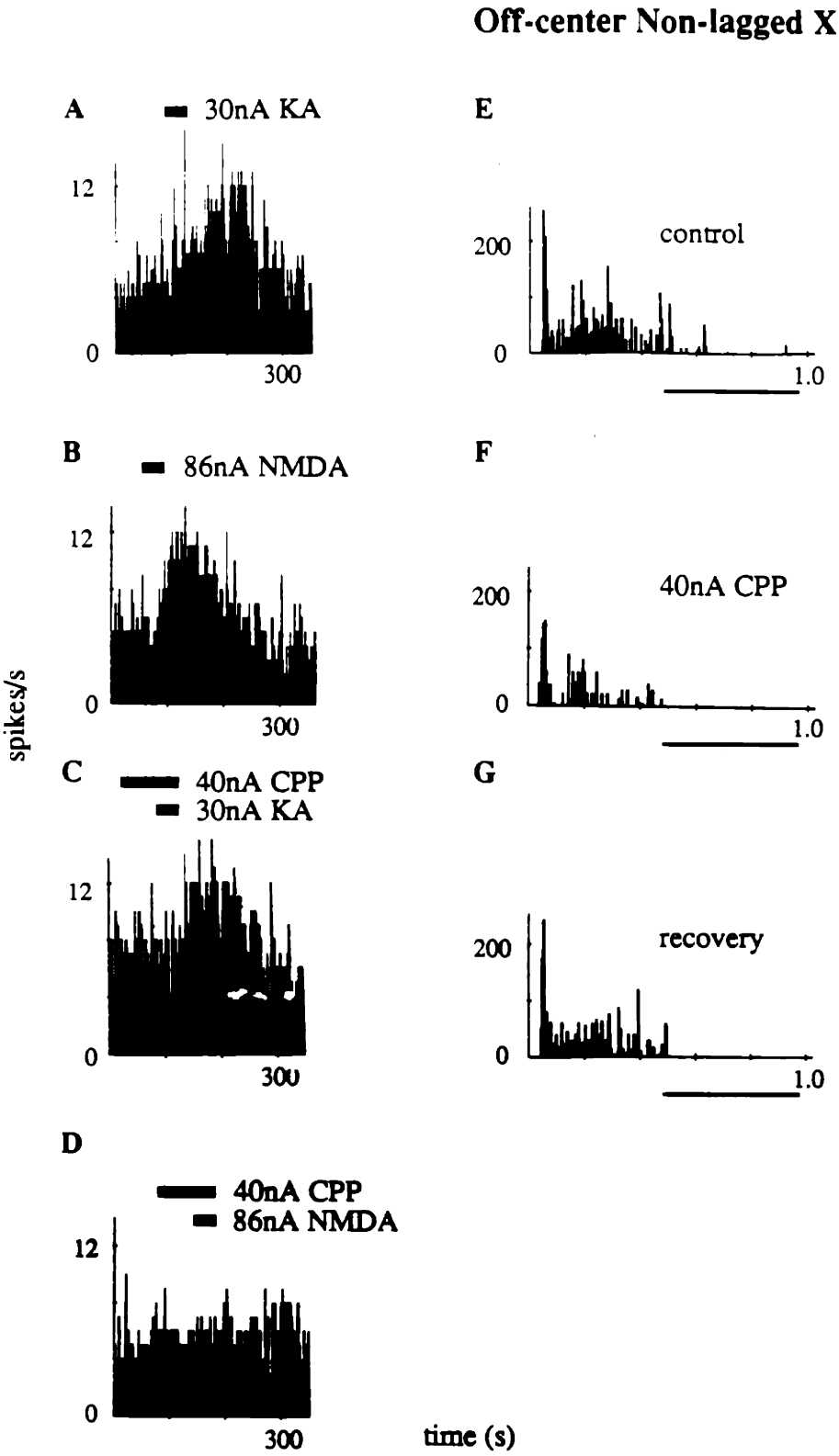
Off-center Non-lagged X
A
30nA KA
12
0
300
B
86nA NMDA
12
0
300
C
40nA CPP
30nA KA
12
0
300
D
40nA CPP
86nA NMDA
12
0
300
spikes/s
time (s)
E
control
200
0
1.0
F
40nA CPP
200
0
1.0
G
recovery
200
0
1.0

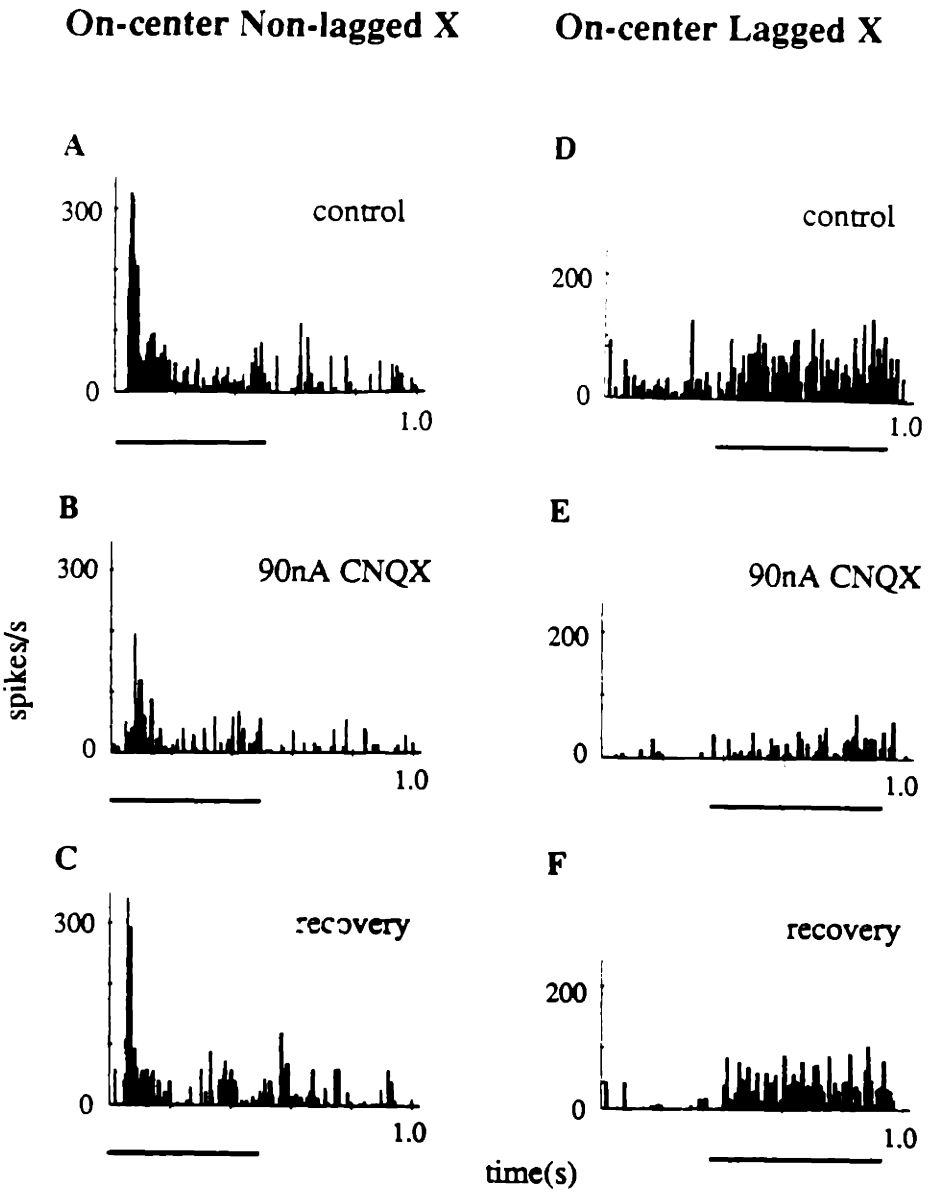
On-center Non-lagged X
On-center Lagged X
A
300
control
0
1.0
D
control
200
0
1.0
B
300
90nA CNQX
0
1.0
E
90nA CNQX
200
0
1.0
spikes/s
C
300
recovery
0
1.0
F
recovery
200
0
1.0
time(s)

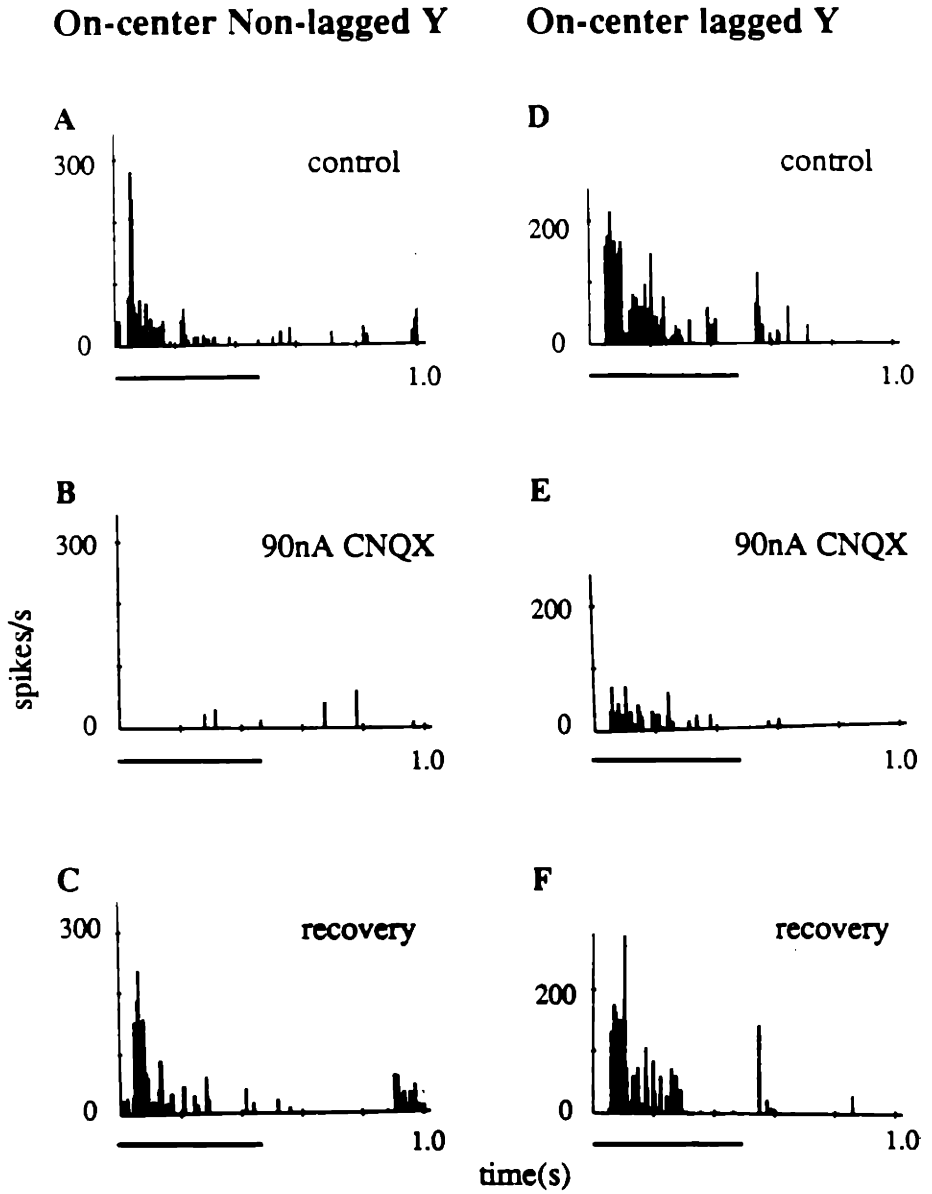
On-center Non-lagged Y
On-center lagged Y
A
control
300
0
1.0
D
control
200
0
1.0
B
90nA CNQX
300
0
1.0
E
90nA CNQX
200
0
1.0
spikes/s
C
recovery
300
0
1.0
F
recovery
200
0
1.0
time(s)

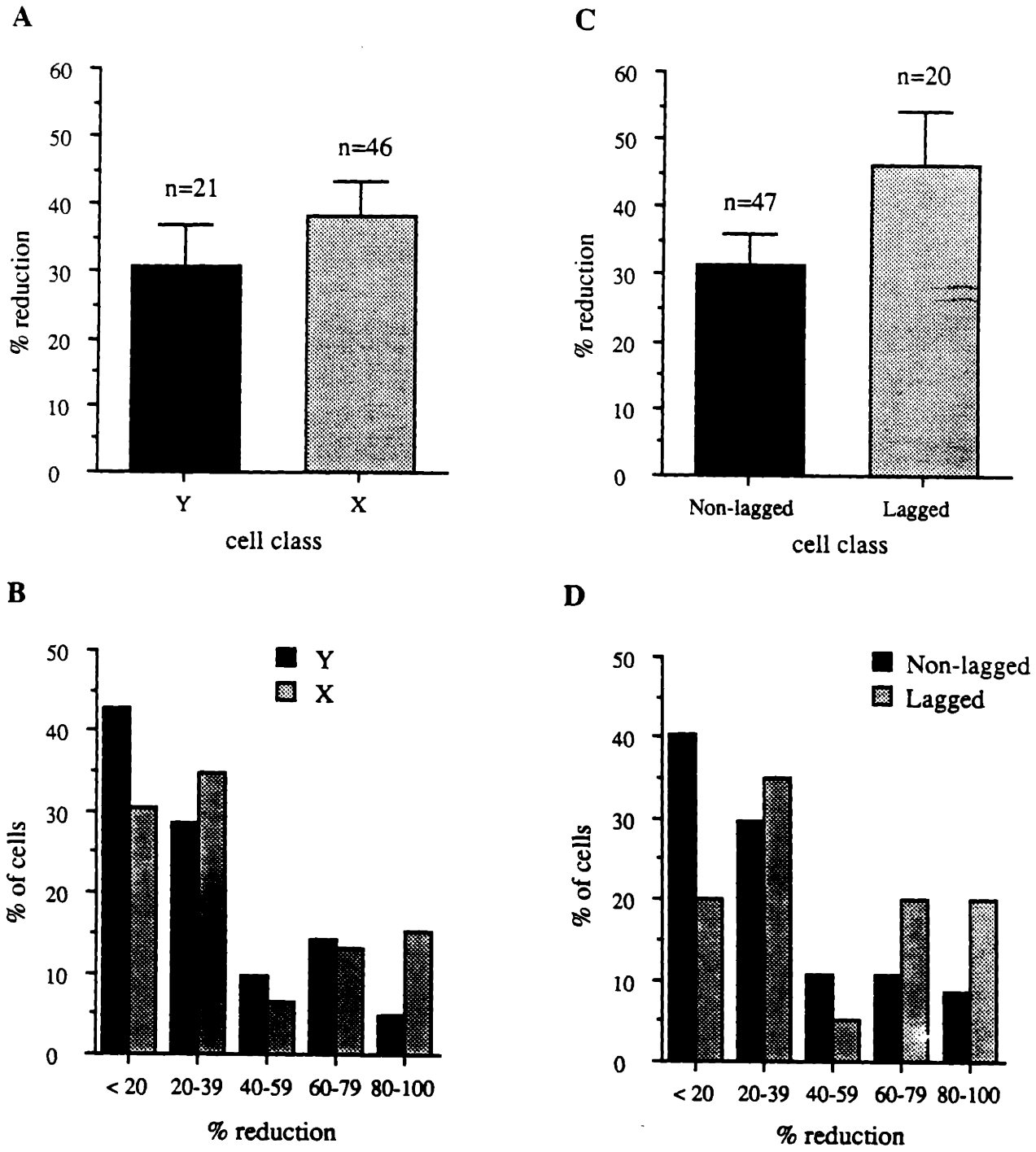
A
60
50
40
30
20
10
0
% reduction
n=21
n=46
Y
X
cell class
C
60
50
40
30
20
10
0
% reduction
n=47
n=20
Non-lagged
Lagged
cell class
B
50
40
30
20
10
0
% of cells
Y
X
< 20
20-39
40-59
60-79
80-100
% reduction
D
50
40
30
20
10
0
% of cells
Non-lagged
Lagged
< 20
20-39
40-59
60-79
80-100
% reduction

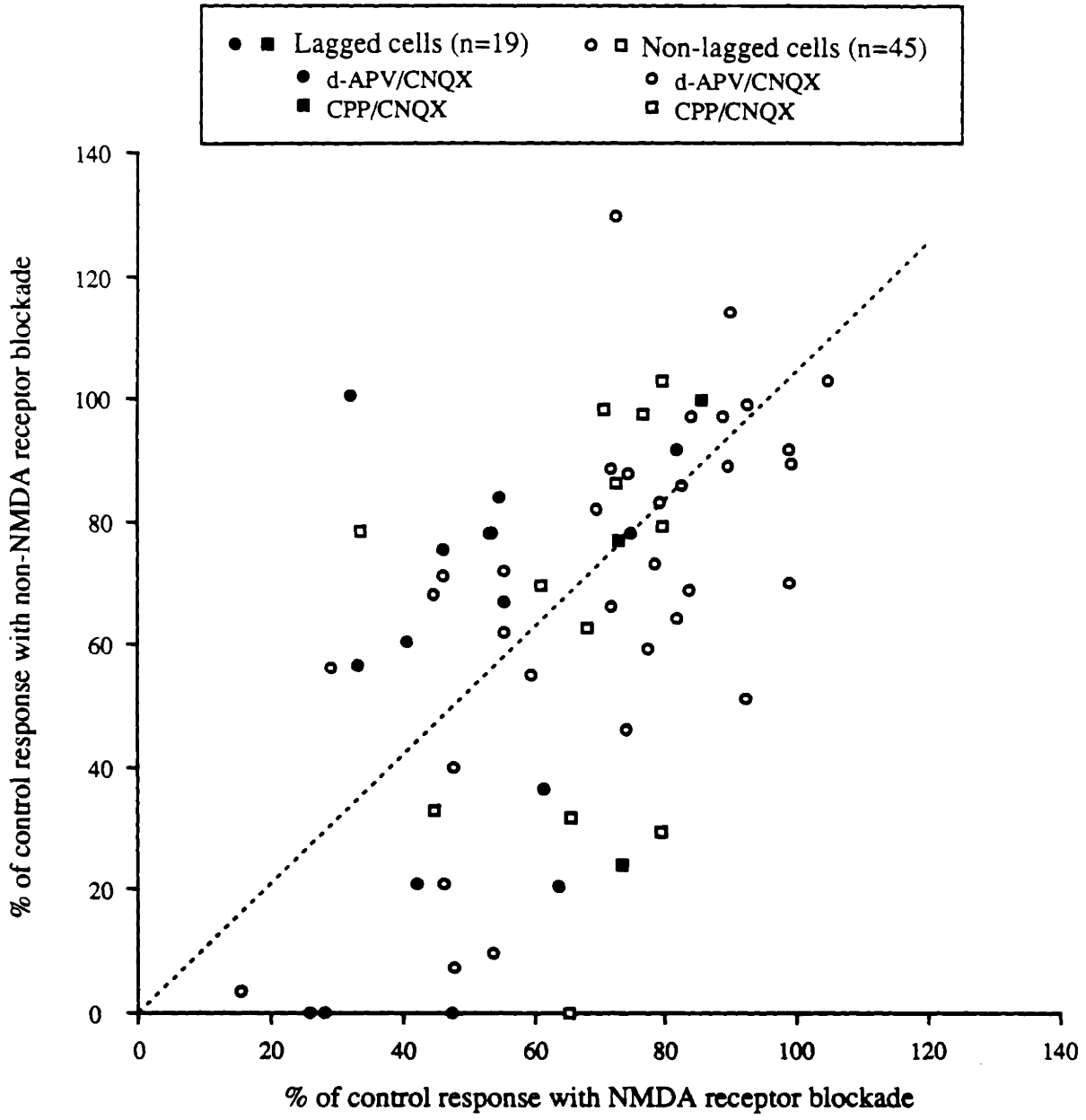
Lagged cells (n=19)
d-APV/CNQX
CPP/CNQX
Non-lagged cells (n=45)
d-APV/CNQX
CPP/CNQX
% of control response with non-NMDA receptor blockade
% of control response with NMDA receptor blockade
0
20
40
60
80
100
120
140

TABLE 1. Visual latencies of X cells. [All values represented as mean ± SE.]

Cell type	Onset latencies (ms)		Offset latencies (ms)	
	start-rise	half-rise	start-fall	half-fall
Non-lagged X	32.6±1.4 (n=39)	40.8±1.3 (n=39)	22.4±1.7 (n=33)	30.1±1.9 (n=33)
Lagged X	63.0±3.9 (n=23)	79.0±5.9 (n=23)	67.0±7.9 (n=14)	84.4±7.1 (n=14)

TABLE 2. Visual latencies of Y cells.
[All values represented as mean ± SE.]

Cell type	Onset latencies (ms)	
	start-rise	half-rise
Non-lagged Y	29.6±1.5 (n=34)	38.7±1.5 (n=34)
Lagged Y	54.4±3.9 (n=5)	64.9±3.1 (n=5)

TABLE 3. Effect of d-APV on early and late components of visual responses.
[All values represented as mean percent reduction ± SE.]

Cell type	*n*	Early component	Late component
Non-lagged X	16	29.1±5.9	29.6±8.6
Lagged X	16	30.7±8.6	61.4±5.4
Non-lagged Y	12	37.1±7.4	33.4±6.3
Lagged Y	1	57.2	59.3

TABLE 4. Effect of CNQX on early and late components of visual responses.
[All values represented as mean percent reduction ± SE.]

Cell type	*n*	Early component	Late component
Non-lagged X	21	35.8±8.6	44.1±7.6
Lagged X	16	43.7±11.7	36.4±9.5
Non-lagged Y	13	30.6±7.4	27.5±6.9
Lagged Y	3	58.1±23.1	30.8±25.2

TABLE 5A. Effect of d-APV on On- and Off-center cells.
[All values represented as mean percent reduction ± SE.]

Cell type	On-center	Off-center
X	35.2±4.0 (n=27)	40.0±6.7 (n=10)
Y	33.1±9.2 (n=10)	30.9±6.1 (n=10)
All	34.6±3.7 (n=37)	35.5±4.5 (n=20)

TABLE 5B. Effect of CNQX on On- and Off-center cells.
[All values represented as mean percent reduction ± SE.]

Cell type	On-center	Off-center
X	36.2±5.9 (n=33)	46.1±9.7 (n=13)
Y	40.9±9.4 (n=12)	17.3±3.1 (n=9)
All	37.4±4.9 (n=45)	34.3±6.5 (n=22)

CHAPTER 3

EFFECT OF STIMULUS CONTRAST AND SIZE ON NMDA RECEPTOR ACTIVITY IN THE CAT'S LATERAL GENICULATE NUCLEUS

SUMMARY AND CONCLUSIONS

1. We studied the effect of varying excitatory and inhibitory drive on the N-Methyl-D-Aspartate (NMDA) receptor-mediated component of the visual responses of neurons in the cat dorsal lateral geniculate nucleus (dLGN), by varying the contrast and size of stimuli presented to the receptive fields of these cells.

2. Cells were classified as either on- or off-center, X or Y and lagged or nonlagged. Stimulus contrast, and hence the amount of excitatory drive, was varied by changing the brightness of a spot, whose size and location matched the cell's receptive field center, relative to a fixed background luminance. Responses to varying contrast were collected from each cell before, during and after iontophoretic application of d-2-amino-5-phosphonovaleric acid (d-APV), a specific NMDA receptor antagonist. From each Contrast-Response plot, a sigmoidal curve fit yielded five parameters on which we examined the effect of d-APV: the threshold contrast, saturation contrast, contrast at half saturation (C_{50}), slope (gain) at C_{50}, and saturation response.

3. In most cells, application of d-APV reduced both the saturation response and the gain of the Contrast-Response curve, but did not reduce or change significantly the threshold contrast, saturation contrast or C_{50}.

4. Cells varied in their sensitivity to d-APV, but for any given cell the d-APV sensitive component was nearly always a *linear* function of the control visual response level. Thus, for a spot of optimal size, there was a constant proportion of the visual response attributable to NMDA receptors, regardless of the amplitude of the response.

5. When the effect of d-APV on the visual responses to an optimal spot at varying contrasts was compared among different classes of dLGN cells, the visual responses of lagged X cells were reduced to a greater extent than those of either nonlagged X cells or the combined population of nonlagged X and Y cells (see also Heggelund and Hartveit 1990; Kwon et al. 1991).

6. Stimulus size (spot diameter) was also varied systematically at a fixed contrast in order to vary the inhibitory drive to dLGN cells. As stimulus size was increased, the response first increased due to increased stimulation of the receptive field center, and then decreased due to increasing amounts of surround inhibition.

7. The d-APV sensitive component was greater when the stimulus spot was less than or equal to optimal size than when the spots were larger. Furthermore, for those cells in which the effect of varying the contrast of a spot of optimal size was studied in addition to the effect of varying spot sizes, the d-APV sensitivity determined at optimal spot size was greater than that when spots were larger than optimal. Thus the contribution of NMDA receptors to the visual response decreased with increasing surround inhibition.

8. These results show that the fraction of the visual response of a dLGN cell mediated by NMDA receptors is not modulated by the amount of retinal excitatory drive. Rather, the proportional contribution of NMDA receptors to the visual response remains the same once the dLGN cell reaches its threshold for firing action potentials. The results also suggest that the relative contribution of NMDA receptors may be decreased by lateral inhibition in the dLGN. Thus modulation of NMDA receptor activation on dLGN cells during visual transmission appears to be a dynamic, ongoing, process subject to the specific spatial distribution of excitation and inhibition on dLGN cells.

INTRODUCTION

Excitatory amino acid (EAA) receptors mediate synaptic transmission in many areas of the vertebrate central nervous system (for reviews see Cotman et al. 1987; Mayer and Westbrook 1987). These receptors can be broadly categorized into two groups: the N-Methyl-D-Aspartate (NMDA) receptors, and non-NMDA receptors. The latter group includes quisqualate and kainate receptors, which may or may not comprise separate classes. The two types of EAA receptors differ not only in their responses to various agonists, but also in their ionic selectivities and voltage dependence. Non-NMDA receptors conduct primarily monovalent Na^{+}/K^{+} ions when activated (MacDermott and Dale 1987; see, however, Gilbertson et al. 1991), while NMDA receptors also conduct divalent cations such as Ca^{++}. In addition, the NMDA receptor channel, unlike most other ligand-gated channels, is voltage-dependent; at hyperpolarized, but not depolarized, potentials it is blocked by physiological levels of Mg^{++} ions (Mayer and Westbrook 1987). These properties of the NMDA receptor enable postsynaptic neurons to increase their permeability to Ca^{++} in response to pre- and postsynaptic coactivation. Increases in intracellular Ca^{++} can then trigger long-term changes in transmission. Thus, activation of NMDA receptors has been shown to be necessary for the induction of a long-term potentiation in the hippocampus (e.g. Kauer et al 1988) and visual cortex (Artola and Singer 1987), and to play an important role in establishing specific connections within the developing optic tectum (Cline et al. 1987), lateral geniculate nucleus (Hahm et al. 1991), and visual cortex (Bear et al. 1990).

In addition to the NMDA receptor's well established role in synaptic plasticity, there is growing evidence that NMDA receptors are also involved in normal sensory transmission. A number of *in vivo* and *in vitro* studies have shown that both types of EAA receptors contribute to retinogeniculate transmission (Kemp and Sillito 1982; Sillito

et al. 1990a,b; Crunelli et al. 1987; Scharfman et al. 1990; Esguerra et al. 1989; Heggelund and Hartveit 1990; Hartveit and Heggelund 1990; Kwon et al. 1991). Given the unique properties of the NMDA receptor, an important goal of pharmacological studies of retinogeniculate transmission is to characterize similarities and differences in the responses of dLGN cells mediated by the two types of EAA receptor. Iontophoretic studies in the cat dorsal lateral geniculate nucleus (dLGN) have shown that both receptors mediate visual responses in each of the major classes of relay cells (on- and off-center, X and Y). Although individual cells vary widely in their sensitivites to blockade of NMDA and non-NMDA receptors, no consistent differences in the role of the two receptor types are observed between these dLGN cell classes (Sillito et al. 1990a,b; Kwon et al. 1991).

Recently, relay neurons in the cat dLGN have also been classified with respect to the temporal properties of their responses to stimuli turning on or off within their receptive fields (Mastronarde 1987a,b; Mastronarde 1988; Humphrey and Weller 1988a; Saul and Humphrey 1990). Nonlagged cells respond to such stimuli with a time course that is similar to that of retinal ganglion cell responses. Their responses are characterized by transient discharge at short latency following stimulus onset. In contrast, lagged cells have a long visual latency to a flashing stimulus and lack the initial onset transient burst of discharge. Most lagged cells also have an offset discharge that decays slowly to background levels. Lagged X cells have very tonic or sustained responses to maintained stimuli. Lagged and nonlagged cells may represent unique dLGN cell classes (Humphrey and Weller 1988b), or different response modes of the same neuron (Uhlrich et al. 1990). Iontophoretic studies *in vivo* have shown that although both types of cell are susceptible to NMDA and non-NMDA receptor blockade, the visual responses of lagged cells are affected more by NMDA receptor anatgonists than those of nonlagged cells (Heggelund and Hartveit 1990; Kwon et al. 1991).

A motivation for the present study was to examine the differences in sensitivity to

NMDA receptor blockade which we and others have observed both within and across relay cell classes. Given the voltage-dependence of the NMDA response in the LGN *in vitro* (Esguerra et al. 1991), we wished to test the hypothesis that differences in sensitivity to NMDA receptor blockade reflect differences in the balance of excitation and inhibition evoked by visual stimulation. In a previous study we found that the difference between lagged and nonlagged cells in the sensitivity to NMDA receptor blockade was *not* correlated with the visual activity levels of the two populations (Kwon et al. 1991). Comparisons across cells may however be complicated by technical difficulties of iontophoretic experiments. It is difficult to know, for example, whether differences between cells reflect different cellular properties or variations in the efficacy of antagonism. In the present study, we have examined this issue more carefully by studying the NMDA receptor contribution to individual cell responses while presenting a range of different visual stimuli. By varying the contrast of a small spot, we varied the amount of *excitatory* drive to the cell (see also Fox et al. 1990). By varying the size of the spot, we varied the amount of *inhibitory* drive to the cell through surround inhibition (Hubel and Wiesel 1961).

Our results show that the fraction of the visual response mediated by NMDA receptors remains the same when the excitatory drive to dLGN cells is varied by varying stimulus contrast. Hence the NMDA receptor component at low visual response levels is proportionately the same as at high response levels. However, the contribution of NMDA receptors becomes proportionately smaller as the amount of inhibitory input is increased by increasing the stimulus size.

METHODS

Animal Preparation

Experiments were performed on adult cats that were prepared for extracellular electrophysiological recording as described previously (Sur et al. 1987, Kwon et al. 1991). Briefly, animals were anesthetized (induction and surgery using 3% halothane in 70% N2O / 30% O2; maintenance on 0.6-1% Halothane), paralyzed (3.6mg/hr gallamine triethiodide and 0.7 mg/hr d-tubocurarine) and artificially ventilated. End-tidal CO_2 was maintained at 4% and body temperature at 38 °C. An electrocardiogram was continuously monitored to maintain the heart rate at the pre-paralysis rate by appropriately adjusting the halothane dose. Pupils were dilated and a set of contact lenses were fitted to focus the eyes on an oscilloscope screen 57cm in front of the animal. The precision of focus was insured by using an ophthalmic retinoscope as well as by reflecting an image of the retinal surface onto a tangent screen. A pair of bipolar stimulating electrodes was placed across the optic chiasm. A 1-2 cm diameter craniotomy was made to expose the cortex overlying the dLGN.

Microiontophoresis

A six-barreled glass micropipette electrode assembly was used for extracellular recording as well as for iontophoretic application of various drugs (Kwon et. al, 1991). The recording micropipette was filled with 3M KCl and each of the other pipettes was filled with one of the following solutions (in H_2O): NMDA (50mM, pH 8.0), kainic acid (KA 20mM, pH 8.0), d-APV (50mM, pH 8.0), and 6-cyano-7-nitroquinoxaline-2,3-dione (CNQX 12.5mM, pH 9.8). A barrel filled with 150mM NaCl was used as a

balance barrel, and in a few cases was used to assess direct effects of iontophoretic current.

Antagonists were applied at doses found to be adequate yet specific with respect to responses to applied agonists. This was achieved by carefully titrating the antagonist dose until it completely blocked the appropriate agonist response (NMDA for the antagonist d-APV and KA for the antagonist CNQX), but not responses to other agonists (see Kwon et al., 1991 for details). Visual responses at various spot contrasts and sizes were collected before, during and after application of each antagonist.

Cell Classification

The receptive field of each cell was plotted on a tangent screen and was classified as either on- or off-center and X or Y. The latter classification was based on the receptive field size at a given eccentricity, latency to optic chiasm stimulation, and linearity of spatial summation determined with a counterphasing grating (Sherman and Spear 1982; Shapley and Lennie 1985; Sur et al. 1987). Cells were also divided into lagged and non-lagged types based on their visual latencies at onset of a spot of the appropriate contrast (Mastronarde 1987a, 1988; Humphrey and Weller 1988a; Saul and Humphrey 1990, Heggelund and Hartveit 1990; Hartveit and Heggelund 1990; see Kwon et al. 1991 for specific criteria). Lagged cells had start-rise and half-rise visual latencies greater than 45 and 55ms respectively; those of non-lagged cells were smaller than these values.

Visual Stimulus

The stimulus was produced with a "Picasso" stimulus generator (Innisfree Inc., Cambridge, MA) under microcomputer (IBM compatible PC) control and presented on a

Tektronix 620 monitor. The visual stimulus consisted of a spot whose luminance varied from darker than background to brighter than background. Contrast was calculated as (Center Luminance - Background Luminance) / (Center Luminance + Background Luminance). In the case of on-center cells, for example, negative contrast consisted of spots darker than background and positive contrast, the spots brighter than background. In one set of experiments, spot contrast was modulated from light to dark at 2 Hz and spot size was matched to the receptive field center size . To minimize the effect of any systematic changes in response during the test period, 12 to 24 different contrast levels were interleaved in a random order for a given cell and each contrast level was presented a total of 10 times. Background screen luminance was 5.87 cd/m^2 and represented the zero contrast level; the response at zero contrast was taken to be the background firing level. (In later experiments, mean luminance was varied between two values, 3.00 and 8.14 cd/m^2, for on- and off-center cells respectively, to obtain a greater positive range of contrasts.) Maximal ranges of contrasts obtained this way were between -0.85 to 0.73 for on-center and between -0.4 to 0.95 for off-center cells. In a second set of experiments, stimulus spot size was systematically varied between 0.5, 1, 2, 4, and 8 times the cell's receptive field center size; spots were presented randomly and each size was presented 10 times. Stimulus contrast was kept constant for a given cell and ranged between 0.5 and 0.72 for on-center cells and 0.85 and 0.95 for off-center cells. All responses were collected on-line and stored in the microcomputer as well as onto videotape using a data encoder for off-line analysis (Neurocorder DR-886, Neuro Data Instruments, New York, NY).

Data Analysis

Averaged peristimulus time histograms (PSTH) were constructed from the 10

trials for each spot contrast and sizeo obtained before, during and after antagonist application. Mean firing rate over entire response period (500ms) as well as peak firing rate (using a 100ms moving average window) was computed and plotted as a function of spot contrast and size.

Contrast-Response plots were constructed by plotting mean firing rate against stimulus contrast. The plot was fitted with an expression of the form:

$R = R_s \times C^n / (C^n + C_{50}{}^n) + R_m,$

where R = response, C = contrast, Rs = saturation response, Rm = minimum response, , C_{50} = contrast at half saturation response, and n = measure of steepness of the linear portion. The function, when plotted, is of a sigmoidal shape. Thus the curve fit assumes the response has a stable minimum and a maximum (saturation), and a linear range between the two. The saturation response, minimum response and C_{50} are directly determined by the curve fit. The slope at C_{50} can be derived by differentiating the expression and evaluating R at C_{50}. We defined the threshold and saturation contrasts as the points on the abscissa where the line crossing the C_{50} point with the slope calculated as above crosses the minimum and maximum response respectively. The five parameters from the Contrast-Response function that we used to examine the effect of d-APV were the threshold contrast, saturation contrast, contrast at half saturation (C_{50}), slope at C_{50} and saturation response (see Fig. 1). Note that the threshold and saturation contrasts define the linear range and the slope defines the gain of the function.

In order to determine whether or not the NMDA receptor-mediated component of the response remains constant with response level, we plotted the d-APV sensitive component of the visual response as a function of the control response amplitude (that is, before the application of antagonist). The d-APV sensitive component was calculated by subtracting the response obtained during d-APV application from the control response. A linear plot would indicate that NMDA receptors contribute a constant fraction of the overall response, with the fraction determined by the slope of the line. The d-APV

sensitive fractions were compared between different cell classes using an unpaired nonparametric statistical test (Mann-Whitney U test).

The responses to different sized spots were divided into two groups. The (receptive field) "center" responses comprised those responses collected at sizes equal to or smaller than the optimal size; the "center+surround" responses comprised responses collected at sizes greater than the optimal spot size. The optimal size was defined as the stimulus size at which the cell's response was the greatest, therefore representing the size closest to the receptive field center size. The d-APV sensitive fractions of the "center" and "center+surround" responses were compared with each other as well as with the d-APV sensitive fractions obtained from the contrast study using a paired nonparametric test (Wilcoxon signed rank test).

RESULTS

We report on a total of 39 cells recorded from the A laminae of the dLGN, including 24 X cells and 15 Y cells. The X cells included 20 nonlagged cells and 4 lagged cells. All the Y cells were nonlagged; we recorded no lagged Y cell in the present study. Our criteria for classifying cells as X or Y and as lagged or nonlagged have been described in detail previously (Kwon et al. 1991), and these criteria were adhered to strictly in the present study. Of the total, 38 cells were tested with varying stimulus contrast (19 nonlagged X cells, 4 lagged X cells, and 15 nonlagged Y cells) and 34 cells were tested with varying stimulus size (20 nonlagged X cells, 1 lagged X cell, and 13 nonlagged Y cells).

Effect of contrast on the d-APV sensitive components of visual responses

Fig. 1 shows the effect of contrast on the visual response of an off-center nonlagged X cell. The cell's response approximates a sigmoidal shape, with a minimum and saturation response and linear range inbetween. Positive contrasts indicate spots darker than background luminance and negative contrasts indicate brighter spots (see Methods). At zero contrast (no visible spot, background mean luminance of 5.87 cd/m^2) there was still a fair amount of response and only for negative contrast values, did the cell's response reach a sustained minimum. We always presented spots with both negative and positive contrasts to ensure a full range of visual responses. A sigmoidal curve fit yielded the parameters that are useful for characterizing the function (see Methods). The linear contrast range for this cell was -0.08/0.28; the C_{50} was 0.10. The slope at C_{50} was 49.09 ($r = 0.990$), and the saturation response was 19.14 spikes/s. The slope provides a measure of the *gain* with which the input (contrast) is encoded into

firing rate. The Contrast-Response plots of most cells were similar to the one shown in Fig. 1 (see Fig. 2, 3 and 5).

Fig. 1 about here

Fig. 2A shows the Contrast-Response curve from the same cell before, during and after 60nA of d-APV application. The levels of d-APV ejection current used in the study were carefully adjusted to block NMDA receptor responses without affecting responses to applied kainate, and were generally between 60 and 90nA (Methods; see also Kwon et al. 1991). The Contrast-Response curve obtained during d-APV application was similar in its overall shape to that obtained prior to drug ejection. There was no significant change in the threshold or saturation contrasts. The slope at C_{50}, however, decreased significantly from 49.09 to 21.67 (a reduction of 56%) and the saturation response decreased from 19.14 to 11.38 spikes/s. Thus the blockade of NMDA receptors appeared to have significantly decreased the contrast gain and saturation response while having only limited influence on the threshold contrast, saturation contrast and C_{50}. Conversely the contribution of NMDA receptors was to increase the gain and saturation response of the Contrast-Response curve without significantly changing the contrasts at which the response reached threshold or saturation. That is, the function of NMDA receptors was to amplify the visual signal in the linear range of the response.

Fig. 2 about here

Sigmoidal curves were fitted to the Contrast-Response curves of all 38 cells. A subset of 25 (13 nonlagged X and 12 nonlagged Y) cells that yielded a reasonably good fit ($r \geq 0.80$; mean $r = 0.95$) was chosen for population analysis. [In 9 of the remaining

13 cells, curve fits to the sigmoidal function were not appropriate; visual responses of the 9 cells (4 nonlagged X, 4 lagged X and 1 nonlagged Y) were so severely reduced by d-APV application (86.1 ± 4.7 % reduction) that sigmoidal curve fits of responses obtained during d-APV application produced threshold and saturation contrasts that were rather arbitrary. Four of these 13 cells generally produced poor fits to the sigmoidal function. The variations in data points were likely due to several sources, including fluctuations in the "background" firing level of the cells. Importantly, all 4 cells had their saturation response severely affected by d-APV]. Table 1 compares five relevant parameters of the Contrast-Response curve before and after d-APV application. Consistent with the results obtained from the cell shown in Fig. 2A, the population parameters show little change in the threshold contrast, saturation contrast and C_{50} during d-APV application ($p > 0.2$ for all three parameters, Wilcoxon signed rank test). Of the 25 cells pooled, 1 cell showed a significant change in threshold contrast with d-APV application while 5 cells showed a significant change in the saturation contrast. The slope at C_{50} and the saturation response however showed significant decreases with d-APV ($p < 0.001$ for both parameters, Wilcoxon signed rank test).

Table 1 about here

In Fig. 2B the d-APV sensitive component of the visual response (as calculated by subtracting the response during d-APV application from the control response) is plotted as a function of the magnitude of the control visual response (visual response minus background activity). The relationship is *linear*, implying that the d-APV sensitive component remained proportionally the *same* throughout the entire range of visual response. The points are well fitted by a line of slope 0.52 (r=0.982) indicating that 52% of the visual response at any contrast was due to NMDA receptors and was

hence sensitive to NMDA receptor blockade. This value (which will be referred to as the "d-APV sensitive fraction" hereafter) also corresponds closely to the change in the gain of the Contrast-Response curve in Fig. 2A. This linear relationship, though initially unexpected because of the nonlinear relationship between the ionic conduction of the NMDA receptor and membrane voltage (see Introduction), was quite consistent from cell to cell (see below). It is important to point out that varying the contrast of a spot confined to the receptive field center effectively changes the amount of *excitatory* retinal drive to a dLGN cell. Furthermore, extracellular recording monitors only the responses that are *suprathreshold* to the generation of action potentials.

Similar results were obtained from other cells, despite variation in the degree of d-APV sensitivity. Fig. 3A shows the Contrast-Response curves of another off-center nonlagged X cell before, during and after 86nA of d-APV application. The slope (or the gain) decreased significantly from 52.32 to 19.56 (reduction of 62.6%). Fig. 3B shows that the same cell's d-APV sensitive component is again a linear function of the visual response, with a slope of 0.75 (r=0.996). Fig. 3C shows a Contrast-Response curves from an on-center nonlagged Y cell. The visual response did not reach saturation up to a stimulus contrast of over 0.7. Nevertheless it is evident that d-APV affected the gain of the linear portion of the curve, which decreased from 152.37 to 52.93. Fig. 3D shows that the d-APV sensitive component was a linear function of the control response for the cell with a slope of 0.60 (r=0.996). Importantly, the three cells illustrated in Figs. 2 and 3 all showed a *linear* relationship between the d-APV sensitive component and the amplitude of the control visual response despite different absolute values of the d-APV sensitive fractions (Figs. 2B, 3B and 3D).

Fig. 3 about here

The linear relationship between the d-APV sensitive component and control visual

response was observed in *all* physiological classes of cells that we recorded. Fig. 4A shows an on-center nonlagged X cell for which slope of the d-APV sensitive component vs. control response line (the d-APV sensitive fraction) was 0.75 ($r = 0.99$). Fig. 4B shows an off-center lagged X cell in which the d-APV sensitive fraction of the visual response was also 1.00 ($r = 1.000$). That is, the visual response of this non-lagged X cell was completely abolished with the application of d-APV. All four lagged X cells that we recorded showed linear relationships and high values of the d-APV sensitive fraction of their visual responses (see below). Fig. 4C shows an on-center nonlagged Y cell in which the d-APV fraction was 0.58 ($r = 0.98$). A linear plot of the d-APV sensitive component as a function of the control response was found in most of the cells that we tested; 27 of the 38 cells we tested could be fit with a straight line with correlation coefficient (r) greater than 0.9. Of the remaining 11, 2 could be fit with $r > 0.8$ and 1 with $r > 0.7$. The mean correlation coefficient (r) for the entire population was 0.837 ± 0.044 ($n = 38$).

Fig. 4 about here

Fig. 5 shows two cells that did not show linear relationships between the d-APV sensitive component and the control visual response. Fig. 5A shows Contrast-Response curves from an off-center nonlagged X cell. As in the previous examples, the sigmoidal shape of the curve was retained during the d-APV application. The gain of the curve decreased from 102.66 to 44.53 while the saturation response decreased from 30.25 to 12.72 with d-APV. The plot of the d-APV sensitive component against the control response showed a slight nonlinearity (Fig. 5B). This was the only cell which showed an increase in the d-APV sensitive fraction with increasing control responses. Fig. 5C shows Contrast-Response curves from another off-center nonlagged X cell. Application

of 83nA of d-APV seemed to reduce the visual responses by a constant amount (except at the highest contrast), and the gain of the curve changed very little. The linear range of contrast decreased significantly from -0.13/0.72 to 0.17/0.47 but the C_{50} changed little from 0.29 to 0.32. The slope actually *increased* from 78.42 to 97.39 with d-APV. Fig. 5D shows that the cell's d-APV sensitive component is a highly nonlinear function; however, for the most part, the function is roughly constant (with a value near 14). The plot indicates that the absolute contribution of NMDA receptors to the visual response was approximately constant at all levels of response. Similar result has been reported in deeper layers of the cat visual cortex (see Fig. 4D of Fox et al. 1990). In general however, these nonlinear effects of d-APV were not common in the dLGN (observed in 8 of 38 cells); most cells showed a linear relationship between the d-APV sensitive component and control visual response level, with a slope between 0 and 1.

Fig. 5 about here

Proportion of the visual response mediated by NMDA receptors in different cell classes

The d-APV sensitive proportions obtained by varying stimulus contrast can be used to compare the NMDA receptor-mediated fractions of visual responses among different cell classes. Fig. 6 shows the frequency distribution histogram of the d-APV sensitive proportions in the three different cell types we recorded. The lagged X cells as a group had the greatest proportion of their visual responses mediated by NMDA receptors (mean of 0.896 ± 0.065, $n = 4$). The nonlagged X cells were next with a mean proportion of 0.636 ± 0.070 ($n = 19$) while the nonlagged Y cells showed a mean of 0.567 ± 0.100 ($n = 15$). The difference between lagged X and nonlagged Y cells was

statistically significant ($p < 0.04$, Mann-Whitney U test) as was the difference between lagged X cells and the combined population of nonlagged X and Y cells ($p < 0.04$, Mann-Whitney U test).

Fig. 6 about here

Simultaneous blockade of NMDA and non-NMDA receptors

Finally, in a few cells (n = 3) we also applied CNQX, a specific non-NMDA receptor antagonist, to see whether the remaining visual response in the presence of d-APV, the NMDA receptor antagonist, is mediated by non-NMDA receptors. Fig. 7 shows the Contrast-Responses curves of an off-center nonlagged X cell (the same cell as in Fig. 5A). Application of d-APV significantly decreased the visual response; simultaneous application of d-APV and CNQX completely abolished the visual response, indicating that all of the visual response of this neuron was mediated by EAA receptors.

Fig. 7 about here

Effect of spot size on the d-APV sensitive component of the visual response

Fig 8 shows the visual responses of an off-center nonlagged X cell to a spot of increasing size (at a fixed contrast of 0.92). Peak firing rates using a 100 ms moving average window are shown because they showed slightly greater depth of modulation with changes in stimulus size than average firing rates over 500 ms response period. Both measures, however, yielded the same qualitative results. The cell's response

increased as the spot diameter increased from 0 (no spot) to 1.2 to 2.4 cm (the optimal size). As the size increased further to 4.8 and 9.6 cm, the response decreased as a result of increasing surround inhibition (due to both retinal and geniculate mechanisms). It is apparent that two different spot sizes can produce the same magnitude of response. For example, in Fig. 8, the response are similar at spot diameters of 1.2 and 9.6 cm (62.0 and 64.0 spikes/s at 1.2 and 9.6 cm respectively). However the mechanism by which this sub-maximal response is achieved differs for the two spot sizes: the small spot does not provide enough excitatory drive, while the large spot likely engages intraretinal inhibition (causing some reduction in retinal excitatory drive) as well as increased lateral intrageniculate inhibition (Sillito and Kemp 1983; see also below). In order to facilitate comparison, we divided these responses into two groups: "center" responses which included responses to spots equal to or smaller than the optimal size, and "center+surround" responses which included responses to spots greater than the optimal size (the dotted line shows the division between the two groups in Fig. 8). We were interested in determining whether the responses mediated solely by the receptive field center and responses that were also subject to surround inhibition were equally sensitive to d-APV. While such a division is somewhat arbitrary, reducing spot sizes into the two groups allowed us to address the question easily. Furthermore, results obtained from different cells could be easily combined by "normalizing" spot sizes with respect to the receptive field center diameter.

Fig. 8 about here

Fig 9A shows the responses of the same cell (as shown in Fig. 8) before, during and after 86nA of d-APV application. While d-APV decreased the background activity and the responses at all spot sizes, the extent of the decrease was greater for the "center" responses than for the "center+surround" responses. To compare the effect of d-APV on

the visual response alone, the background response (either pre- or during d-APV application) was subtracted from each of the responses (Fig. 9B). The two "center" responses (at 1.2 and 2.4 cm) decreased significantly (by 92% and 71% respectively), while one of the "center+surround" responses (at 4.8 cm) decreased only slightly (by 33%) and the other (at 9.6 cm) actually *increased* (by 92%) with d-APV (Fig. 9C). This differential effect of d-APV is especially clear if one compares the responses at 1.2 and 9.6 cm. Even though the control responses at the two sizes were similar, d-APV decreased the former but increased the latter. Proportional reductions were computed for each of the two groups by combining the 2 "center" responses (at 1.2 and 2.4 cm) together as well as the 2 "center+surround" responses (4.8 and 9.6 cm) together; the sum of the reductions by d-APV was divided by the sum of the control responses in each of the two groups. Fig. 9D shows that the d-APV sensitive fraction of the "center" responses was substantially greater than that of the "center+surround" responses (0.76 and -0.04 respectively).

Fig. 9 about here

Different levels of contribution of NMDA receptors to the two groups of responses were evident in all cell classes. Fig. 10 shows results from four different cell types. In each case, the d-APV sensitive proportion was greater for the "center" than for the "center+surround" responses. Figs. 10A and 10B show an off-center nonlagged X cell whose d-APV sensitive fractions of the "center" and "center+surround" responses were 0.70 and -0.23 respectively. Figs. 10C and 10D show an on-center nonlagged X cell whose d-APV sensitive fractions of the "center" and "center+surround responses" were 1.00 and 0.52 respectively. Figs. 10E and 10F show an off-center lagged X cell whose d-APV sensitive fractions were 1.00 and 0.64, while 10G and 10H show an on-

center nonlagged Y cell whose d-APV sensitive fractions were 0.80 and 0.41. Fig. 10 shows that neither the particular optimal spot size nor the particular value of the d-APV sensitive fraction for a given cell affect the fact that increased (intrageniculate) surround inhibition (via larger spots) decreased the proportional contribution of NMDA receptors to the visual response.

Fig. 10 about here

For each cell tested we calculated the difference between the d-APV sensitive fractions of the "center" and "center+surround" responses ("center" minus "center+surround"). The results are shown in the frequency distribution histogram of Fig. 11. The "0" column contains cells whose d-APV sensitive fraction of the "center" responses was within ± 0.05 of the "center+surround" responses. The positive columns show cells in which the d-APV sensitive fraction of the "center" responses was greater than that of the "center+surround" responses. The negative columns represent cells in which the reverse was true. The data show that although cells vary widely in the relative d-APV sensitivity of their "center" and "center+surround" responses, the distribution is biased in favor of cells showing greater d-APV sensitivity for "center" responses. The mean d-APV sensitive proportion of the "center" responses was 0.581 ± 0.053 (n=34) and that of the "center+surround" responses was 0.353 ± 0.106 (n=34). The mean of the individual differences between the two was 0.228 ± 0.085 (marked by triangle in Fig. 11) and this difference was statistically significant ($p < 0.02$, Wilcoxon signed rank test). These results suggest that intrageniculate inhibition induced by stimulating larger regions of retina (and dLGN) reduces the activation of NMDA receptors mediating the visual responses of dLGN neurons.

Fig. 11 about here

Comparison between responses evoked by varying contrast and spot sizes

The Contrast-Response functions before and after d-APV application, and hence the contribution of NMDA receptors to the visual responses at different contrasts, were obtained with the spot size fixed at optimal. The Size-Response functions, on the other hand, were obtained with spots at a fixed contrast. However, given the linear relationship between the d-APV sensitive fraction and control visual response at different contrasts (Figs. 2-4), the fraction obtained from the first study should match closely the "center" responses obtained from the second study. We wished to establish if this was true for individual cells. We also wished to compare the fraction obtained from the first study to the fraction from the "center+surround" responses obtained from the second study.

Fig 12A shows the frequency distribution histogram of the difference in the d-APV sensitive fraction between the value obtained by varying contrast at optimal spot size and the value for "center" responses (for the same cell) obtained by varying spot sizes at a fixed contrast. The positive columns indicate cells whose d-APV sensitive proportion was greater for the optimal spot than for the "center" spots. The difference in the d-APV sensitive fractions was not statistically significant (mean of the individual differences = 0.073 ± 0.050, represented by the triangle in Fig. 12A; $p > 0.2$, Wilcoxon signed rank test). On the other hand, the difference between the d-APV sensitive fraction at optimal spot size and "center+surround" responses (0.288 ± 0.113, marked by triangle in Fig. 12B) was statistically significant ($p = 0.02$; mean for optimal spots, 0.634 ± 0.053; mean for "center+surround", 0.346 ± 0.113; $n = 32$). Thus, the d-APV sensitive fraction is smaller with surround inhibition than with center stimulation alone, whether the center

was driven with varying contrasts at a fixed optimal spot size or by varying sizes (up to and including the optimal size) at a fixed contrast.

Fig. 12 about here

In summary, these results suggest that different levels of retinal excitatory drive activate a *constant* proportion of NMDA receptors on dLGN neurons and therefore do not modulate NMDA receptor activation, at least when monitored extracellularly. However, increasing (the spatial extent of) intrageniculate inhibition does reduce the proportion of the visual response mediated by NMDA receptors. That is, altering the balance of excitation and inhibition on dLGN neurons *via* intrageniculate inhibition *can* modulate the level of NMDA receptor activation.

DISCUSSION

There are three main results of the present study. First, NMDA receptors contribute to visual responses of dLGN cells, but predominantly in the linear range of the Contrast-Response curve. Second, the magnitude of the d-APV sensitive component of the visual response is a *linear* function of the control visual response level. Third, the d-APV sensitive component of the visual response decreases with increasing surround inhibition.

Contribution of NMDA receptors to visual responses

Blockade of NMDA receptors reduced the slope and the amplitude of the saturation response of the Contrast-Response curve. It did not, however, significantly change the threshold contrast, saturation contrast or the contrast at half saturation (C_{50}). These results are similar to those obtained in a recent report on the role of NMDA receptors in the superficial layers of the cat's visual cortex (Fox et al. 1990). In order to directly assess the magnitude of the NMDA receptor component at varying levels of visual responses, we plotted the d-APV sensitive component as a function of control response (Figs. 2, 3 and 4). This showed clearly that for most cells the NMDA receptor component is a *linear* function of the visual response amplitude. Hence d-APV reduced the smallest responses (near threshold contrast) just as much as it did the responses near saturation. However, even though the extracellularly recorded responses show a linear relationship, the *subthreshold* response need not be so. Indeed, recent *in vitro* studies both in the LGN (Esguerra et al 1991) and visual cortex (Jones and Baughman 1988) have shown nonlinear, voltage-dependent excitatory postsynaptic potentials (EPSPs) that are mediated by NMDA receptors.

Previous studies of hippocampus (Herron et al. 1986) or ventrobasal thalamus (Salt 1986) neurons have suggested that only high frequency inputs can activate NMDA receptors. In these studies, low frequency stimulation was apparently not sufficient to overcome the Mg^{++} block of NMDA receptors. On the basis of these studies, one might have predicted that NMDA receptor activation would be a non-linear function of retinal input; specifically one would predict little or no activation of NMDA receptors at low levels of excitatory input (and therefore low response levels) and proportionally greater activation at high levels of input (high response levels). This was *not* observed in the present study. The proportion of NMDA receptors involved in the visual response remained similar at low ("just suprathreshold") responses as well as at higher responses. Therefore, the threshold for complete activation of NMDA receptors must be equal to or lower than the threshold for spike generation; by the time a dLGN cell fires action potentials (ca. 54 mV; McCormick & Feeser 1990; Esguerra et al. 1991), the voltage-dependent block of NMDA receptors is essentially relieved completely, so that the receptor functions in classic linear fashion. A similar conclusion was reached regarding NMDA receptors on visual cortical neurons (Fox et al. 1990).

There are several possible explanations for the apparent differences between dLGN neurons and neurons in systems that have shown the necessity of high frequency stimulation for NMDA receptor activation. First, the visual responses that we measured extracellularly in the dLGN are driven by afferent retinal ganglion cells with background firing rates of 40 - 50 Hz (Kaplan et al. 1987). In addition, retinogeniculate afferent input is likely to be sustained in many cells for as long as the visual stimulus persists (0.5 s in our experiments). These more natural stimulus conditions are very different from the single electrical shocks delivered to afferent fibers that were used in the other studies. Tonic afferent inputs of 40 - 50 Hz are likely to provide sufficient postsynaptic depolarization to overcome the voltage-dependent Mg^{++} block of the NMDA receptor.

Second, dLGN cells *in vivo* receive input not only from retinal afferents but also from a variety of non-retinal sources (for review, see Sherman and Koch 1986). These inputs may serve to maintain the membrane potential of dLGN neurons at more depolarized levels than neurons in other systems. Third, ambient levels of glutamate (Sah et al. 1989) may tonically activate EAA receptors on dLGN neurons. Indeed even a single electrical shock to the optic tract has been found to be sufficient to activate NMDA receptors that contribute to excitatory postsynaptic potentials (EPSPs) in the LGN *in vitro* (Esguerra et al. 1989; Esguerra and Sur 1990; Scharfman et al. 1990), and single electrical stimuli can activate NMDA receptors in the ventrobasal thalamus of the rat as well (Salt and Eaton 1991).

Interaction of intrageniculate inhibition and NMDA receptor-mediated excitation

GABAergic inhibition is known to play a significant role in the processing of retinal signals in the dLGN (Sillito and Kemp 1983; Berardi and Morrone 1984; for review, see Sherman and Koch 1986). Local application of bicuculline in the dLGN reduces the strength of surround inhibition (Sillito and Kemp 1983). We used the fact that large stimuli generate increased lateral intrageniculate inhibition to study the effect of that inhibition on d-APV sensitivity. We found that responses to large stimuli were reduced less by d-APV than were responses to small stimuli. One interpretation of these results is that NMDA receptor activation decreases with increasing intrageniculate inhibition. Intracellular studies *in vivo* and *in vitro* suggest some possible synaptic mechanisms by which this could occur. *In vivo*, inhibitory postsynaptic potentials (IPSPs) in LGN relay neurons are of 3 types: short-, medium- and long-duration (Bloomfield and Sherman 1988). Based on reversal potential, the short-duration IPSPs

are believed to be mediated by $GABA_A$ receptors and the medium- and long-duration IPSPs, by $GABA_B$ receptors. *In vitro* studies have confirmed the presence of two pharmacologically distinct IPSPs in LGN neurons, a short-lasting (3-5 ms) IPSP mediated by $GABA_A$ receptors and a delayed (20-40 ms) long-lasting IPSP mediated by $GABA_B$ receptors (Hirsch and Burnod 1987; Crunelli et al. 1988; Soltesz et al 1989; for review see Crunelli and Leresche 1991). Both types of IPSPs can be elicited by optic tract stimulation in a LGN slice preparation that does not contain the perigeniculate nucleus, a potential source of inhibitory input to LGN relay cells. This leaves the intrinsic interneurons in the LGN as the source of the two IPSP types. The $GABA_A$ receptor mediated IPSP produces a shunting inhibition through Cl^- channels and the $GABA_B$ receptor produces hyperpolarization through K^+ channels.

Optic tract evoked EPSPs recorded in the LGN reveal NMDA receptor-mediated components which are relatively sustained (Scharfman et al. 1990; Esguerra et al. 1991). Similar results have been found in the ventrobasal thalamus (Salt and Eaton 1991) and visual cortex (Jones and Baughman 1988). Taken together with what we know of the two types of GABAergic inhibitions in the dLGN, it seems not unlikely that the long-lasting $GABA_B$ receptor mediated IPSP may be able to selectively reduce the sustained component of the EPSPs mediated by NMDA receptors in the dLGN. Furthermore, $GABA_B$ receptor mediated hyperpolarization can lead to Mg^{++} block of NMDA receptors, while actually increasing non-NMDA responses by increasing driving force. Indeed such $GABA_B$-mediated inhibition of the NMDA component of synaptic potentials has recently been reported in the hippocampus (Morrisett et al. 1991). However in the visual cortex, it has been also shown that NMDA receptor activation is blocked by $GABA_A$ receptor mediated inhibition (Artola and Singer 1987).

An alternative explanation for the observed difference between "center" and "center+surround" responses is that iontophoretic application of d-APV reduces excitation to relay cells as well as to intrageniculate interneurons, thus altering the balance

of excitation and inhibition on relay cells (this assumes that our results pertain mainly to relay cells). We observed several cells that increased their spontaneous firing rate with the application of d-APV (data not shown), and the response to the largest spot (presumably leading to the greatest amount of intrageniculate inhibition) was in several instances increased by d-APV (Fig. 10). A similar paradoxical increase in response with NMDA blockade in the dLGN has been recently reported for some cells by Hartveit and Heggelund (1990). Indirect evidence suggests that postsynaptic membranes of interneurons contain NMDA receptors. Retinal axons synapse onto relay cell and interneuronal elements in close proximity to each other within synaptic triads (Guillery 1969; Wilson et al. 1984; Hamos et al. 1987). In few cells recorded in slices of the LGN *in vitro*, optic tract evoked IPSPs (as well as the EPSPs) decrease with application of d-APV in dLGN slices (Esguerra et al. unpublished results). Similar findings have also been described in the dorsolateral septal nucleus of the rat (Gallagher and Hasuo 1989).

A simple model derived in the *Appendix*, that expresses the response of a dLGN relay cell as a linear function of afferent ganglion cell input (at least at a fixed contrast; cf. Kaplan et al. 1987), provides some insight into why the fraction of the visual response mediated by NMDA receptors decreases as the spot size increases to include center and surround. Briefly, this would happen if the d-APV sensitivity at retinal-interneuron synapses comes to be greater than that at retinal-relay cell synapses for large spot sizes. For a large enough increase in the former, application of d-APV would actually cause an increase in a relay cell's response to a large spot.

NMDA component of the visual response in different cell classes

When we compared the proportion of the visual response due to NMDA receptors among different physiological classes of cells in the dLGN, we found that NMDA

receptors contributed more to the responses of lagged X cells than nonlagged X or Y cells (we recorded no lagged Y cells in this study). This result is consistent with those of previous studies (Heggelund and Hartveit 1990; Kwon et al. 1991). The present results show that the difference in the proportional contribution of NMDA receptors between cell classes and indeed, between different cells, cannot be due to differences in visual response levels. This is also consistent with results from our previous study in which we found no correlation between the average level of (pre-drug) visual activity and the effect of d-APV on visual responses of lagged or nonlagged cells (Kwon et al. 1991).

Our results using large spots suggest that one possible reason why the fraction of the visual response mediated by NMDA receptors varies between cells is the amount of inhibition on cells. However, we found different NMDA-mediated proportions using spots of optimal size, that elicited little or no surround inhibition. It is also possible that the variable contribution of NMDA receptors results from technical aspects of microiontophoresis (e.g. distance of the iontophoretic barrel from dendrites, differences between cells in rates of diffusion, rates of uptake etc.). We consider this unlikely for two reasons. First, we were careful to wait a period of time (> 2 min) after the start of iontophoresis to allow drugs to reach a "steady-state" concentration around the cell from which we were recording. Second, optic tract evoked EPSPs in LGN neurons in a slice preparation also differ in their d-APV sensitivity even under the same concentration of d-APV (Esguerra et al. 1991). Therefore, the variability in the NMDA component of the visual response among different cells and cell classes is likely to be a reflection of different amounts of NMDA receptors that are either present on these cells or that are recruited for the visual response.

It is useful here to distinguish between two possible kinds of intrageniculate inhibition: feedforward inhibition and lateral inhibition (Fig. 13). It is reasonable to postulate that feedforward inhibition arises from the same afferents that provide the major

excitatory drive to a relay cell. Feedforward inhibition would increase as the excitatory drive from retinal afferents increases (such as with increasing stimulus contrast). However, the balance of excitation and inhibition would remain the same at different levels of contrast. Lateral inhibition arises from afferents that are spatially separate from those that provide the major excitatory drive to a relay cell; lateral inhibition would increase as stimulus size increases to include greater retinal area. Thus, the balance of excitation and inhibition would change as spot size is varied. Our results suggest strongly that the proportional contribution of NMDA receptors to dLGN cell responses can be modulated by lateral inhibition but not by feedforward inhibition at least at suprathreshold levels of response. Consistent with this view, we find that lagged cells, that are thought to receive greater feedforward inhibition (Mastronarde 1987b; Humphrey & Weller 1988b), are actually more sensitive to NMDA receptor blockade. Even for lagged cells, feedforward inhibition may be only part of the mechanism that gives rise to the lagged responses, for application of bicuculline results in only partial uncovering of the initial "inhibition" in their responses (Heggelund and Hartveit 1990). Other non-retinal inputs such as inputs from the brain stem (Uhlrich et al. 1990) or even intrinsic membrane properties of dLGN cells themselves (McCormick. 1990) may also contribute to generating lagged responses.

Role of NMDA receptors in the dLGN

At subthreshold levels, NMDA receptors on dLGN cells can mediate nonlinear transfer of retinal input to cortex (Esguerra et al. 1991). The nonlinear nature of NMDA receptor activation has been hypothesized to underlie the gating of retinogeniculate transmission by corticofugal input to the dLGN (Koch 1987) and this possibility has been recently demonstrated *in vitro* (Esguerra and Sur 1990). The current results show

that intrageniculate (GABAergic) inhibition can also modulate the efficacy of NMDA receptors in the dLGN. GABAergic interneurons in turn receive inputs from a variety of sources, including retinal, corticofugal (Weber et al. 1989) and cholinergic brain stem (Singer and Dräger 1972; Singer 1973; Ahlsén et al. 1984) afferents. For a given cell responding to a particular stimulus at suprathreshold levels however, NMDA receptor modulation does not seem possible simply by varying retinal excitatory drive alone.

In general thalamic cells have been shown to display two different intrinsic firing modes, known as the "burst" and "relay" modes (e.g. McCormick and Feeser, 1990; for review see McCormick, 1989; Lo et al. 1991). In the relay mode, incoming sensory information is faithfully transmitted to the cortex, whereas in the burst mode the cell's membrane is relatively hyperpolarized and the cell fires in bursts that bear little relation to the input pattern. The current study as well as our previous iontophoretic study of the role of NMDA receptors in dLGN visual activity (Kwon et al. 1991) underscore the importance of NMDA receptors in the relay mode of dLGN cell firing with concomitant faithful transmission of the retinal input to cortex. A dLGN cell in the burst mode, with a relatively hyperpolarized membrane potential, is unlikely to activate a large amount of NMDA receptors due to the voltage-dependent Mg^{2+} block of the receptor channel (Esguerra et al. 1991). If follows then that switching between the two modes, possibly by input from the peribrachial region of the brain stem (Hu et al. 1989), may also modulate the activation of NMDA receptors on dLGN cells.

NMDA receptors have been implicated in development and plasticity in the visual pathway (Artola and Singer 1987; Cline et al. 1987; Kleinschmitdt et al. 1987; Hahm et al. 1991). The present results describe the role of NMDA receptors in the ongoing transmission of visual signals through the dLGN. Gating of sensory information by NMDA receptors on dLGN cells appears then to be critically dependent on the modulation of the activity of these cells by intrageniculate inhibition or by extraretinal inputs.

ACKNOWLEDGEMENTS

We thank Manuel Esguerra and Anna W. Roe for general advice and comments and Anthony Passera and Robert Dolan for technical advice on data analysis programs. Supported by NIH grant EY 07023.

APPENDIX

Suppose the response of a relay cell in the dLGN is expressed as

$y = Ax - Bx$ (1)

where y = LGN relay cell response

x = retinal afferent input

A = net excitatory transfer ratio at retinal-relay cell synapse

B = net lateral inhibitory contribution from interneurons via retinal interneuron-relay cell contacts.

The assumptions for the model include: 1) Linear retinogeniculate transfer; 2) Identical retinal input (x) to a relay cell and to interneurons that impinge on the relay cell; 3) Excitation and inhibition add linearly.

Let Fr be the fractional contribution from NMDA receptors at the retinal-relay cell contract, and Fi be the fractional contribution of NMDA receptors to inhibitory interneurons.

The d-APV sensitive (or NMDA-mediated) component of the visual response is then

$y(NMDA) = FrAx - FiBx.$

$$\text{Overall NMDA fraction, } F = \frac{y(NMDA)}{y} = \frac{FrA - FiB}{A-B} \quad (2)$$

Equation (2) shows that the net contribution of NMDA receptors to relay cell responses is given by the balance of excitation and inhbition and the proportional contribution of

NMDA receptors to each.

i) For a small spot stimulating the center alone, $B \approx 0$ (very little net intrageniculate lateral inhibition), so that the NMDA fraction $F(c) \approx Fr$. That is, the overall NMDA fraction is essentially the same as the fraction at the retinal-relay cell synapse.

ii) For increasing spot sizes, and in particular for simultaneous center+surround stimulation, the NMDA fraction F(c+s) is given by equation 2.

a) If $Fr = Fi$, then $F(c+s) = F(c) = Fr$. That is, the fractional contribution of NMDA receptors would remain independent of spot size.

b) If $Fr > Fi$ (either due to a greater contribution from NMDA receptors at retinal-relay cell synapses or due to the effect of d-APV being greater at the retinal-relay cell synapse than at the retinal-interneuron synapse), then
$F(c+s) > F(c)$ for any A, B where $A > B \geq 0$.

c) If $Fr < Fi$ (due to a greater contribution from NMDA receptors at retinal-interneuron synapses than at retinal-relay cell synapses), then
$F(c+s) < F(c)$ for any A, B where $A > B \geq 0$.

Our results (Figs. 9, 10) indicate that $F(c+s) < F(c)$ when $A > B$ (a situation where cells continue to respond even at large spot sizes). The model suggests t hat one possible way this would happen is if $Fi > Fr$ as spot sizes increase to include center and surround. Indeed, for large enough Fi, $FiB > FrA$, so that the overall NMDA fraction F (c+s) goes negative (Eqn. 2). Then application of d-

APV would actually increase the cell's response, which is what we observe in some cells responding to very large spots (Fig. 10).

REFERENCES

Ahlsén, G., Lindström, S. and Lo, F.-S. Inhibition from the brain stem of inhibitory interneurons of the cat's dorsal lateral geniculate nucleus. J. Physiol. 347: 593-609, 1984.

Artola, A. and Singer, W. Long-term potentiation and NMDA receptors in rat visual cortex. *Nature* 330: 649-652, 1987.

Bear, M.F., Kleinschmidt, A., Gu, Q. and Singer, W. Disruption of experience-dependent synaptic modifications in striate cortex by infusion of an NMDA receptor antagonist. J. Neurosci. 10:909-925, 1990.

Berardi, N. and Morrone, M.C. The role of g-aminobutyric acid mediated inhibition in the response properties of cat lateral geniculate nucleus neurones. J. Physiol. 357:505-523, 1984.

Bloomfield, S.A. and Sherman, S.M. Postsynaptic potentials recorded in neurons of the cat's lateral geniculate nucleus following electrical stimulation of the optic chiasm. J. Neurophysiol. 60: 1924-1945,1988.

Cline, H. T., Debski, E. A., and Constantine-Paton, M. N-methyl-D-aspartate receptor antagonist desegregates eye-specific stripes. *Proc. Natl. Acad. Sci.USA* 84: 4342-4345, 1987.

Cotman, C.W., Monaghan, D.T., Ottersen, O.P. and Storm-Mathisen, J. Anatomical

organization of excitatory amino acid receptors and their pathways. *Trends in Neurosci.* 10: 273-280, 1987.

Crunelli, V., Haby, M., Jassik-Gerschenfeld, D., Leresche, N. and Perchio, M. Cl^- and K^+-dependent inhibitory postsynaptic potentials evoked by interneurones of the rat lateral geniculate nucleus. J. Physiol. 399: 153-176, 1988.

Crunelli, V., Kelly, J.S., Leresche, N. and Perchio, M. On the excitatory post-synaptic potential evoked by stimulation of the optic tract in the rat lateral geniculate nucleus. J. Physiol. Lond. 384: 603-618, 1987.

Crunelli, V. and Leresche, N. A role for $GABA_B$ receptors in excitation and inhibition of thalamocortical cells. TINS 14: 16-21, 1991.

Esguerra, M., Kwon, Y.H. and Sur, M. NMDA and non-NMDA receptors mediate retinogeniculate transmission in cat and ferret LGN in vitro. Soc. for Neurosci. Abstr. 15:175, 1989.

Esguerra, M., Kwon, Y.H. and Sur, M. Retinogeniculate EPSPs recorded intracellularly in the ferret lateral geniculate nucleus in vitro: role of NMDA receptors. submitted, 1991.

Esguerra, M. and Sur, M. Corticogeniculate feedback gates retinogeniculate transmission by activating NMDA receptors. *Soc. Neurosci. Abstr.* 16: 159, 1990.

Fox, K., Sato, H. and daw, N. The effect of varying stimulus intensity on NMDA-

receptor activity in cat visual cortex. J. Neurophysiol. 64: 1413-1428, 1990.

Gallagher, J.P. and Hasuo, H. Bicuculline- and phaclofen-sensitive components of N-Methyl-D-Aspartate-induced hyperpolarizations in rat dorsolateral septal nucleus neurones. J. Physiol. 418: 367-377, 1989.

Gilbertson, T.A., Scobey, R. and Wilson, M. Permeation of calcium ions through non-NMDA glutamate channels in retinal bipolar cells. Science 251: 1613-1615, 1991.

Guillery, R.W. The organization of synaptic interconnections in the laminae of the dorsal lateral geniculate nucleus of the cat. Z. Zellforsch. 96: 1-38, 1969.

Hahm, J., Langdon, R.B. and Sur, M. Disruption of retinogeniculate afferent segregation by antagonists to NMDA receptors. Naure (Lond.) in press.

Hamos, J.E., VanHorn, S.C., Raczkowski, D. and Sherman, S.M. Synaptic circuits involving an individual retinogeniculate axon in the cat. J. Comp. Neurol. 259: 165-192, 1987.

Hartveit, E. and Heggelund, P. Neurotransmitter receptors mediating excitatory input to cells in the cat lateral geniculate nucleus. II. Nonlagged cells. *J. Neurophys.* 63: 1361-1372, 1990a.

Heggelund, P. and Hartveit, E. Neurotransmitter receptors mediating excitatory input to cells in the cat lateral geniculate nucleus. I. Lagged cells. *J. Neurophys.* 63: 1347-1360, 1990.

Herron, C.E., Lester R.A.J., Coan, E.J. and Coolingridge, G.L. Frequency-dependent involvement of NMDA receptors in the hippocampus: a novel synaptic mechanism. Naure Lond. 322: 265-267, 1986.

Hirsch, J.C. and Burnod, Y. Optic tract induced late hyperploarization in the lateral geniculate body of the rat. Neurosci. Letters. 22: S 307, 1987.

Hu, B., Steriade, M. and Deschênes, M. The effects of brainstem peribrachial stimulation on neurons of the lateral geniculate nucleus. Neuroscience. 31:13-24, 1989.

Hubel, D.H. and Wiesel, T.N. Integrative action in the cat's lateral geniculate body. J. Physiol. (Lond.) 155: 385-398, 1961.

Humphrey, A.L. and Weller, R.E. Functionally distinct groups of X-cells in the lateral geniculate nucleus of the cat. *J. Comp. Neurol.* 268: 429-447, 1988a.

Humphrey, A.L. and Weller, R.E. Structural correlates of functionally distinct X-cells in the lateral geniculate nucleus of the cat. *J. Comp. Neurol.* 268: 448-468, 1988b.

Jones, K.A. and Baughman, R.W. NMDA- and non-NMDA-receptor components of excitatory synaptic potentials recorded form cells in layer V of rat visual cortex. J. Neurosci. 8: 3522-3534, 1988.

Kaplan, E., Purpura, K. and Shapley, R.M. Contrast affects the transmission of visual information through the mammalian lateral geniculate nucleus. J. Physiol. 391: 267-288, 1987.

Kauer, J.A., Malenka, R.C. and Nicoll, R.A. A persistent postsynaptic modification mediates long-term potentiation in the hippocampus. Neuron. 1: 911-917, 1988.

Kemp, J.A. and Sillito, A.M. The nature of the excitatory transmitter mediating X and Y cell inputs to the cat dorsal lateral geniculate nucleus. *J. Physiol.* 323: 377-391, 1982.

Kleinschmidt, A., Bear, M. F., and Singer, W. Blockade of "NMDA" receptors disrupts experience-dependent plasticity of kitten striate cortex. *Science* 238: 355-358, 1987.

Koch, C. The action of the corticofugal pathway on sensory thalamic nuclei: a hypothesis. *Neuroscience* 23: 399-406, 1987.

Kwon, Y.H., Esguerra, M. and Sur, M. NMDA and non-NMDA receptors mediate visual responses of neurons in the cat's lateral geniculate nucleus. J. Neurophysiol. in press.

Lo, F.-S., Lu, S.-M. and Sherman, S.M. Intracellular and extracellular in vivo recording of different response modes for relay cells of the cat's lateral geniculate nucleus. Exp. Brain Res. 83: 317-328, 1991.

Mastronarde, D.N. Two classes of single-input X-cells in cat lateral geniculate nucleus. I. Receptive-field properties and classification of cells. *J. Neurophysiol.* 57: 357-380, 1987a.

Mastronarde, D.N. Two classes of single-input X-cells in cat lateral geniculate nucleus.

II. Retinal inputs and the generation of receptive-field properties. *J. Neurophysiol.* 57: 381-413,1987b.

Mastronarde, D.N. Branching of X and Y functional pathways in cat lateral geniculate nucleus. *Soc. Neurosci. Abstr.* 14: 309, 1988

Mayer, M.L. and Westbrook, G.L. The physiology of excitatory amino acids in the vertebrate central nervous system. *Progress in Neurobiology* 28: 197-276, 1987.

McCormick, D. A. Cholinergic and noradrenergic modulation of thalamocortical processing. *Trends in Neurosci.* 12: 215-221, 1989.

McCormick, D.A. Possible ionic basis for lagged visual responses in cat LGNd relay neurons. *Soc. Neurosci. Abstr.* 16: 159, 1990.

McCormick, D.A. and Feeser, H.R. Functional implications of burst firing and single spike activity in lateral geniculate nucleus neurons. Neurosci. 39: 103-113, 1990.

McDermott, A.B. and Dale, N. Receptors, ion channels and synaptic potentials underlying the integrative actions of excitatory amino acids. Trends in Neurosci. 10: 280-284, 1987.

Morrisett, R.A., Mott, D.D., Lewis, D.V., Swartzwelder, H.S. and Wilson, W.A. $GABA_B$-receptor-mediated inhibition of the N-Methyl-D-Aspartate component of synaptic transmission in the reat hippocampus. J. Neurosci. 11: 203-209, 1991.

Sah, P., Hestrin, S. and Nicoll, R.A. Tonic activation of NMDA receptors by ambient glutamate enhances excitability of neurons. Science 246: 815-818, 1989.

Salt, T.E. Mediation of thalamic sesnsory input by both NMDA receptors and non-NMDA receptors. *Nature (Lond.)* 322: 263-265, 1986.

Salt, T.E. and Eaton, S.A. Sensory excitatory postsynaptic potentials mediated by NMDA and non-NMDA receptors in the thalamus *in vivo*. European J. Neurosci. 3: 296-300, 1991.

Saul, A and Humphrey, A.L. Spatial and temporal response properties of lagged and non-lagged cells in the cat lateral geniculate nucleus. *J. Neurophys.* 64: 206-224, 1990.

Scharfman, H.E., Lu, S.-M., Guido, W., Adams, P.R. and Sherman, S.M. N-Methyl-D-Aspartate receptors contribute to excitatory postsynaptic potentials of cat lateral geniculate neurons recorded in thalamic slices. Proc. Natl. Acad. Sci. USA. 87: 4548-4552, 1990.

Shapley, R. and Lennie, P. Spatial frequency analysis in the visual system. *Ann. Rev. Neurosci.* 8: 547-583, 1985.

Sherman, S.M. and Koch, C. The control of retinogeniculate transmission in the mammalian lateral geniculate nucleus. Exp. Brain Res. 63: 1-20, 1986.

Sherman, S.M. and Spear, P.D. Organization of visual pathways in normal and visually deprived cats. Physiol. Rev. 62: 738-855, 1982.

Sillito, A.M., and Kemp, J.A. The influence of GABAergic inhibitory processes on the receptive field structure of X and Y cells in cat dorsolateral geniculate nucleus (dLGN). Brain Research 277: 63-77, 1983.

Sillito, A.M., Murphy, P.C. and Salt, T.E. The contribution of the non-N-Methyl-D-Aspartate group of excitatory amino acid receptors to retinogeniculate transmission in the cat. *Neuroscience* 34: 273-280, 1990a.

Sillito, A.M., Murphy, P.C., Salt, T.E. and Moody, C.I. Dependence of retinogeniculate transmission in cat on NMDA receptors. *J. Neurophys.* 63: 347-355, 1990b.

Singer, W. The effect of mesencephalic reticular stimulation on intracellular potentials of cat lateral geniculate neurons. Brain Res. 61: 35-54, 1973.

Singer, W. and Dräger, U. Postsynaptic potentials in relay neurons of cat lateral geniculate nucleus after stimulation of the mesencephalic reticular formation. Brain Res. 41: 214-220, 1972.

Soltesz, I., Lightowler, S., Leresche, N. and Crunelli, V. On the properties and origin of the $GABA_B$ inhibitory prostsynaptic potential recorded in morphologically identified projection cells of the cat dorsal lateral geniculate nucleus. Neurosci. 33: 23-33, 1989.

Sur, M., Esguerra, M., Garraghty, P. E., Kritzer, M. F., and Sherman, S. M. Morphology of physiologically identified retinogeniculate X- and Y-axons in the cat. J.

Neurophysiol. 52: 1- 32, 1987.

Uhlrich, D.J., Tamamaki, N. and Sherman, S.M. Brainstem control of response modes in neurons of the cat's lateral geniculate nucleus. *Proc. Natl. Acad. Sci. USA* 87: 2560-2563, 1990.

Weber, A.J., Kalil, R.E. and Behan, M. Synaptic connections between corticogeniculate axons and interneurons in the dorsal lateral geniculate nucleus of the cat. J. Comp. Neurol. 289: 156-164, 1989.

Wilson, J.R., Friedlander, M.J. and Sherman, S.M. Fine structural morphology of identified X- and Y-cells in the cat's lateral geniculate nucleus. Proc. R. Soc. Lond. B 221: 411-436, 1984.

FIGURE LEGENDS

Fig. 1. Contrast-Response curve of an off-center nonlagged X cell. Positive contrast values refer to dark spots and negative contrast to bright spots, relative to a fixed background luminance of 5.87 cd/m^2; zero contrast refers to an uniform illumination of the visual field. Average firing rate is computed over 0.5 s which was the period of stimulus presentation. The error bars indicate the standard error of the mean (SEM) of 10 trials. The Contrast-Response curve is sigmoidal in shape and a curve fit was performed as described in the Methods ($r = 0.990$).

Fig. 2. Effect of d-APV on the Contrast-Response plot of the cell in Fig. 1. **A.** Contrast-Response plot before (open circle), during (filled circle) and 2 min. after (open triangle) 60nA of d-APV application. Conventions as in Fig. 1. **B.** The d-APV sensitive component is calculated by subtracting the responses during d-APV application from those before application. The line represents the least squares fit with a slope of 0.515 ($r = 0.982$). The d-APV sensitive component was approximately linear function of the control visual response level.

Fig. 3. Effect of d-APV on the Contrast-Response plots of two cells with different d-APV sensitive fractions in their visual responses. Conventions as in Fig. 2. **A.** Contrast-Response plots of an off-center nonlagged X cell before, during, and after 86nA of d-APV application. **B.** The same cell as in A. The best linear fit has a slope of 0.753 ($r = 0.996$). **C.** Contrast-Response plots of an on-center nonlagged Y cell before, during and 1.5 min. after 91nA of d-APV application. **D.** The same cell as in C. The line of best fit has a slope of 0.604 ($r = 0.996$). There is a linear relationship between the d-APV sensitive component and the control visual response level in both cells even at

different absolute values of the slopes.

Fig. 4. Plots of the d-APV sensitive component as a function of the control level of response in different dLGN cell classes. There is a constant contribution from NMDA receptors to the visual responses of all three cells. **A.** On-center nonlagged X cell with 85nA of d-APV application. Slope = 0.748 (r = 0.99). **B.** Off-center lagged X cell with 86nA of d-APV application. Slope = 1.002 (r = 1.0). **C.** On-center nonlagged Y cell with 85nA of d-APV application. Slope = 0.576 (r = 0.98).

Fig. 5. Contrast-Response curves of two X cells in which the plots of the d-APV sensitive component as a function of the control visual response deviated from linearity. Conventions as in Fig. 2. **A.** Off-center nonlagged X cell before, during 86nA of d-APV iontophoresis, and 2 min. after iontophoresis. **B.** The same cell as in A. The curve is a second order polynomial fit. **C.** Another off-center nonlagged X cell before, during and 5 min 20 s after 83nA of d-APV application. **D.** The same cell as in C. The curve is a third order polynomial fit.

Fig. 6. Frequency distribution histogram of the d-APV sensitive fractions (derived from the contrast study) among different cell types. Mean for lagged X cells, 0.896 ± 0.065, n = 4; nonlagged X cells, 0.636 ± 0.070, n = 19; nonlagged Y cells 0.567 ± 0.100, n = 15.

Fig. 7. The Contrast-Response curves of an off-center nonlagged X cell (same cell as in Fig. 5A), before (open circle), during 86nA of d-APV iontophoresis (filled circle), during simultaneous application of 86nA of d-APV and 83nA of CNQX (star), and 2 min. after iontophoresis (open triangle). Note the significant decrease in the gain of the

Contrast-Response curve by d-APV and complete abolition of visual responses with the additional application of CNQX application.

Fig. 8. Size-Response plot for an off-center nonlagged X cell. Error bars indicate the SEM of the peak firing rate averaged over 10 trials. The dotted line indicates the division between the "center" and "center+surround" responses (see text).

Fig. 9. Effect of d-APV on the Size-Response plot of the cell in Fig. 8. **A.** Size-Response plot before (open circle), during (filled circle) and after (open triangle) 86nA of d-APV application. Conventions as in Fig. 8. **B.** Same plot with only the pre-drug control and d-APV responses, each with their respective background firing rate subtracted. The arrows indicate the direction and magnitude of the d-APV effect for each of the four responses. **C.** Histogram of the d-APV sensitive component as a fraction of the control responses at each spot size. Note that there is an inverse relationship between the d-APV sensitive fraction and spot size. **D.** Histogram of the d-APV sensitive components as proportions of the control for "center" and "center+surround" responses. The d-APV sensitive fraction was greater for the "center" responses than for the "center+surround" responses.

Fig. 10. Effect of d-APV on Size-Response plots of four different dLGN cells. **A.** Off-center nonlagged X cell before and during application of 85nA of d-APV. **B.** same cell as in A. Histogram of d-APV sensitive fraction of the "center" and "center+surround" responses. **C** and **D.** On-center nonlagged X cell before and during application of 86nA of d-APV. Histogram convention same as B. **E** and **F.** Off-center lagged X cell before and during application of 86nA of d-APV. **G** and **H.** On-center nonlagged Y cell before and during application of 86nA of d-APV. In all four cells, the d-APV sensitive

fraction is greater for the "center" responses than for the "center+surround" responses.

Fig. 11. Frequency distribution histogram of the difference in the d-APV sensitive fraction between the "center" and "center+surround" responses (n = 34 cells). The actual values are computed by subtracting the d-APV sensitive fraction of the "center+surround" responses from that of the "center" responses. Thus positive columns represent bigger d-APV sensitive fractions for the "center" responses and the negative columns represent the reverse. The open triangle represents the mean difference.

Fig. 12. Frequency distribution histogram of the differences between the d-APV sensitive fraction obtained using an optimal spot size at different contrasts and that of (**A**) "center" response and (**B**) "center+surround" response. Conventions as in Fig. 11. See text for details.

Fig. 13. Two different kinds of inhibition on dLGN relay cells, and their spatial relationship to the center (+) and surround (-) of a dLGN cell receptive field. The results of this study suggest that varying feedforward inhibition does not alter the proportional contribution of NMDA receptors to the visual responses of dLGN cells, while varying lateral inhibition does. See text for details.

Fig. 1

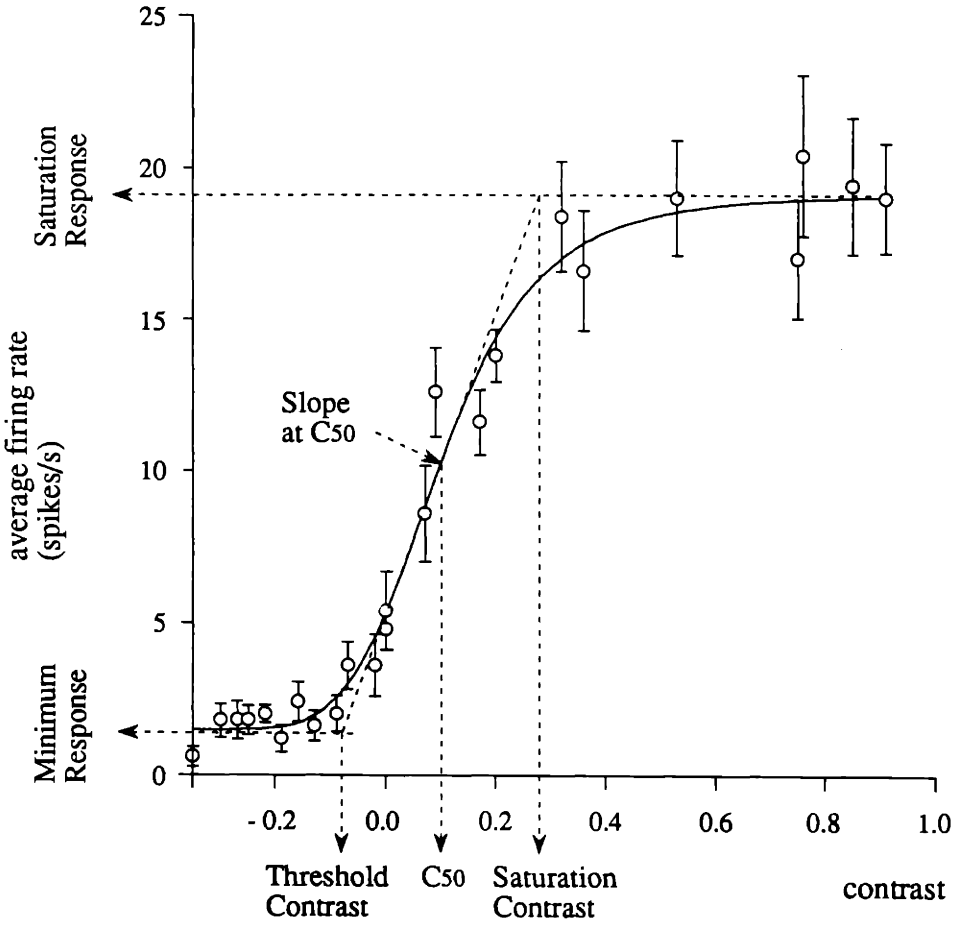
25
20
15
10
5
0
Saturation Response
Minimum Response
average firing rate (spikes/s)
Slope at C50
- 0.2
0.0
0.2
0.4
0.6
0.8
1.0
Threshold Contrast
C50
Saturation Contrast
contrast

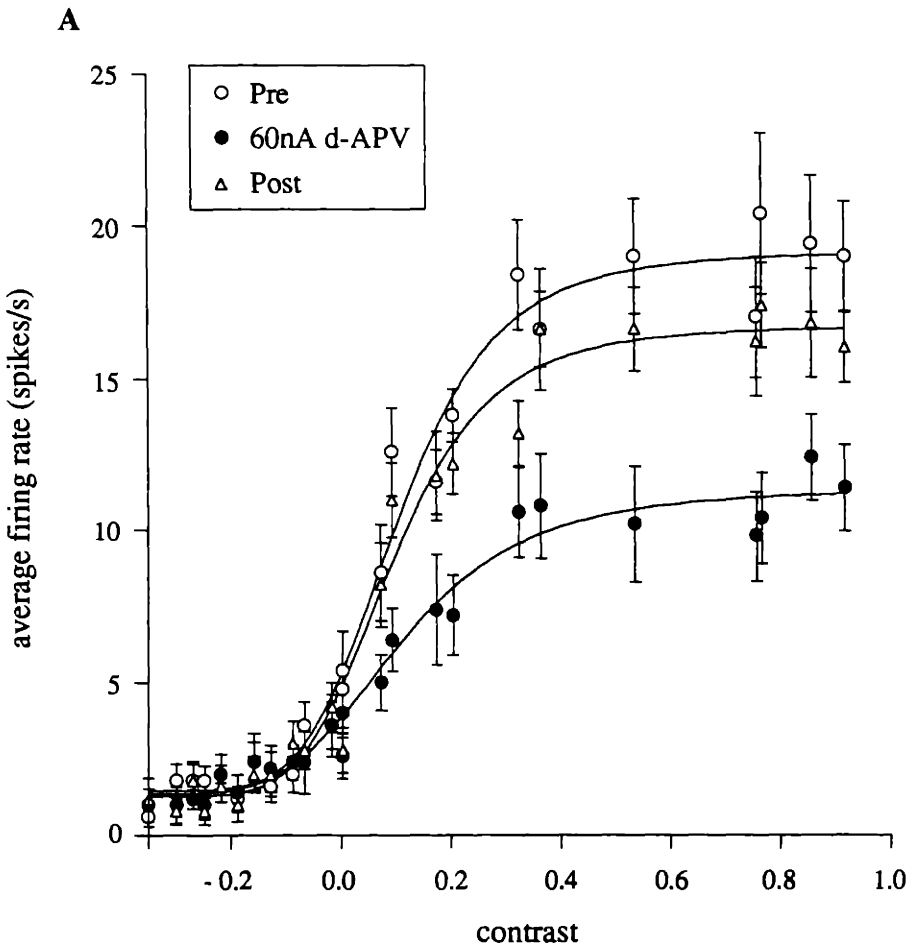
A
Pre
60nA d-APV
Post
average firing rate (spikes/s)
25
20
15
10
5
0
-0.2
0.0
0.2
0.4
0.6
0.8
1.0
contrast

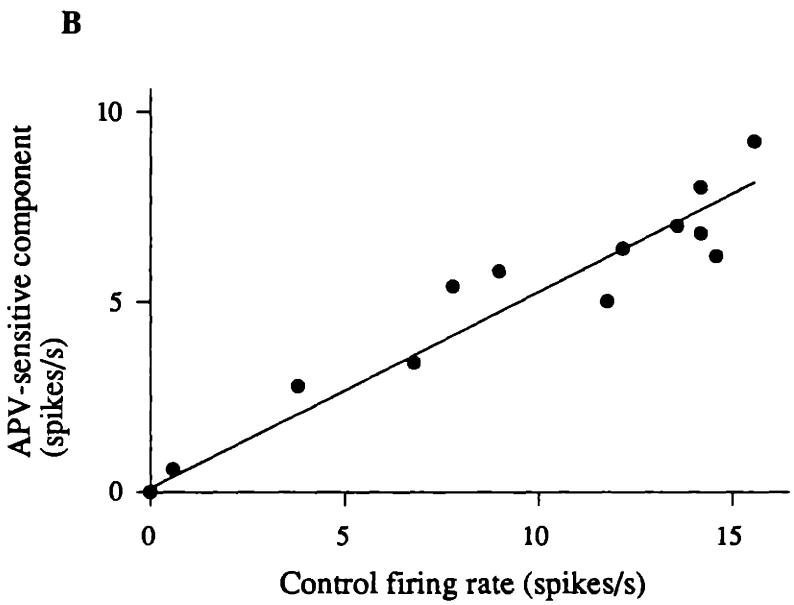
B
APV-sensitive component (spikes/s)
10
5
0
0
5
10
15
Control firing rate (spikes/s)

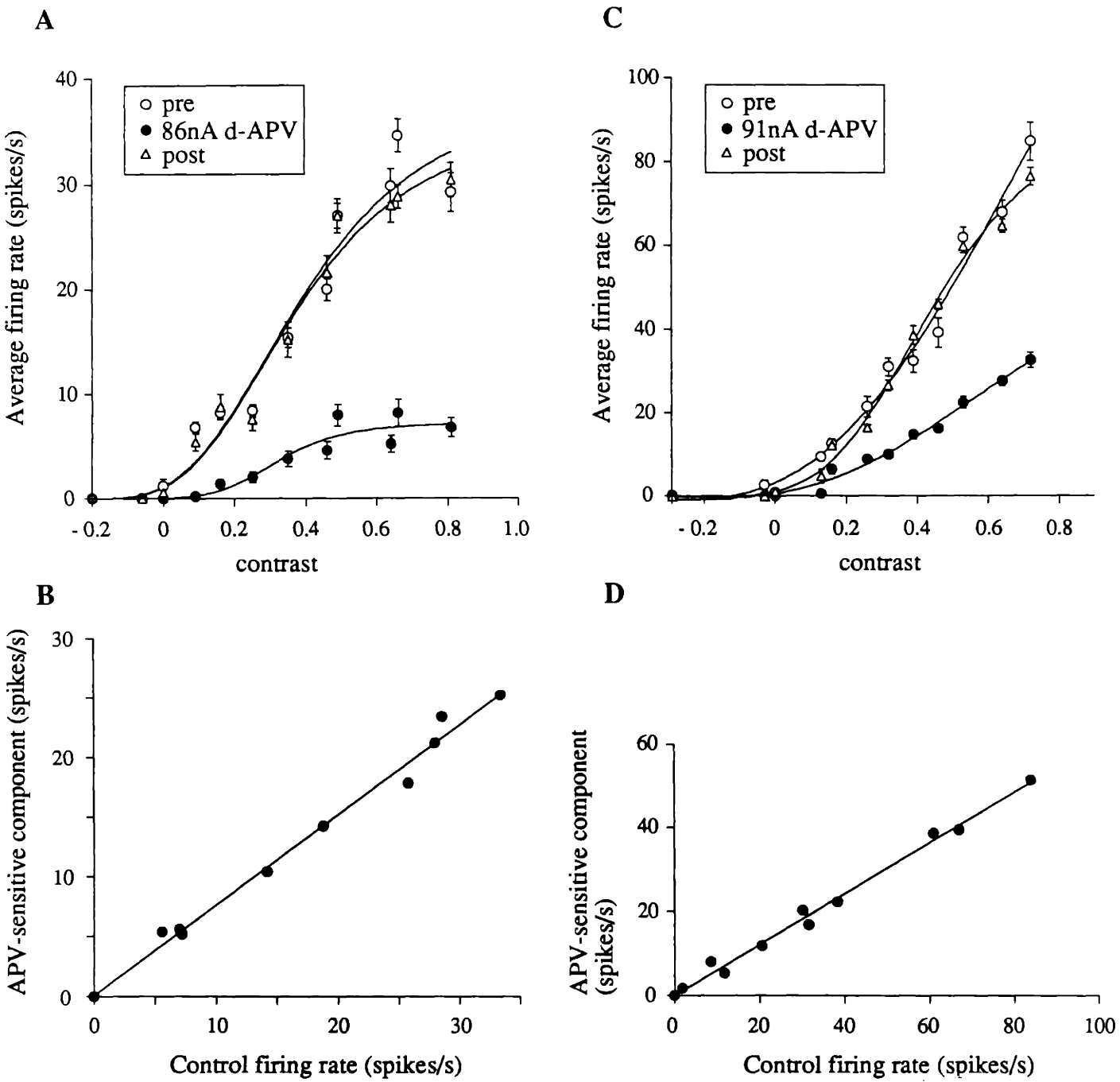
A
pre
86nA d-APV
post
Average firing rate (spikes/s)
contrast
C
pre
91nA d-APV
post
Average firing rate (spikes/s)
contrast
B
APV-sensitive component (spikes/s)
Control firing rate (spikes/s)
D
APV-sensitive component (spikes/s)
Control firing rate (spikes/s)

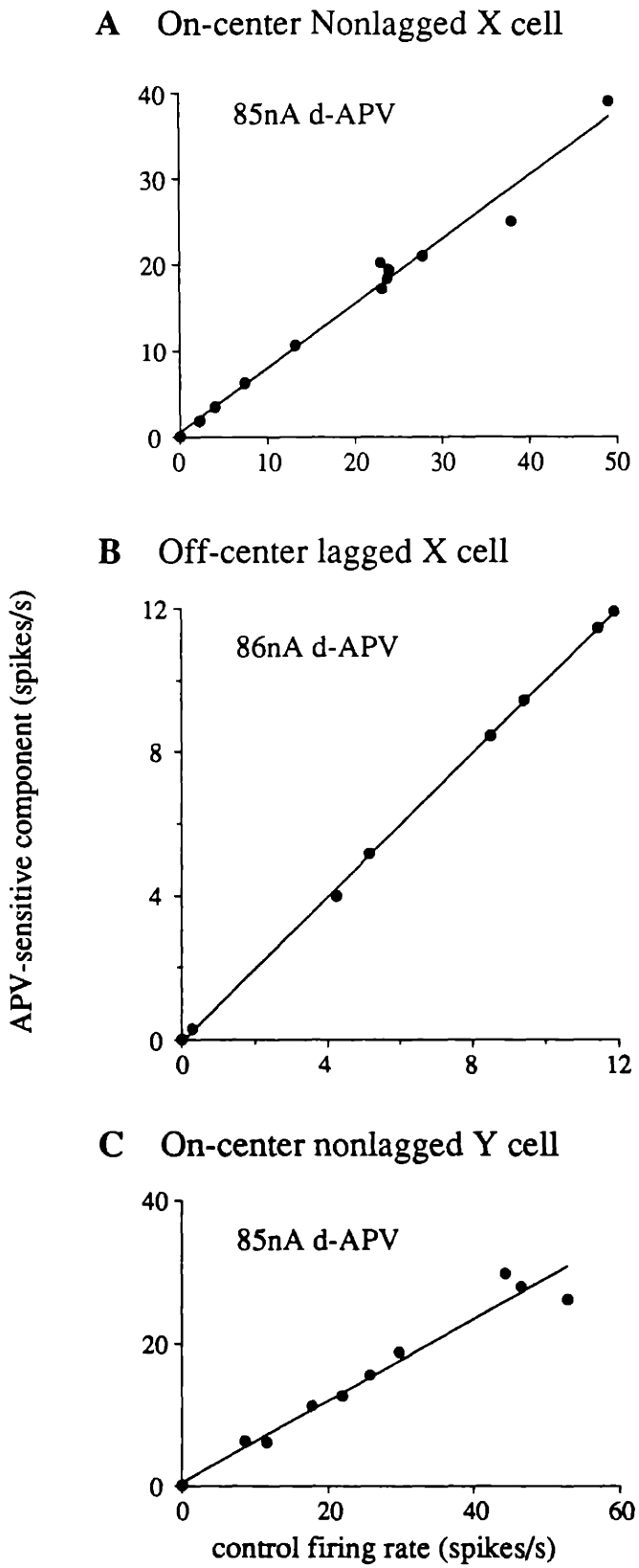
A On-center Nonlagged X cell
85nA d-APV
40
30
20
10
0
0
10
20
30
40
50
B Off-center lagged X cell
86nA d-APV
12
8
4
0
0
4
8
12
APV-sensitive component (spikes/s)
C On-center nonlagged Y cell
85nA d-APV
40
20
0
0
20
40
60
control firing rate (spikes/s)

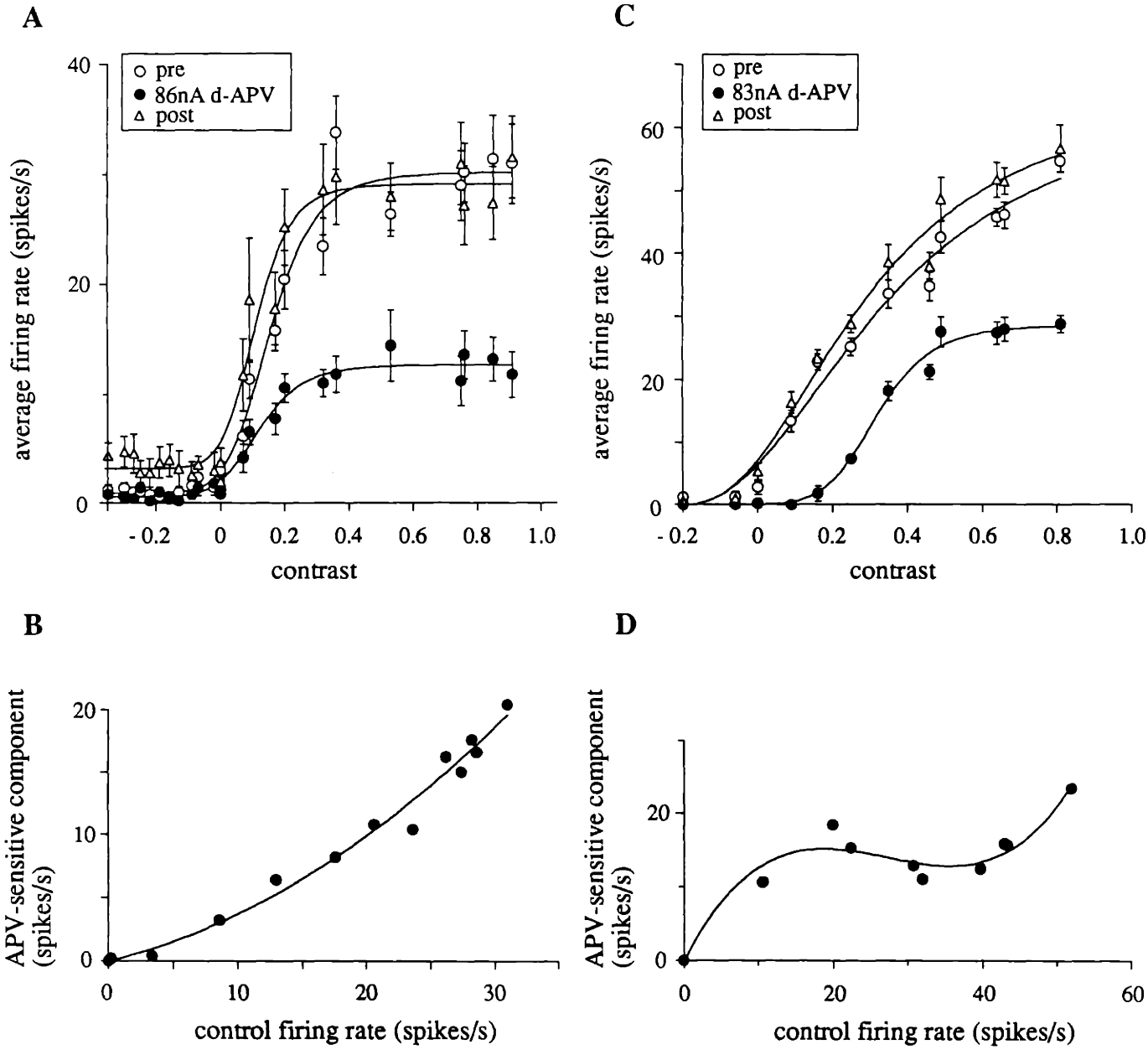
A
pre
86nA d-APV
post
average firing rate (spikes/s)
contrast
C
pre
83nA d-APV
post
average firing rate (spikes/s)
contrast
B
APV-sensitive component (spikes/s)
control firing rate (spikes/s)
D
APV-sensitive component (spikes/s)
control firing rate (spikes/s)

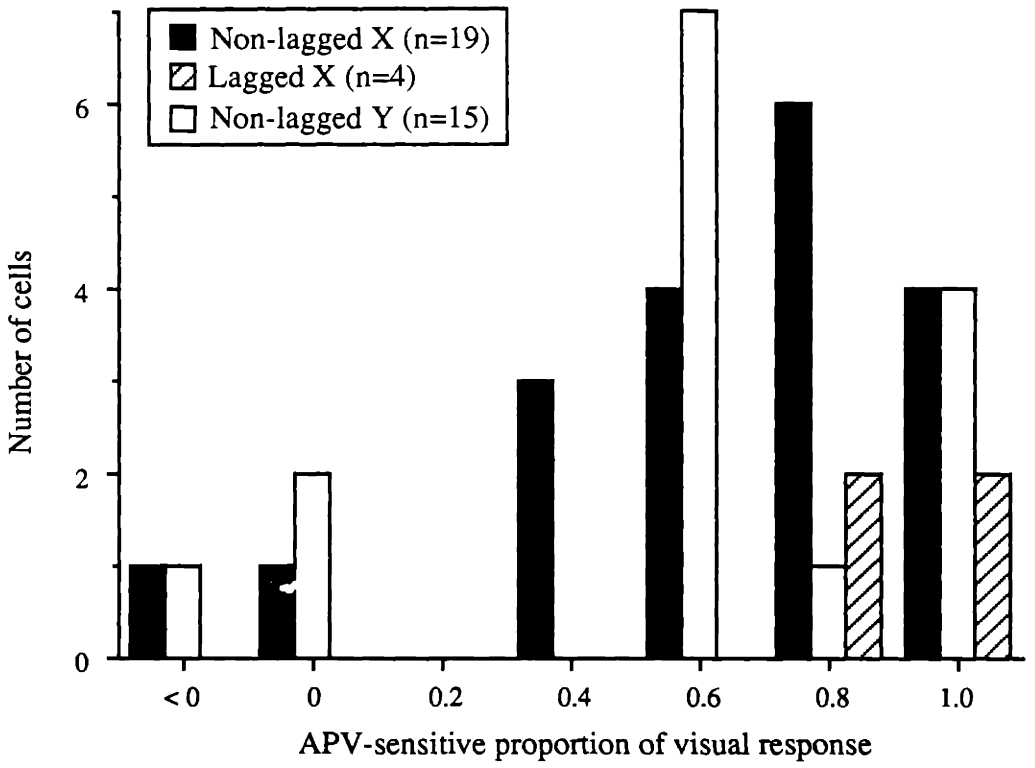
Non-lagged X (n=19)
Lagged X (n=4)
Non-lagged Y (n=15)
Number of cells
0
2
4
6
< 0
0
0.2
0.4
0.6
0.8
1.0
APV-sensitive proportion of visual response

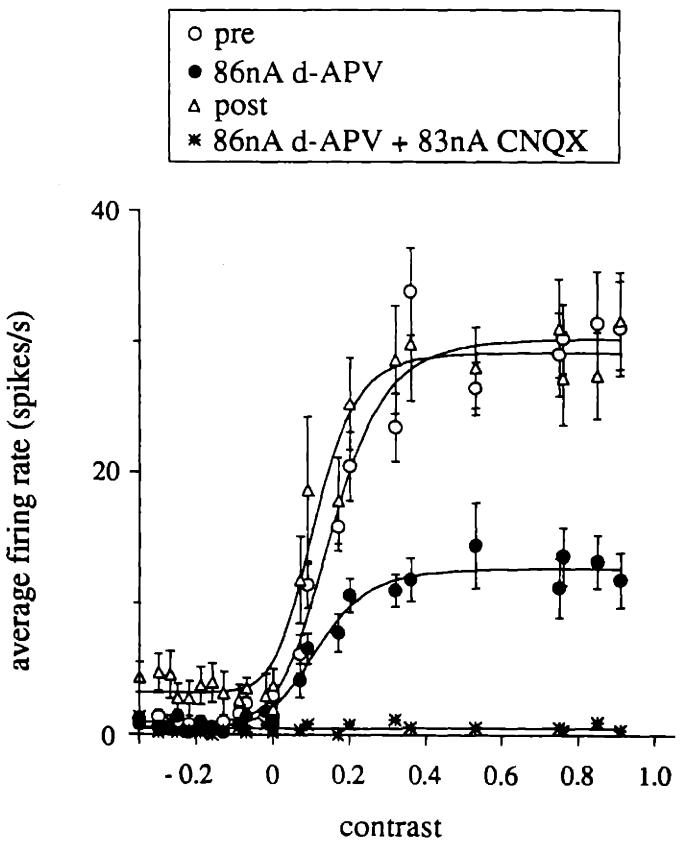
pre
86nA d-APV
post
86nA d-APV + 83nA CNQX
average firing rate (spikes/s)
40
20
0
-0.2
0
0.2
0.4
0.6
0.8
1.0
contrast

Off-center Nonlagged X cell

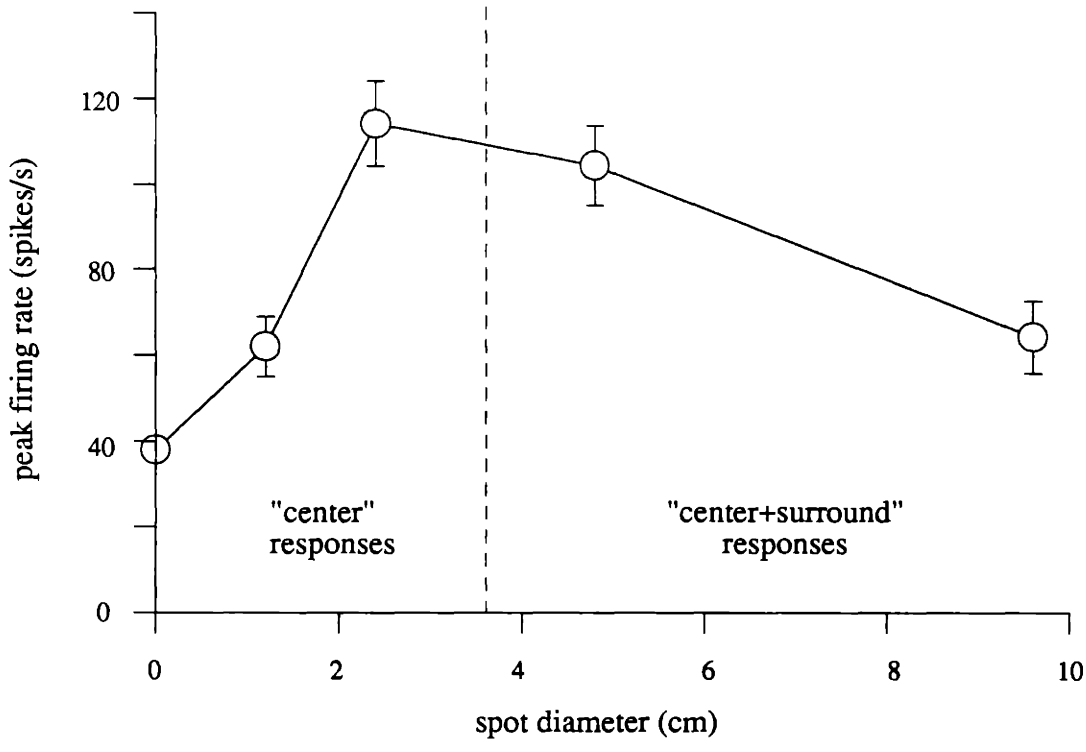

Fig. 9

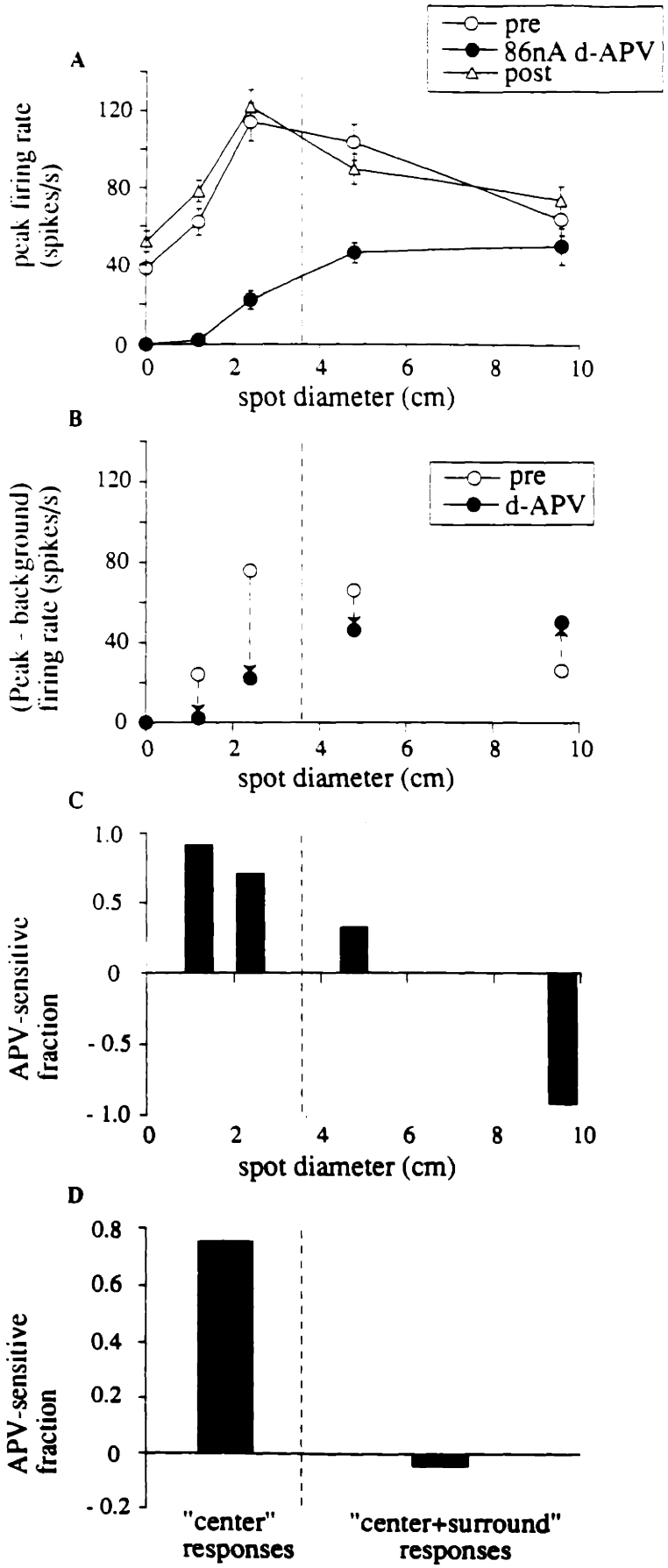
A
pre
86nA d-APV
post
peak firing rate (spikes/s)
120
80
40
0
0
2
4
6
8
10
spot diameter (cm)
B
pre
d-APV
(Peak - background) firing rate (spikes/s)
120
80
40
0
0
2
4
6
8
10
spot diameter (cm)
C
APV-sensitive fraction
1.0
0.5
0
- 0.5
- 1.0
0
2
4
6
8
10
spot diameter (cm)
D
APV-sensitive fraction
0.8
0.6
0.4
0.2
0
- 0.2
"center" responses
"center+surround" responses

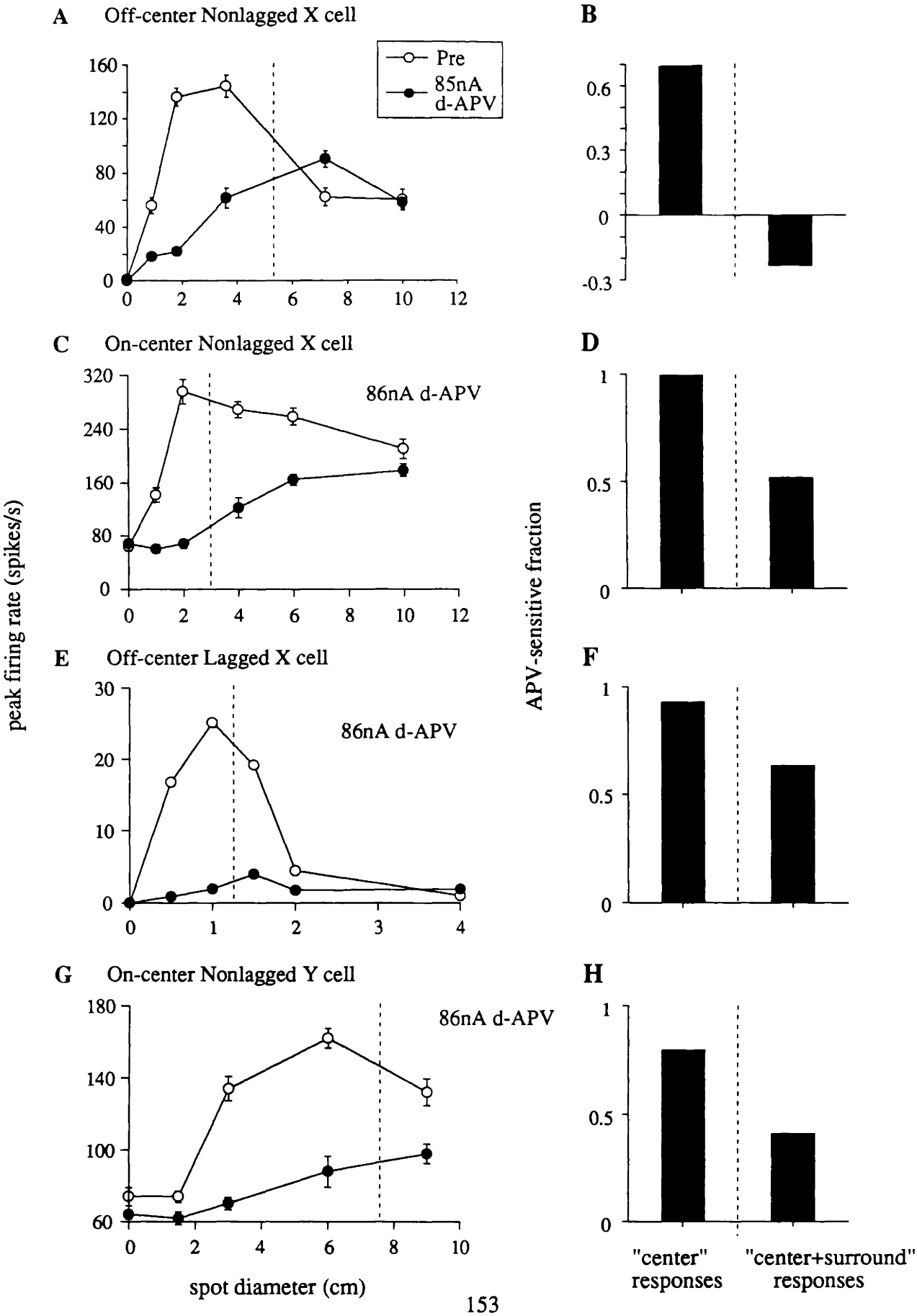
A
Off-center Nonlagged X cell
Pre
85nA d-APV
160
120
80
40
0
0 2 4 6 8 10 12
B
0.6
0.3
0
-0.3
C
On-center Nonlagged X cell
86nA d-APV
320
240
160
80
0
0 2 4 6 8 10 12
D
1
0.5
0
E
Off-center Lagged X cell
86nA d-APV
30
20
10
0
0 1 2 3 4
F
1
0.5
0
G
On-center Nonlagged Y cell
86nA d-APV
180
140
100
60
0 2 4 6 8 10
spot diameter (cm)
H
1
0.5
0
"center" responses
"center+surround" responses
peak firing rate (spikes/s)
APV-sensitive fraction

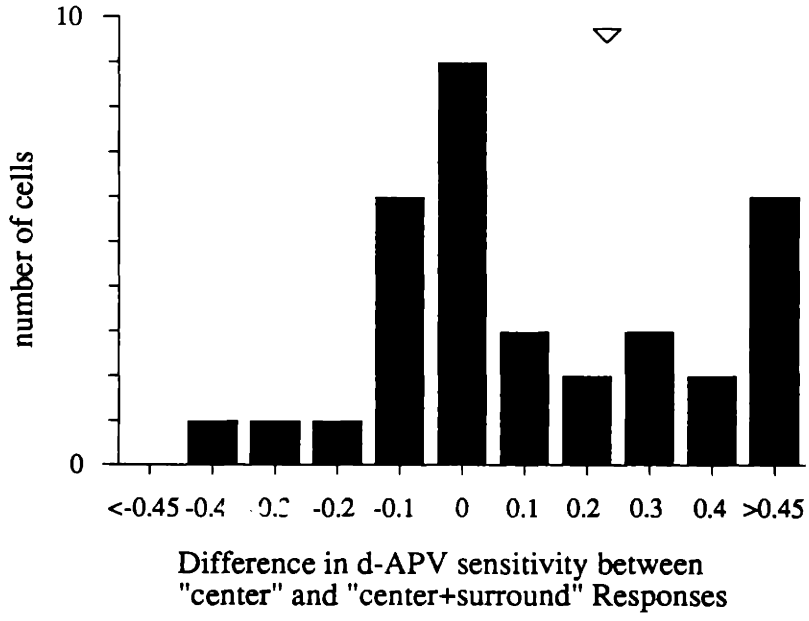
10
0
number of cells
<-0.45
-0.4
-0.2
-0.1
0
0.1
0.2
0.3
0.4
>0.45
Difference in d-APV sensitivity between
"center" and "center+surround" Responses

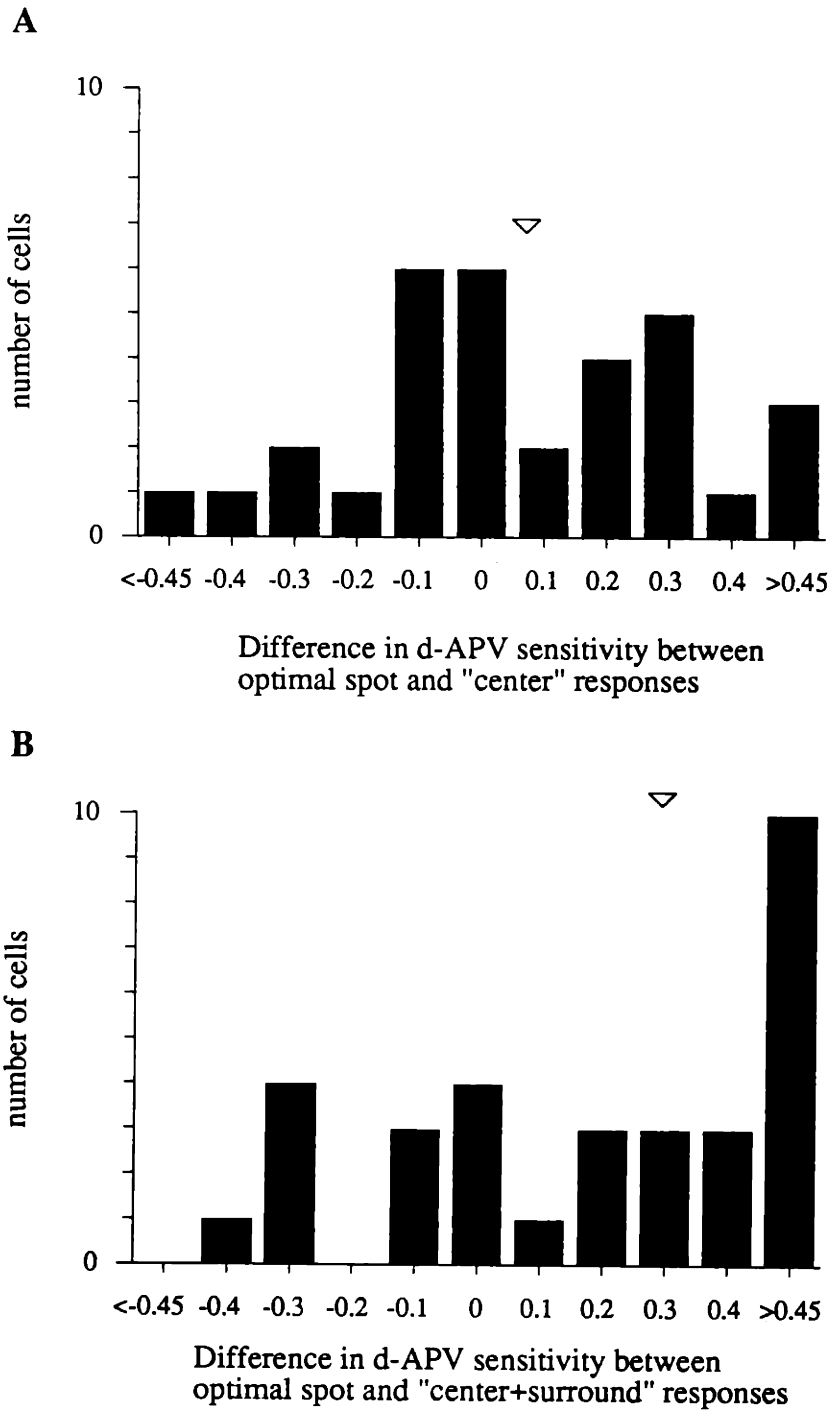
A
10
0
number of cells
<-0.45 -0.4 -0.3 -0.2 -0.1 0 0.1 0.2 0.3 0.4 >0.45
Difference in d-APV sensitivity between optimal spot and "center" responses
B
10
0
number of cells
<-0.45 -0.4 -0.3 -0.2 -0.1 0 0.1 0.2 0.3 0.4 >0.45
Difference in d-APV sensitivity between optimal spot and "center+surround" responses

Fig. 13

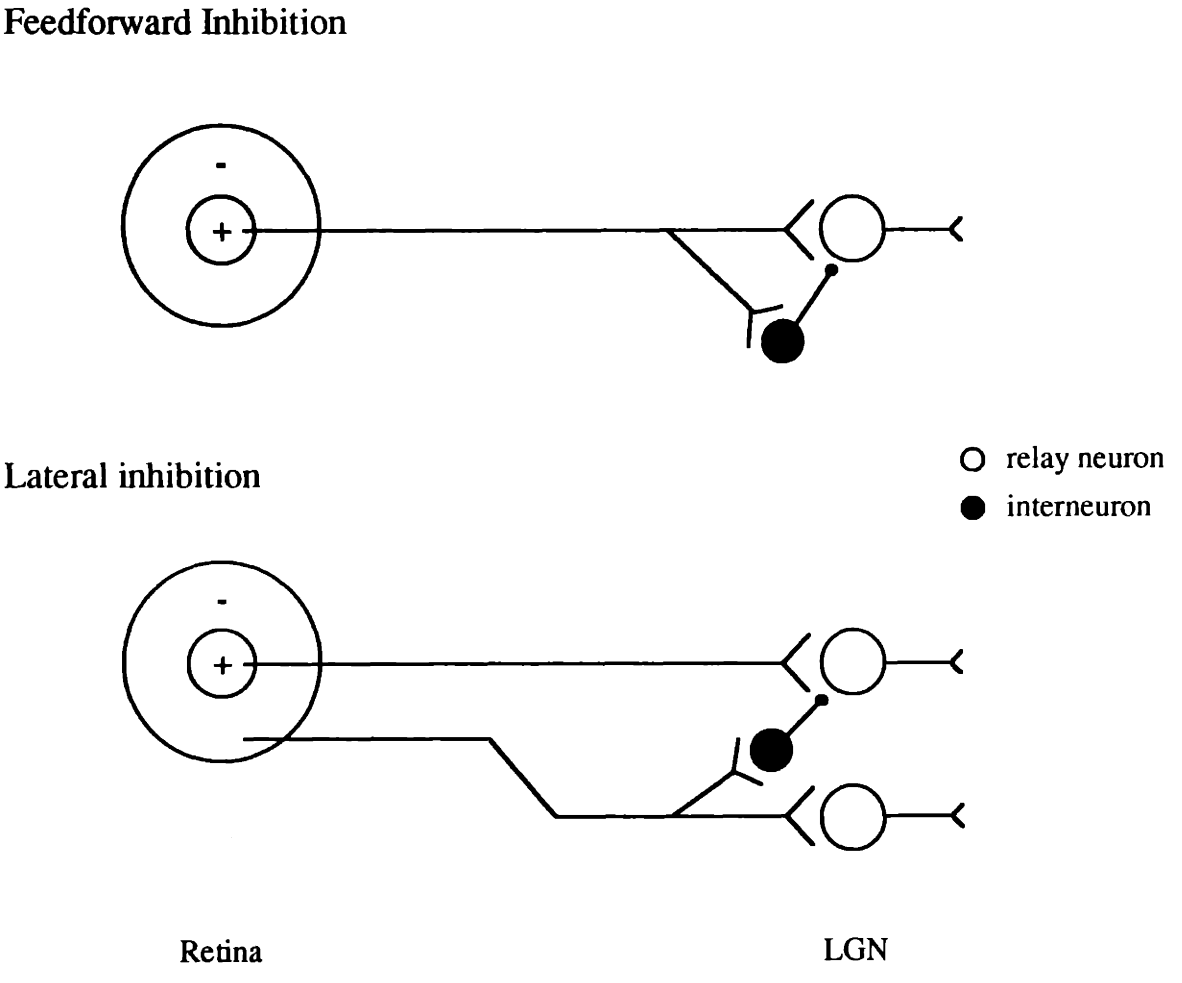
Feedforward Inhibition
-
+
Lateral inhibition
relay neuron
interneuron
-
+
Retina
LGN

Table 1. Parameters of the Contrast-Response function and the effect of d-APV (n=25)

	Control	d-APV	APV - control
Threshold Contrast	0.017±0.021	0.019±0.028	0.001±0.024 (p = 0.84)
Saturation Contrast	0.398±.047	0.367±0.062	-0.031±0.05 (p = 0.57)
Contrast at half saturation (C_{50})	0.208±0.027	0.193±0.041	-0.015±0.024 (p = 0.25)
Slope at C_{50}	174.103±26.408	75.924±14.893	-98.179±24.241 (p = 0.0005)
Saturation Response (spikes/s)	51.49±5.91	24.546±4.49	-26.945±5.814 (p = 0.0001)

All values are represented as mean±SE. Statistical comparisons employed the Wilcoxon signed rank test. The only two parameters of the Contrast-Response curve that signficantly changed with d-APV application were the slope at half saturation and saturation response; other parameters did not change significantly.

CHAPTER 4

ACTION OF ACETYLCHOLINE ON TEMPORAL FEATURES OF VISUAL RESPONSES IN THE CAT'S LATERAL GENICULATE NUCLEUS

ABSTRACT

Acetylcholine (ACh) was applied iontophoretically to neurons of the cat dorsal lateral geniculate nucleus (dLGN). Neurons were classified as on or off-center, X or Y, and "lagged" or "nonlagged" (Mastronarde, 1987a; Humphrey & Weller, 1988a). On the majority of dLGN neurons, ACh had an excitatory effect on both the background firing and the visual response; on a small number of neurons, it had either an inhibitory effect or little discernible effect on average response levels. The cells excited by ACh included both on-center and off-center as well as X and Y cells, but were all nonlagged. ACh altered the temporal pattern of the visual responses of these cells so that the responses became more sustained. None of the lagged cells had their overall level of response altered by ACh, but the temporal features of their responses were markedly changed: the latency and/or tonicity of responses decreased, so that the responses resembled nonlagged responses. The results show that ACh input to the dLGN can have a strong influence on the temporal characteristics of neuronal responses in the dLGN, and are consistent with a hypothesis that ACh facilitates more faithful transfer of retinal signals to cortex.

INTRODUCTION

Ascending brain-stem inputs capable of modulating the excitability of neurons in the mammalian thalamus (Steriade, 1970), and in the dorsal lateral geniculate nucleus (dLGN) in particular (Singer, 1977; Burke & Cole, 1978), have been extensively studied. One such input is the cholinergic projection to the thalamus originating in the mesencephalic reticular formation (for example, see Francesconi et al., 1984). The anatomical features of this input to the dLGN have been well documented (Sakai, 1980; Kimura et al., 1981; De Lima et al., 1985; DeLima & Singer, 1987), and it has been proposed that the cholinergic innervation plays an important role in the functional modulation of thalamic transmission of its afferent input to cortex (Steriade & Dechênes, 1984; McCormick, 1989).

Acetylcholine (ACh) directly excites most neurons in the LGN when iontophoretically applied *in vivo*, while it inhibits neurons of the perigeniculate nucleus (PGN) (Sillito et al., 1983; Eysel et al., 1986). *In vitro*, ACh is capable of exciting relay neurons while inhibiting intrinsic interneurons in the cat LGN (McCormick & Prince, 1987; McCormick & Pape, 1988).

A physiological group of neurons, called lagged cells, has been recently reported in the LGN, based on their temporal patterns of visual response to flashing stimuli (Mastronarde, 1987a; Humphrey & Weller, 1988a). The visual responses of lagged cells differ from those of nonlagged cells in that lagged cells have longer visual latencies, lack initial onset discharges and have anomalous offset responses. Importantly, the lagged property is not found in the retinal afferents to lagged cells (Mastronarde, 1987a). Instead, retinal inputs to both lagged and nonlagged cells in the dLGN are exclusively of the nonlagged type, demonstrating that the lagged property is an emergent property of the dLGN. It is unclear at present as to whether lagged and nonlagged cells represent

separate classs of neurons in the dLGN or different physiological modes of the same neuron. The evidence for the former view comes from Humphrey and Weller (1988b) who showed that lagged cells were different from nonlagged cells not only in physiological but also in morphological properties. Evidence also exists however, to support the latter view; stimulation of parabrachial regions of the brain-stem alters at least some features of lagged responses into nonlagged ones (Uhlrich et al., 1990). Therefore, it is of some interest to examine whether ACh, a likely neurotransmitter candidate of the parabrachial innervation of the dLGN (Francesconi et al., 1984), can also bring about similar changes in the visual responses of lagged cells. More generally, lagged and nonlagged responses represent different kinds of temporal processing of retinal input by dLGN cells, and we wished to examine the action of ACh on temporal aspects of the visual responses of dLGN cells.

Our results show that ACh excited a majority of dLGN cells while it actively inhibited the visual responses of others. The latter groups of neurons may represent intrinsic interneurons (McCormick & Pape, 1988). In a few cells ACh had little effect on the mean/overall visual response. Among the cells excited by Ach or on which it had little effect on the overall response level, there was a clear effect on the temporal properties of visual responses: the responses of nonlagged cells became more sustained, while most of the lagged cells showed decreases in visual latency and/or tonicity. Thus Ach markedly reduced the differences between lagged and nonlagged responses of dLGN cells. These results support the hypothesis that brain-stem cholinergic input may act to facilitate faithful transmission of retinal signals through the thalamus on to cortex.

METHODS

Animal Preparation

The experiments were performed on adult cats that were prepared for standard extracellular electrophysiological recording (see Sur et al., 1987; Kwon et al., 1991). Briefly, animals were anesthetized (induction and surgery with 3% halothane in 70% N_2O / 30% O_2 mixture, then maintained on 0.6 - 1 % halothane), paralyzed (by continuous intravenous infusion of 3.6 mg/hr gallamine triethiodide and 0.7 mg/hr d-tubocurarine) and supported on a ventilator through a tracheostomy. End-tidal CO_2 was kept at 4% and the body temperature was maintained at 37 °C using a heating blanket. A 5-lead EKG was monitored throughout the experiment and the heart rate was maintained at the pre-paralysis level. An adequate level of anesthesia was maintained at all times by adjusting the halothane dose. The pupils were dilated with atropine and appropriate contact lenses were fitted to focus the eyes on an oscilloscope screen 57 cm in front of the animal. The accuracy of the focus was checked using an ophthalmic retinoscope as well as by reflecting the image of retinal blood vessels and the optic discs onto the tangent screen. A pair of bipolar stimulating electrodes was placed across the optic chiasm. A 1 - 2 cm diameter craniotomy was made over the LGN.

Recording and Microiontophoresis

A six-barreled glass micropipette electrode assembly was used for extracellular recording as well as for iontophoretic application of acetylcholine (ACh) according to methods described previously from this laboratory (Kwon et. al. 1991). The recording pipette was filled with 3M KCl. One of the drug barrels was filled with ACh (200mM

pH 4.5). The remaining barrels were filled with other drugs as part of another study. One of the barrels was filled with 150mM NaCl as a balance barrel and was, in a few cases, used to assess any direct effect of iontophoretic current. Two or three levels of iontophoretic current (usually around 50 and 90nA) were chosen and the current levels were tried in increasing order until there was a clear excitatory or inhibitory effect.

Cell Classification

The receptive field of each cell was plotted on a tangent screen and classified as on- or off-center and X or Y. The latter classification was based on a number of criteria including the receptive field size (adjusted for eccentricity), latency to optic chiasm stimulation and linear summation of the response to a counterphasing grating stimulus (Sherman & Spear, 1982; Shapely & Lennie, 1985; Sur et al., 1987). Cells were also divided into lagged and nonlagged types based on the start-rise and half-rise visual latencies to a flashing stimulus that filled (only) the receptive field center (Mastronarde, 1987a, 1988; Humphrey & Weller, 1988a; Saul & Humphrey, 1990). We strictly adhered to previously established criteria in classifying cells as lagged or nonlagged (cf. Kwon et al., 1991).

Visual stimulus

Visual stimuli were produced by a stimulus generator (Picasso, Innisfree Inc., Cambridge, MA) under microcomputer (IBM PC compatible) control and presented on a Tektronix 620 monitor. The visual stimulus consisted of a spot whose luminance was brighter than the background (for on-center cells) or darker than the background (for off-center cells). The size of the stimulus was matched to the size and location of the

receptive field center. The spot was modulated at 1 Hz (stimulus "on" period of 0.5 s followed by background luminance of 0.5 s). The background luminance was 5.87 cd/m^2 and the response at this luminance was taken to be the background firing level.

In some cells, excitatory effect of ACh was compensated for by reducing the stimulus contrast, in order to characterize the effect of ACh on the temporal pattern of the response without the confounding factor of overall response increase. The background luminance was varied between two values, 3.00 and 8.14 cd/m^2, for on- and off-center cells respectively. Contrast was computed by the formula,

$$\text{Contrast} = \frac{\text{Center luminance - Background luminance}}{\text{Center luminance + Background luminance}}$$

Contrasts was varied between -0.85 to 0.73 for the on-center cells and between -0.4 to 0.95 for the off-center cells.

All responses were collected on the microcomputer on-line as well as onto tape using a data encoder for off-line analysis (Neurocorder DR-886, Neuro Data Instruments, New York, NY).

Data Analysis

Peristimulus time histograms (PSTHs, 5 ms bin width) were constructed from 10 trials of visual stimulation before, during and after each ACh application. For each trial the mean firing rate during the stimulation period (500 ms) as well as the peak firing rate (using a 100 ms moving average window) were computed. Average responses obtained before and during ACh applications were compared for each cell. Effects of ACh were considered significant if responses increased or decreased by at least twice the standard error of the control response.

Two temporal parameters, the start-rise and half-rise latencies, useful in distinguishing lagged from nonlagged responses, were measured from each PSTH as described previously (Kwon et al., 1991). The start-rise latency was determined from the start of the stimulus to the midpoint of the first bin that contained a response whose magnitude exceeded twice the standard error of the mean (SEM) of the background firing rate. The half-rise visual latency was determined from the start of the stimulus to the midpoint of the bin that contained a response that was equal to or just greater than half the peak amplitude.

In addition, third temporal parameter termed the "Tonicity Index" was also measured. The Tonicity Index is a measure of the strength of the sustained (or late) component of the visual response with respect to the onset transient (or early) component. Fig. 1 shows the how the sustained and onset transient components were obtained from the visual response of a representative dLGN cell. The onset response was defined as the average firing rate during the first 0.1 s following the stimulus onset and the sustained response was defined as the average firing rate from 0.2 to 0.5 s. For each cell we calculated the Tonicity Index as the fraction of the sustained response to the sum of the sustained and onset responses. A Tonicity Index close to 1 implies that the sustained response is much greater than the onset response, as would be the case for some lagged cells in which the initial discharge at stimulus onset is minimal. A Tonicity Index near 0 implies that the sustained response is near minimal, as would be the case for cells in which the response is highly phasic. Finally, a Tonicity Index of 0.5 implies that the sustained response is equal to the onset response. (Tonicity Index for the cell in Fig. 1 was 0.49).

Population values are presented as mean ± S.E.M. All statistical comparisons (unless otherwise noted) were done using the nonparametric, paired, Wilcoxon signed rank test.

Fig. 1 about here

RESULTS

We recorded a total of 62 neurons from laminae A and A1 of the dLGN. Of these, 28 neurons that showed stable extracellular recording throughout the drug application and recovery period (typically ≥ 2 hours) were analyzed quantitatively and constitute the subject of this report. The 28 cells contained 15 on- and 13 off-center cells and 19 X and 9 Y cells. Of the X cells, 15 were nonlagged and 4 were lagged; we encountered no lagged Y cells in the present study.

Effect of ACh on the visually-evoked and background firing of dLGN neurons

ACh excited 14 cells in the dLGN (50%) while inhibited 8 cells (29%), and did not change the response level of the remaining 6 cells (21%).

The most common effect of ACh application on dLGN cells was an increase in the visual response and sometimes in the background discharge. Fig. 2A-D shows an off-center nonlagged X cell whose average visually evoked response (during the 0.5 s of stimulus 'on' time) increased with iontophoretic application of ACh. Fig. 2A shows that the cell's visual response prior to ACh contained an initial onset discharge burst followed by a low, sustained, firing that lasted until the end of the stimulus. This type of response was typical of nonlagged cells that we recorded in our sample. In addition, start-rise and half-rise visual latencies (see Methods) were 25 and 35 ms respectively, which are well within the nonlagged range (Kwon et al., 1991). There was no background discharge (as evident during the last 0.25s of the PSTH). Fig. 2B shows the increase in the visual response during ACh application (84nA). The excitation was most pronounced during the late, sustained, portion of the response, making the response more "tonic" (see below). This effect on the visually evoked response was not, however, accompanied by

a similar increase in the background firing of the cell. The response returned to the original level 2 min. post ejection (Fig. 2C). Fig. 2D shows the control for a direct effect of the iontophoretic current. Application of NaCl through the balance pipette at 70nA had little effect on the cell's response (70nA was the maximal current possible through the barrel).

Fig. 2 about here

The excitatory effect of ACh was found in both on- and off-center as well as X and Y cells. Fig. 3 shows an off-center nonlagged Y cell in which the visually evoked response increased with ACh application. In this cell, both the background firing level and visual response increased significantly during ACh application at 50nA (Fig. 3B). Note again that the ACh effect is more pronounced in the sustained portion of the visually evoked response.

Fig. 3 about here

In other dLGN neurons, however, the effect of ACh was the opposite of that shown in Figs. 2 and 3; ACh *decreased* the background firing and visually evoked response. Fig. 4 shows two cells whose visual responses significantly decreased with ACh application. Fig. 4A shows a PSTH obtained before ACh application from an off-center nonlagged X cell. ACh application almost completely abolished the visual response (Fig. 4B) which subsequently recovered (Fig. 4C). The background firing also decreased during ACh application. Inhibitory effects of ACh were seen in both on- and off-center as well as in X and Y cells. Figs. 4D-F show PSTHs obtained from an off-center nonlagged Y cell in which the visual response also decreased significantly with

ACh. While control visual responses (that is, responses before application of ACh) of the cells that were subsequently found to be inhibited by ACh were often indistinguishable from those that were found to be excited by it, one consistent feature of the former was that their visually evoked responses were rather sustained. Thus both cells in Fig. 4 show tonic responses (Figs. 4A and 4D); seven out of the 8 cells that were inhibited by ACh showed Tonicity Indices of ≥ 0.3 (see Methods). The Tonicity Index of the ACh-inhibited cells (0.36 ± 0.042, n = 8) was greater than that of the ACh-excited cells (0.27 ± 0.038, n = 14).

Fig. 4 about here

Fig. 5 shows a population scatter plot showing the effects of ACh on the mean amplitude of visual responses. The x-axis represents the average control response and the y-axis represents the response during ACh application. The forty-five degree line thus represents no change with ACh. Open circles represent those cells in which the visual response significantly increased. (Significant change is defined by an increase or decrease greater than twice the standard error of the control response, where each response is an average of 10 trials, see Methods). The population responses of these cells increased from 25.0 ± 6.26 to 45.0 ± 6.33 (in spikes/s, n = 14); the mean percent increase during ACh application was 141 ± 39.5 and this increase was statistically significant ($p = 0.001$). ACh also increased the background firing rate in 13 of the 14 cells (data not shown). All 14 cells were nonlagged and included 9 on- and 5 off-center cells and 10 X and 4 Y cells. Closed circles in Fig. 5 represent cells in which the visual response was significantly decreased by ACh. The population response amplitude decreased from 31.7 ± 9.17 to 16.0 ± 5.56 (n = 8); the mean percent decrease was 70.6 ± 6 ($p = 0.01$). ACh also decreased the background firing level in 6 of these 8 cells (data

not shown). All 8 cells were nonlagged and included 4 on- and 4 off-center cells and 3 X and 5 Y cells. Finally, in the remaining 6 cells, the mean amplitude of visual responses did not significantly change during ACh application (25.1 ± 3.2 for control; 24.7 ± 3.15 during ACh; $p = 0.92$). The 6 cells included both on- and off-center cells. All of these cells however, were X cells and 4 of the 6 were lagged cells. We were not able to significantly increase or decrease the response level of these cells despite using maximal levels of currents (≥ 84nA in 4 of the 6 cells). However, in 4 of these 6 cells a significant change in temporal response patterns occurred during ACh application (see below).

Fig. 5 about here

Effect of ACh on the temporal pattern of visual responses in lagged and nonlagged cells

We were interested in finding out how the temporal aspects of dLGN cell responses, exemplified by lagged and nonlagged responses, changed with ACh application. We excluded the ACh-inhibited cells from this analysis because measurements of temporal response properties become meaningless when the response decreases significantly (see Fig. 4). We examined two temporal parameters of the visual response that distinguish lagged and nonlagged responses, the start-rise and half-rise latencies, and a third parameter, the Tonicity Index. The Tonicity Index represents a normalized measure of the strength of the late, sustained, component relative to the onset transient component (see Fig. 1 and Methods). The measure is useful because lagged responses contain little or no onset transient components while nonlagged responses usually contain strong onset transients. Thus, the Tonicity Index of the lagged cell responses in our sample was 0.73 ± 0.143 (n = 4) while that of the nonlagged responses was 0.28 ± 0.034 (n =16); the difference between the two populations was statistically

significant ($p = 0.01$, Mann-Whitney U test). Each of the three temporal parameters, the start-rise latency, half-rise latency and Tonicity Index, was examined before and during ACh application.

Fig. 6 shows an off-center nonlagged X cell whose visual response increased with application of ACh, similar to the responses shown previously (Figs. 2 and 3). The cell's start-rise (35 ms) and half-rise (45 ms) latencies did not change during ACh application (Figs. 6B and C). However, there was a significant change in the Tonicity Index with ACh. The control visual response had a minimal sustained component (Tonicity Index of 0.05, Fig. 6A). The cell's response became more sustained during ACh application with an increase in the Tonicity Index to 0.37 (Fig. 6B). We examined whether this increase was specific to the sustained component of the visual response in the following way. We reduced the stimulus contrast to a level such that the overall response (in total spike count) matched that before ACh application. The cell still exhibited a sustained response with a high Tonicity Index (0.42), indicating that the increase in the Tonicity Index was due to a specific increase in the sustained component and not due to a general increase in the amplitude of the response (Fig. 6C). The response pattern (to a stimulus of the original contrast) returned to that of the control within 2 min. after stopping ACh application (Fig. 6D).

Fig. 6 about here

As described earlier, the average level of visual response of the 4 lagged cells did not change significantly during ACh application. However, in these lagged cells, there were significant changes in temporal response patterns. Fig. 7 shows the effects of ACh on the visual responses of two lagged cells. Fig. 7A shows an off-center lagged X cell with long visual latencies (start-rise time of 125 ms and half-rise time of 320 ms), little or

no initial onset discharge, and an offset response at the end of the stimulus period at 0.5 s with slow "fall" time. Application of ACh did not significantly change the average response level (14.3 to 12.1 spikes/s, Fig. 7A and 7B respectively); however, the temporal patterns of the response changed dramatically. Specifically, the start-rise latency decreased by 75 ms to 50 ms; the half-rise latency decreased by 265 ms to 55 ms. In addition, an onset discharge burst emerged, shifting the peak response to the beginning of the stimulus period. The onset discharge was followed by a significantly less sustained response; the Tonicity Index decreased from 0.99 to 0.43 (Fig. 7A and 7B respectively). The offset response (at 0.5 s) also decreased significantly (Fig. 7B). These changes made the response of this lagged cell appear to be *nonlagged* during ACh application. These nonlagged features disappeared and the response became lagged once again following recovery from ACh (Fig. 7C). Fig. 7D-F shows another off-center lagged X cell in which temporal response patterns were less dramatically affected by ACh. The start-rise latency increased slightly from 55 to 60 ms; the half-rise latency remained at 75 ms (Fig. 7D and E). However, application of ACh clearly increased the initial onset discharge; the Tonicity Index decreased from 0.65 (Fig. 7D) to 0.55 (Fig. 7E). The response returned to the control pattern following recovery from ACh (Fig. 7F).

Fig. 7 about here

Fig. 8 shows population scatter plots of the three temporal parameters measured in the lagged and nonlagged cells. Fig. 8A shows the changes in the start-rise latency during ACh application. The x-axis represents the start-rise latency of the control responses; the y-axis represents the responses during ACh application. The forty-five degree line represents no change in the latency. The start-rise latencies of the nonlagged

responses before ACh application (25.9 ± 2.7 ms., n = 16) were not significantly different from those during ACh application (27.5 ± 2.7 ms., $p > 0.1$). In contrast, the population start-rise latency of the lagged cells tended to decrease during ACh application, with a reduction from 92.5 ± 23.3 to 60 ± 7.1 ms. (n = 4). Similarly, Fig. 8B shows that the half-rise latencies of the nonlagged cells did not change significantly (40.6 ± 2.04 ms. for the control; 38.8 ± 1.85 ms. during ACh, n = 16, $p > 0.1$). The population half-rise latency of the lagged cells again tended to decrease with a reduction from 168.8 ± 57.28 to 105.0 ± 43.59 (n = 4). Finally, Fig. 8C shows the change in the Tonicity Index during ACh application. The population Tonicity Index for the nonlagged cells (open circles) increased from 0.28 ± 0.034 to 0.41 ± 0.018 (n = 16, $p < 0.005$). Furthermore, when the amplitude of average firing rate during ACh application was matched to that of the control by appropriately varying stimulus contrast, the Tonicity Index still showed an increase from 0.24 ± 0.061 to 0.40 ± 0.044 (n = 7, individual data not shown). In contrast, the Tonicity Index for the lagged cells decreased from 0.73 ± 0.143 to 0.58 ± 0.082 (n = 4).

Fig. 8 about here

In summary, there were significant changes in the temporal characteristics of nonlagged and lagged (relay) cell responses to ACh application. In nonlagged cells, ACh application made the visual response more sustained but did not change the visual latencies. In the small number of lagged cells we recorded, ACh effects were more variable. However, the lagged cells displayed decreases in the Tonicity Index and/or visual latencies with ACh application. In one of the lagged cells, the change was consistent with a nonlagged response (Fig. 7C).

DISCUSSION

There are two main results of this study. First, iontophoretic application of ACh resulted in an excitatory effect on responses of a majority of dLGN cells while it had an inhibitory effect on others. In a small number of cells, it had no significant effect. Second, ACh changed temporal patterns of visual responses such that nonlagged cells had higher Tonicity Indices during ACh application while lagged cells tended to have lower Tonicity Indices and visual latencies.

Inhibitory effects of ACh

The excitatory effect of ACh on dLGN cells is consistent with the results of previous studies (Sillito et al., 1983; Eysel et al., 1986). The latter study demonstrated that ACh causes direct excitation rather than general disinhibition of dLGN cells because ACh was able to excite cells even when the retinal input was abolished (Eysel et al., 1986). Eysel et al. also reported that cells located in the PGN were inhibited by ACh while dLGN cells were not directly inhibited by it. Our results differ because we show the presence of dLGN neurons that are inhibited by ACh. Five of the 8 cells that were inhibited by ACh were from layer A1 and received monocular input from the ipsilateral eye; these cells were encountered only after the electrode passed through layer A and recorded cells receiving input from the contralateral eye. Like the cells in Fig. 4, all of the other cells inhibited by ACh received a monocular input, had clear distinct borders of the receptive field center and surround, and brisk visual responses, all consistent with LGN responses but not PGN responses (So & Shapley, 1981).

A number of studies support the idea that the dLGN neurons that are inhibited by ACh are intrinsic interneurons. First, ACh inhibits morphologically identified

interneurons in the cat dLGN *in vitro* through muscarinic receptors (McCormick & Pape, 1988). Second, electrical stimulation of a brain-stem area thought to send cholinergic afferents to the dLGN caused inhibition of interneurons in the dLGN (Ahlsén et al., 1984). Third, all physiologically and morphologically identified interneurons recorded *in vivo* are of nonlagged type (Humphrey & Weller, 1988b). All ACh-inhibited cells in the present study were also nonlagged cells. Fourth, the proportion of intrinsic interneurons in the dLGN is thought to be in the range of 20 - 30 % (LeVay & Ferster, 1979; Fitzpatrick et al., 1984; Montero & Zempel, 1985). This corresponds well with the proportion of ACh-inhibited cells (29%) found in the present study.

The effect of ACh on temporal patterns of visual responses

The present results show that ACh had a significant effect not only on the average firing rate of visually-evoked responses but also on their temporal patterns (see Figs. 6 and 7). This is of some interest because the distinction between lagged and nonlagged cells in the dLGN is based on specific temporal characteristics (Mastronarde, 1987a; 1987b; 1988; Humphrey & Weller, 1988a; 1988b; Saul and Humphrey, 1990). We wished to assess what effects, if any, ACh had on the defining characteristics of these cells. In particular, we wished to find out if a lagged response can be switched to a nonlagged response under the influence of ACh, similar to the results obtained by stimulation of parabrachial regions of the brain-stem (Uhlrich et al. 1990). Our results show that ACh increases the sustained portion of the visual response of nonlagged cells, thereby increasing the Tonicity Index, without affecting the visual latencies. On lagged cells on the other hand, ACh tends to decrease the visual latencies and Tonicity Index, thus making them "less lagged." One lagged cell's visual response came to resemble closely a nonlagged response during ACh application (Fig. 7B). Thus, it seems possible

to switch a lagged response to a nonlagged one under the influence of ACh at least in some dLGN cells. These findings are consistent with those of Uhlrich et al. (1990), and lend support to the notion that while two distinct temporal patterns of response exist in dLGN cells, these types do not necessarily represent separate classes of cell. Rather, in at least some population of cells, they may represent different response modes of the same neuron, and lead to state-dependent temporal transformation of retinal signals that are relayed to the cortex.

It has been shown that the retinal ganglion cell input to both nonlagged and lagged cells in the dLGN is of nonlagged type (Mastronarde, 1998a). Simultaneous recording of retinal ganglion cells and dLGN cells postsynaptic to the retinal afferents show that in a nonlagged geniculate cell, the retinal cell that provides the afferent input has generally a similar visual latency (with a difference of $\leq$ 10 ms) but has a stronger sustained response than the postsynaptic geniculate cell (see, for example, Fig. 1 in Mastronarde, 1988a). This response pattern of retinal afferent input resembles closely, in principle, a nonlagged geniculate cell's response during ACh application. Similarly, (nonlagged) retinal ganglion cells that drive geniculate lagged cells are indistinguishable from those that drive nonlagged geniculate cells; they have short visual latencies, a transient onset discharge, and lack an offset response (Fig. 1 in Mastronarde, 1988a). This afferent retinal response is consistent with the changes seen in some of the lagged cells during ACh application. Thus, one way to interpret the effect of ACh on nonlagged and lagged cells in the dLGN is to hypothesize that the cholinergic input facilitates more faithful encoding of retinal signals into dLGN cell responses.

ACKNOWLEGEMENTS

We thank Manual Esguerra and Anna W. Roe for general advice and comments, and Anthony Passera for technical advice on data analysis programs. Supported by NIH grant EY 07023.

REFERENCES

Ahlsén, G., Lindström, S. and Lo, F.-S. (1984). Inhibition from the brain stem of inhibitory interneurons of the cat's dorsal lateral geniculate nucleus. Journal of Physiology, 347, 593-609.

Burke, W. and Cole, A.W. (1978). Extraretinal influences on the lateral geniculate nucleus. Review of Physiological and Biochemical Pharmacology, 80, 105-166.

De Lima, A.D., Montero, V.M. and Singer, W. (1985). The cholinergic innervation of the visual thalamus: An EM immunocytochemical study. Experimental Brain Research, 59, 206-212.

De Lima, A.D. and Singer, W. (1987). The brainstem projection to the lateral geniculate nucleus in the cat: identification of cholinergic and monoaminergic elements. Journal of Comparative Neurology, 259, 92-121.

Eysel, U.T., Pape, H.-C. and van Schayck, R. (1986). Excitatory and differential disinhibitory actions of acetylcholine in the lateral geniculate nucleus of cat. Journal of Physiology, 370, 233-254.

Fitzpatrick, D., Penny, F.R. and Schmechel, D.E. (1984). Glutamic acid decarboxylase-immunoreactive neurons and terminals in the lateral geniculate nucleus of the cat. Journal of Neuroscience, 4, 1809-1829.

Francesconi, W., Muller, C.M. and Singer, W. (1984). Acetylcholine mediates the

effects of mesencephalic reticular formation stimulation in the dorsal geniculate nucleus of the cat. Neuroscience Letters Supplement, 18, S309.

Humphrey, A.L. and Weller, R.E. (1988a). Functionally distinct groups of X-cells in the lateral geniculate nucleus of the cat. Journal of Comparative Neurology, 268, 429-447.

Humphrey, A.L. and Weller, R.E. (1988b). Structural correlates of functionally distinct X-cells in the lateral geniculate nucleus of the cat. Journal of Comparative Neurology, 268, 448-468.

Kimura, H., McGeer, P.L., Peng, J.H. and McGeer, E.G. (1981). The central cholinergic system studied by choline acetyltransferase immunohistochemistry in the cat. Journal of Comparative Neurology, 200, 151-201.

Kwon, Y.H., Esguerra, M. and Sur, M. (1991). NMDA and non-NMDA receptors mediate visual responses of neurons in the cat's lateral geniculate nucleus. Journal of Neurophysiology, in press.

LeVay, S. and Ferster, D. (1979). Proportion of interneurons in the cat's lateral geniculate nucleus. Brain Research, 164, 304-308.

Mastronarde, D.N. (1987a). Two classes of single-input X-cells in cat lateral geniculate nucleus. I. Receptive-field properties and classification of cells. Journal of Neurophysiology, 57, 357-380.

Mastronarde, D.N. (1987b). Two classes of single-input X-cells in cat lateral geniculate nucleus. II. Retinal inputs and the generation of receptive-field properties. Journal of Neurophysiology, 57, 381-413.

Mastronarde, D.N. (1988). Branching of X and Y functional pathways in cat lateral geniculate nucleus. Society for Neuroscience Abstract, 14, 309.

McCormick, D. A. (1989). Cholinergic and noradrenergic modulation of thalamocortical processing. Trends in Neuroscience. 12: 215-221.

McCormick, D.A. and Pape, H.-C. (1988). Acetylcholine inhibits identified interneurons in the cat lateral geniculate nucleus. Nature (London), 334, 246-248.

McCormick, D.A. and Prince, D.A. (1987). Actions of acetylcholine in the guinea-pig and cat medial and lateral geniculate nuclei, *in vitro*. Journal of Physiology, 392, 147-165.

Montero, V.M. and Zempel, J. (1985). Evidence for two types of GABA-containing interneurons in the A-laminae of the cat lateral geniculate nucleus: A double-label HRP and GABA-immunocytochemical study. Experimental Brain Research, 60, 603-609.

Sakai, K. (1980). Some anatomical and physiological properties of pontomesencephalic tegmental neurons with special reference to the PGO waves and postural atonia during paradoxical sleep in the cat. In: Hobson J.A., Brazier, M.A.B. (eds) The reticular formation revisited. Raven Press, New York, pp 427-447.

Saul, A and Humphrey, A.L. (1990). Spatial and temporal response properties of lagged

and non-lagged cells in the cat lateral geniculate nucleus. Journal of Neurophysiology, 64, 206-224.

Shapley, R. and Lennie, P. (1985). Spatial frequency analysis in the visual system. Annual Review of Neuroscience, 8, 547-583.

Sherman, S.M. and Spear, P.D. (1982). Organization of visual pathways in normal and visually deprived cats. Physiological Review, 62, 738-855.

Sillito, A.M., Kemp, J.A. and Berardi, N. (1983). The cholinergic influence of the function of the cat dorsal lateral geniculate nucleus (dLGN). Brain Research, 280, 299-307.

Singer, W. (1977). Control of thalamic transmission by corticofugal and ascending reticular pathways in the visual system. Physiological Review, 57, 386-420.

So, Y.T. and Shapley, R. (1981). Spatial tuning of cells in and around lateral geniculate nucleus of the cat: X and Y relay cells and perigeniculate interneurons. Journal of Neurophysiology, 45: 107-120.

Steriade, M. (1970). Ascending control of thalamic and cortical responsiveness. International Review of Neurobiology, 12, 87-144.

Steriade, M. and Dechênes, M. (1984). The thalamus as a neuronal oscillator. Brain Research Review, 8, 1-63.

Sur, M., Esguerra, M., Garraghty, P. E., Kritzer, M. F., and Sherman, S. M. (1987). Morphology of physiologically identified retinogeniculate X- and Y-axons in the cat.

Journal of Neurophysiology, 52, 1- 32.

Ulrich, D.J., Tamamaki, N. and Sherman, S.M. (1990). Brainstem control of response modes in neurons of the cat's lateral geniculate nucleus. Proceedings of National Academy of Sciences USA, 87, 2560-2563.

FIGURE LEGEND

Fig. 1. Temporal parameters of a peristimulus time histogram (PSTH) used to calculate the Tonicity Index. Sustained response refers to the average firing rate during the last 300 ms of the stimulus "on" period (dotted line below PSTH, showing stimulation with dark spot); onset response refers to the average firing rate over the first 100 ms of the stimulus "on" period. The Tonicity Index is calculated by dividing the sustained response by the sum of the sustained and onset responses. The PSTH was obtained from an off-center nonlagged X cell and represents average response of 10 trials (with 5 ms bin width).

Fig. 2. Excitatory effect of ACh on an off-center nonlagged X cell. Conventions as in Fig. 1. The PSTH was obtained (**A**) before, (**B**) during and (**C**) 2 min. post ACh application at 84nA. **D**. The PSTH of the same cell during 150mM NaCl ejection at 70nA. Note that the sustained portion of the response increased during ACh application.

Fig. 3. Excitatory effect of ACh on a nonlagged Y cell. The PSTHs were obtained (**A**) before, (**B**) during and (**C**) post ACh application at 50nA. Note that the excitatory response is more pronounced during the sustained portion of the response. The background firing level also increased with ACh (during 0.5 - 0.75 s stimulus period).

Fig. 4. Inhibitory effect of ACh on two nonlagged dLGN cells. **A-C**. PSTHs obtained from an off-center nonlagged X cell (**A**) before, (**B**) during and (**C**) after ACh application at 84nA. Note that both the visual response and background firing decreased significantly. **D-F**. PSTHs obtained from an off-center nonlagged Y cell (**D**) before, (**E**) during and (**F**) post ACh application at 84nA.

Fig. 5. Population scatter plot showing changes in the average visual response due to ACh application. The x-axis represents the average visual response before ACh application; the y-axis represents the response during ACh application. Open circles represent cells whose visual responses increased significantly; closed circles represent cells whose response significantly decreased. Triangles represent those cells whose response did not change significantly. Significant change is defined as a change equal to or greater than twice the standard error of the control response. Forty-five degree line represents no change. See text for cell type composition for each of the 3 groups.

Fig. 6. Changes in temporal patterns of the visual response of a nonlagged cell with ACh. The PSTHs were obtained from an off-center nonlagged X cell (**A**) before, (**B** and **C**) during and (**D**) after application of ACh at 84nA. **A**,**B** and **D** are obtained at a stimulus contrast of 0.66 while **C** is obtained at a contrast of 0.25. The start-rise and half-rise visual latencies remained the same during ACh application (**B** and **C**). However, the visual response became more sustained with ACh; the Tonicity Index increased from 0.05 (**A**) to 0.37 (**B**). This increase in tonicity remained even when the average visual response during ACh application was reduced to match that of the control by reducing the stimulus contrast; under this condition, the Tonicity Index remained high (0.42) (**C**). The response pattern returned to that of the control following recovery from ACh (**D**).

Fig. 7. Changes in temporal patterns of lagged visual responses with ACh. **A**-**C**. PSTHs obtained from an off-center lagged X cell (**A**) before, (**B**) during and (**C**) after ACh application at 84nA. The start-rise and half-rise visual latencies decreased from 125 and 320 ms respectively (**A**) to 50 and 55 ms respectively (**B**). The Tonicity Index also

decreased from 0.99 (**A**) to 0.43 (**B**). The initial onset discharge which was absent in the control (**A**) appeared during ACh application (**B**), while the offset response which occured when the stimulus was turned off (**A**) was reduced during ACh application (**B**). These changes were consistent with a *nonlagged* response. **D-F**. PSTHs obtained from another off-center lagged X cell (**D**) before, (**E**) during and (**F**) after ACh application at 90nA. The start-rise and half-rise visual latencies did not decrease. However, there was an increase in the onset discharge in **B**; the Tonicity Index decreased from 0.65 (**D**) to 0.55 (**E**).

Fig. 8. Population scatter plots of the temporal parameters of visual response of lagged and nonlagged cells before and after application of ACh. The x-axis represents the appropriate parameter of control responses; the y-axis represents that of the responses during ACh application. The forty-five degree line represents no change. Open circles represent nonlagged cells and closed circles represent lagged cells. **A**. The start-rise visual latency. **B**. The half-rise visual latency. **C**.The Tonicity Index. See text for the changes in the population mean values of each of the 3 parameters.

Fig. 1

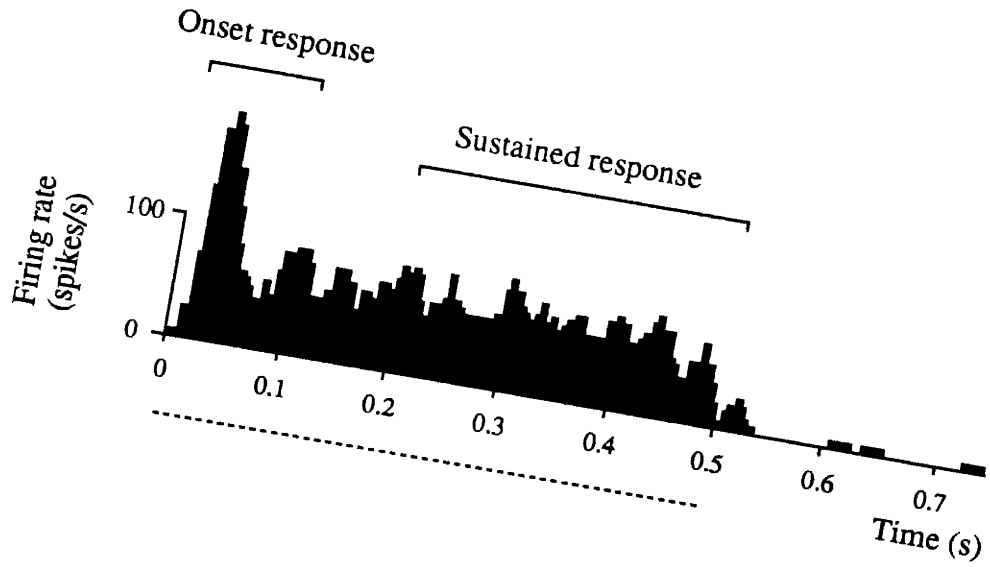
Onset response
Sustained response
Firing rate (spikes/s)
100
0
0
0.1
0.2
0.3
0.4
0.5
0.6
0.7
Time (s)

Off-center nonlagged X cell

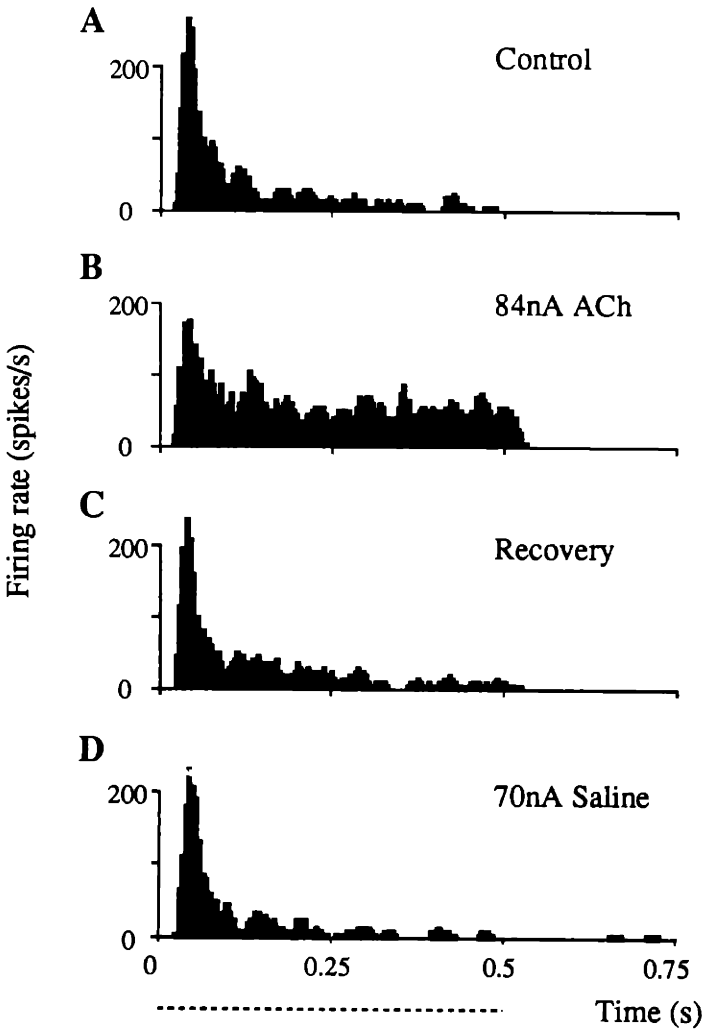

Fig. 3

Off-center nonlagged Y cell

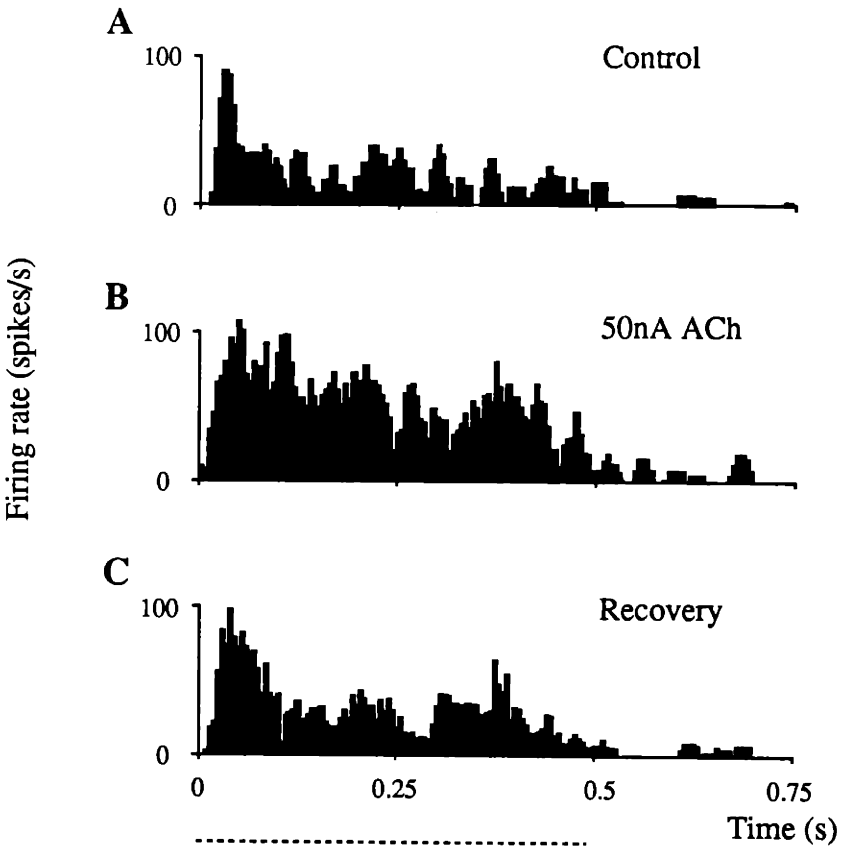

Fig. 4

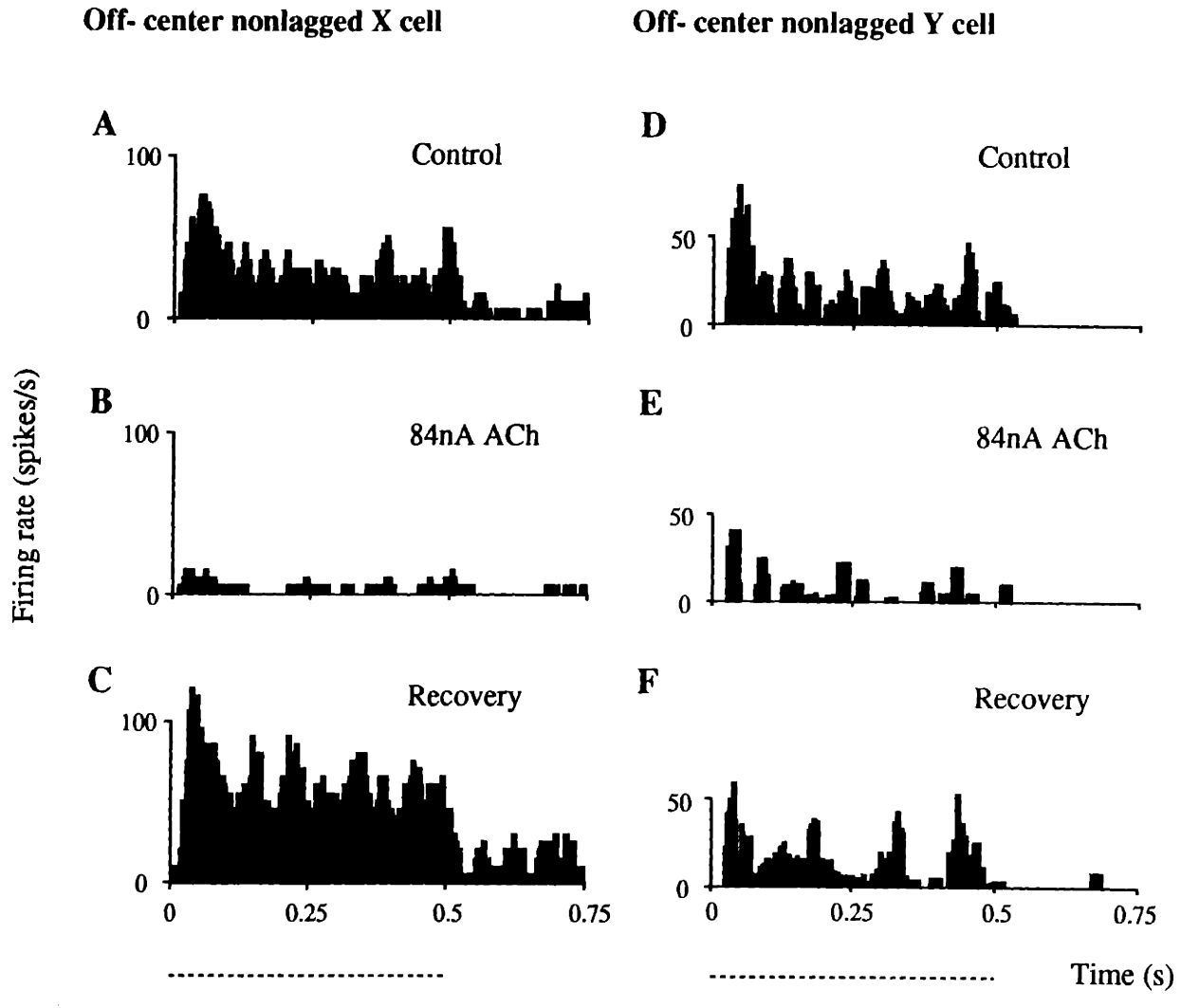
Off- center nonlagged X cell
Off- center nonlagged Y cell
A
Control
100
0
B
84nA ACh
100
0
C
Recovery
100
0
0
0.25
0.5
0.75
D
Control
50
0
E
84nA ACh
50
0
F
Recovery
50
0
0
0.25
0.5
0.75
Firing rate (spikes/s)
Time (s)

Fig. 5

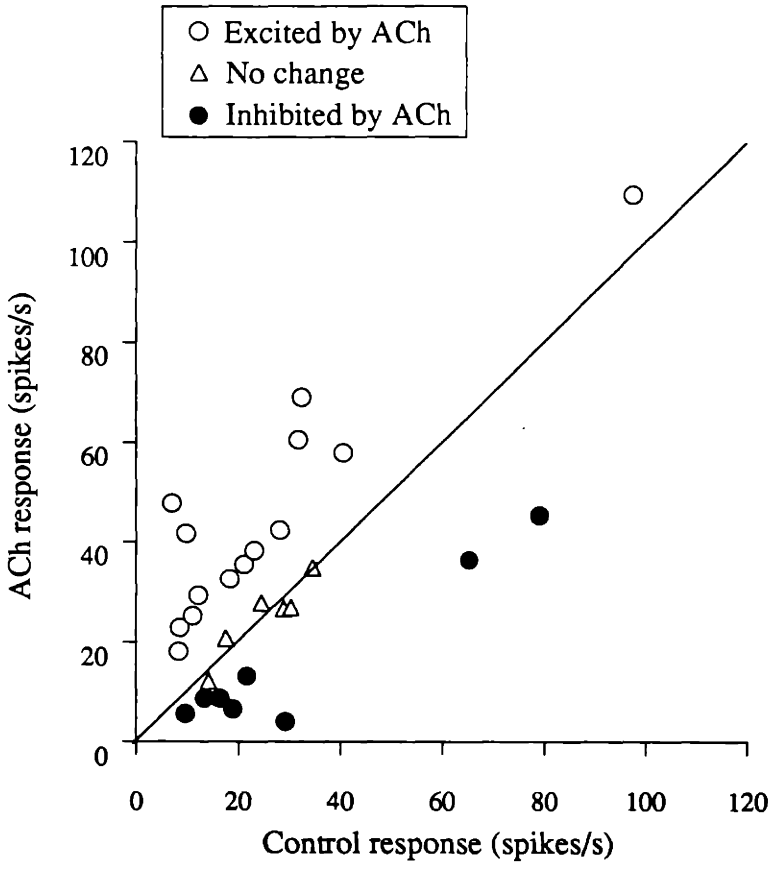
Excited by ACh
No change
Inhibited by ACh
ACh response (spikes/s)
Control response (spikes/s)
0
20
40
60
80
100
120

Off-center nonlagged X cell

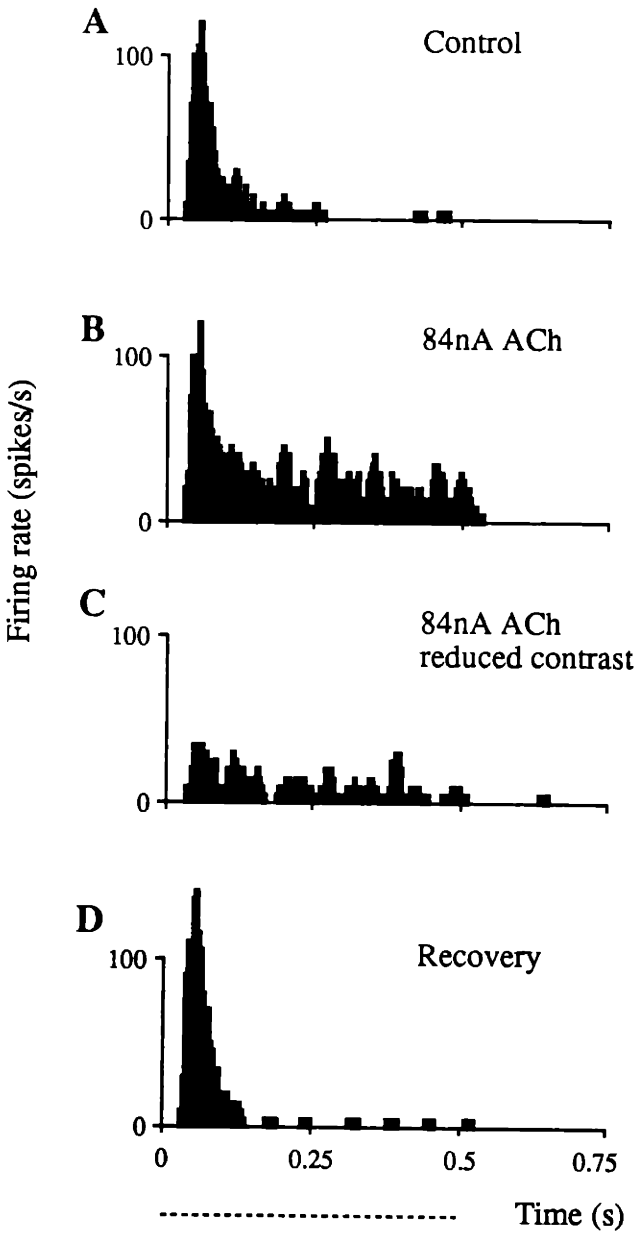

Fig. 7

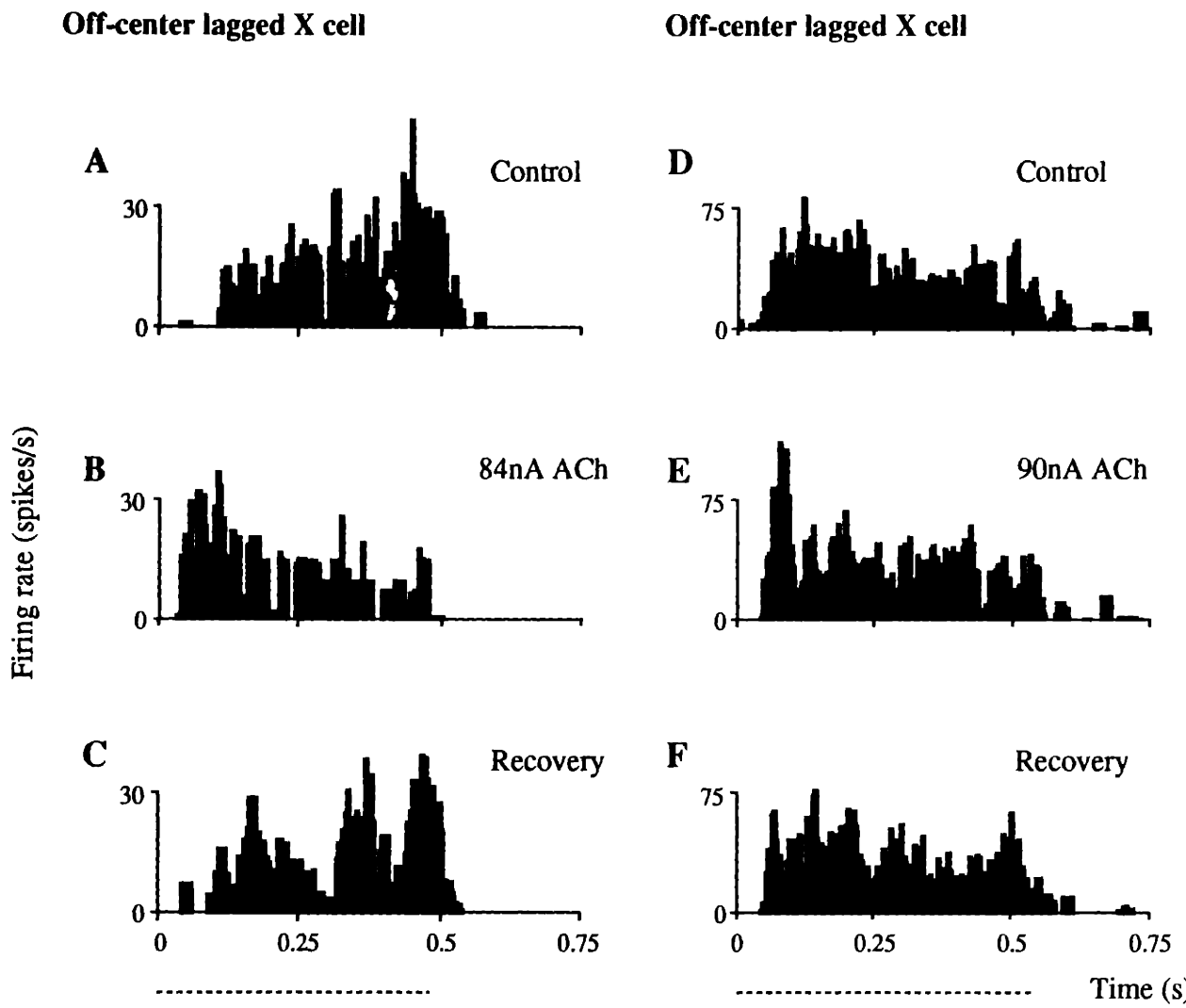
Off-center lagged X cell
Off-center lagged X cell
A
Control
30
0
D
Control
75
0
B
84nA ACh
30
0
E
90nA ACh
75
0
Firing rate (spikes/s)
C
Recovery
30
0
0
0.25
0.5
0.75
F
Recovery
75
0
0
0.25
0.5
0.75
Time (s)

Fig. 8

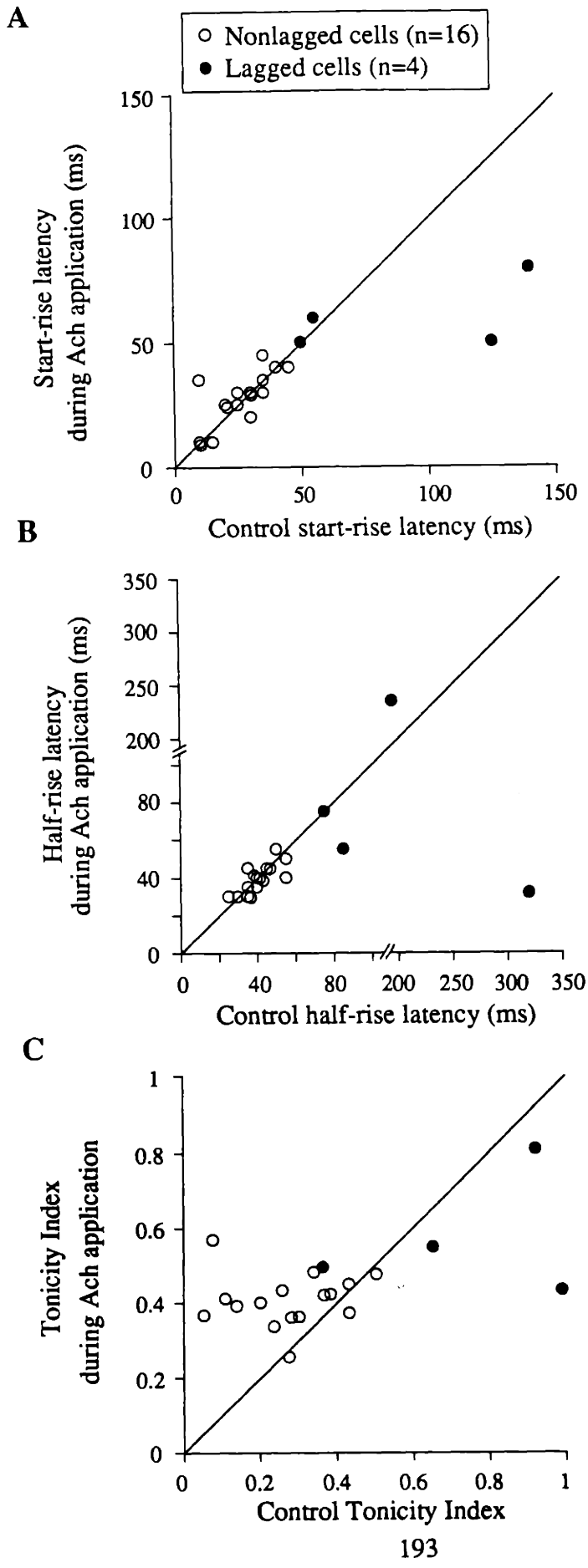
A
Nonlagged cells (n=16)
Lagged cells (n=4)
Start-rise latency during Ach application (ms)
Control start-rise latency (ms)
B
Half-rise latency during Ach application (ms)
Control half-rise latency (ms)
C
Tonicity Index during Ach application
Control Tonicity Index